# NEW POLYNUCLEAR CATALYSTS FOR ATOM-TRANSFER RADICAL ADDITION REACTIONS

THÈSE N$^{O}$ 3344 (2005)

PRÉSENTÉE À LA FACULTÉ SCIENCES DE BASE

Institut des sciences et ingénierie chimiques

SECTION DE CHIMIE ET GÉNIE CHIMIQUE

ÉCOLE POLYTECHNIQUE FÉDÉRALE DE LAUSANNE

POUR L'OBTENTION DU GRADE DE DOCTEUR ÈS SCIENCES

PAR

Laurent QUÉBATTE

chimiste diplômé de l'Université de Lausanne
de nationalité suisse et originaire de Saignelégier (JU)

acceptée sur proposition du jury:

Prof. K. Severin, directeur de thèse
Prof. P. Dyson, rapporteur
Prof. P. Pregosin, rapporteur
Prof. G. Süss-Fink, rapporteur

Lausanne, EPFL
2006

The development and improvement of catalysts is an important field of interest for many contemporary research groups and chemical industries. This not only because new organic molecules and reactions are being developed at a tremendous rate, but also because already existing processes have to be reconsidered and improved for economical and environmental reasons. The use of appropriate catalysts allows to perform reactions with lower energy consumption, but also with higher selectivities and less waste products. Catalysts are therefore required for two purposes a) economical rentability of chemical processes and b) making human activities more respectful towards nature. Many different chemical compounds have found application in catalysis, from simple Bronsted acids to very complex proteins, but the most famous catalysts are found within metal and organometallic complexes.

In this report, I will discuss the synthesis of bi- and polynuclear chloro-bridged complexes of the late transition metals and their application in atom-transfer radical addition catalysis.

# Summary

HOMO- AND HETEROBIMETALLIC complexes of the late transitions metals have been synthesized by metathesis reactions of the corresponding chloro-bridged dimers. These reactions have the advantage of being fast and giving rise to structurally defined products in quantitative yield. Complexes with three chloro-bridges of the general formula [LM($\mu$-Cl)$_3$RuL$_m$] (LM = (arene)Ru, Cp$^\star$Ir, or Cp$^\star$Rh; RuL$_m$ = RuCl(PPh$_3$)$_2$ or RuCp$^\star$) were investigated in detail and several of these were structurally characterized. Evidence is provided that triply bridged complexes of this kind can undergo fast exchange reactions.

The complexes with the fragment {RuCl(PPh$_3$)$_2$} were found to catalyze atom-transfer radical addition (ATRA) reactions. Structurally related complexes with chelating 1,4-*bis*(diphenylphosphino)butane (dppb) or 1,4-*bis*(dicyclohexylphosphino)butane (dcypb) ligands instead of the two PPh$_3$ ligands could likewise be generated. A total of 69 different combinations were prepared and tested in a combinatorial fashion for their ability to catalyze the ATRA of CCl$_4$ to styrene. Two combinations were found to be remarkably active and the corresponding complexes [Cp$^\star$Rh($\mu$-Cl)$_3$RuCl(PPh$_3$)$_2$] and [{(tpc)Rh($\mu$-Cl)$_3$Ru(dcypb)}$_2$($\mu$-N$_2$)] were identified and structurally characterized. They proved to be among the most active catalysts described so far.

Other ATRA catalysts were investigated. The cationic complex [Cp$^\star$Ru(PPh$_3$)$_2$-(CH$_3$CN)]OTf was found to display a higher stability than the related neutral catalyst [Cp$^\star$RuCl(PPh$_3$)$_2$]. Total TONs of up to 890 for the addition of CHCl$_3$ to styrene were obtained at a temperature of only 40 °C.

For the first time, ATRA reactions are reported using a mixture of [(arene)RuCl$_2$]$_2$ and PCy$_3$ as the catalyst precursors. As a product of the reaction between [(C$_6$H$_3$$^i$Pr$_3$)-RuCl$_2$]$_2$ and PCy$_3$, the tetranuclear complex [{(C$_6$H$_3$$^i$Pr$_3$)Ru($\mu$-Cl)$_3$RuCl(PCy$_3$)}$_2$($\mu$-N$_2$)] was isolated, which itself proved to be highly active. When the arene and the N$_2$ ligands of the latter were exchanged for a cymene ligand and an ethylene ligand, respectively, the resulting binuclear complex [(cymene)Ru($\mu$-Cl)$_3$RuCl(PCy$_3$)($\eta^2$-C$_2$H$_4$)] was obtained. It proved to be even more efficient than the dinitrogen complex and allowed the Kharasch addition of CCl$_4$ to 1-olefins to be carried out at a temperature as low as 0 °C. The observed TOFs (1100 h$^{-1}$ at 24 °C and 1550 h$^{-1}$ at 40 °C) are comparable to those reported for the most active catalysts.

# Version Abrégée

DES COMPLEXES homo- et hétérobinucléaires de métaux de transition ont été synthétisés par des réactions de métathèse à partir des dimères chloro-pontés correspondants. Ces réactions ont l'avantage d'être rapides et d'aboutir à des produits de structures bien définies, avec des rendements quantitatifs. Des complexes tripontés de formule générale $[LM(\mu\text{-}Cl)_3RuL_m]$ (LM = (arène)Ru, Cp$^\star$Ir, ou Cp$^\star$Rh; $RuL_m = RuCl(PPh_3)_2$ ou RuCp$^\star$) ont été étudiés en détail. Certains ont été structurellement caractérisés. Nous avons prouvé que des complexes de ce type peuvent subir de rapides réactions d'échange.

Les complexes avec le fragment $\{RuCl(PPh_3)_2\}$ se sont montrés capables de catalyser des réactions d'addition radicalaire par transfert d'atome (ATRA). Des complexes de structures très proches ont été générés de la même manière, avec des ligands chélatants 1,4-*bis*(diphénylphosphino)butane (dppb) ou 1,4-*bis*(dicyclohéxylphosphino)butane (dcypb), au lieu des deux ligands $PPh_3$. Au total, 69 combinaisons différentes ont été préparées et testées de manière combinatoire pour leur capacité à catalyser l'ATRA du $CCl_4$ au styrène. Deux combinaisons se sont montrées remarquablement actives et les complexes correspondants $[Cp^\star Rh(\mu\text{-}Cl)_3RuCl(PPh_3)_2]$ et $[\{(tpc)Rh(\mu\text{-}Cl)_3Ru(dcypb)\}_2(\mu\text{-}N_2)]$ ont été identifiés et caractérisés structurellement. Ces derniers figurent parmi les catalyseurs les plus actifs décrits jusqu'ici.

D'autres catalyseurs pour des réactions d'ATRA ont aussi été étudiés. Il a été trouvé que le complexe cationique $[Cp^\star Ru(PPh_3)_2(CH_3CN)]OTf$ possède une plus grande stabilité que le catalyseur neutre $[Cp^\star RuCl(PPh_3)_2]$. Des TONs totaux de 890 pour l'addition du $CHCl_3$ au styrène ont été atteints à une température de seulement 40 °C.

Pour la première fois, des réactions d'ATRA catalysées par des mélanges de $[(arene)RuCl_2]_2$ et de $PCy_3$ sont décrites. Le complexe tetranucléaire $[\{(C_6H_3{}^iPr_3)Ru(\mu\text{-}Cl)_3RuCl(PCy_3)\}_2(\mu\text{-}N_2)]$ a été isolé en tant que produit de réaction entre $[(C_6H_3{}^iPr_3)RuCl_2]_2$ et $PCy_3$ et a prouvé être très actif. Lorsque les ligands arène et $N_2$ ont été échangés pour respectivement un ligand cymène et un ligand éthylène, le complexe binucléaire $[(cymene)Ru(\mu\text{-}Cl)_3RuCl(PCy_3)(\eta^2\text{-}C_2H_4)]$ a été obtenu. Ce dernier s'est montré encore plus efficace que le complexe avec l'azote et a permis d'entreprendre l'addition de Kharasch du $CCl_4$ au styrène à une température de seulement 0 °C. Les TOFs observées (1100 $h^{-1}$ à 24 °C et 1550 $h^{-1}$ à 40 °C) sont comparables à celles publiées pour les catalyseurs les plus actifs.

# Contents

# Chapter 1

# Introduction

## 1.1 Halogeno-Bridged Mixed Complexes

### 1.1.1 Bimetallic complexes: inspired by nature

With the advance in spectroscopic techniques, the structures of the active sites of many metallo-enzymes and the nature of the key intermediates in enzyme catalyzed processes have been elucidated. With regard to polynuclear systems, it has been shown that a large number of these active sites contain two or more metal ions, that work in a cooperative fashion. The hydrogenases, for example, are enzymes, which catalyze the reversible oxidation of molecular hydrogen and play a vital role in the anaerobic metabolism of some bacteria. The hydrogen oxidation is coupled to the reduction of electron acceptors such as oxygen, nitrate, sulphate, carbon dioxide, or fumarate. In the sulfate-reducing bacterium *Desulfovibrio gigas*, the most numerous of these contain a dinuclear nickel-iron active site [1]. The 3D structure of several Ni-Fe hydrogenases have been determined (Figure 1.1) [2].

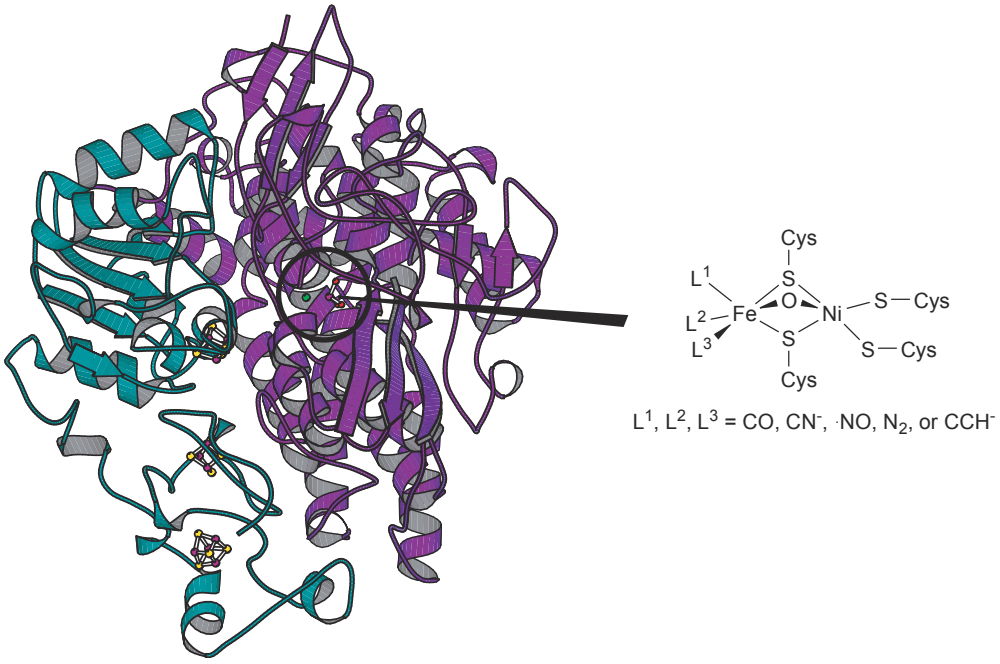


**Figure 1.1:** 3D structure of a Ni-Fe hydrogenase from *Desulfovibrio gigas* and depiction of the heterobimetallic active center.

The heterobimetallic active site is situated in the large subunit. The two metal ions are connected by two bridging $S^{\gamma}$ atoms of Cys residues and one oxygen atom. The nickel ion is connected to two other $S^{\gamma}$ atoms and displays a square pyramidal geometry. The coordination geometry of the Fe ion is a slightly distorted octahedron, with the presence

of three terminal ligands. There is no general agreement on the catalytic mechanism of Ni-Fe hydrogenases. It is presumed that the resting state of the dinuclear cluster is a Ni(II)-Fe(III) complex. First, $H_2$ binds the Fe in the form of a molecular hydrogen complex, which then undergoes heterolytic splitting with participation of the adjacent Cys thiolate ligand. The hydride bound to the Fe center can finally be transfered to the Ni center, on which subsequent proton or electron transport can take place [3].

The high efficiencies and selectivities of bimetallic metalloenzymes have long inspired chemists. It was expected that suitably designed multimetallic complexes could provide distinct reactivity patterns, different and potentially more attractive than those shown by analogous monometallic systems. The reducing power of multimetallic systems, for example, has good chances to be greater, simply because each of the metals could contribute to the reduction process within their normally accessible oxidation states. As a result, the synthesis of structurally defined polynuclear complexes, in particular that of heterobimetallic complexes, has attracted much attention over the last decades. Many of the structures described are based on polydentate ligands, which allow simultaneous coordination of several metal fragments (Figure 1.2, A). More complex molecules, such as the so-called dinucleating ligands, provide binding sites for two different metal ions in close proximity with a fixed geometry (Figure 1.2, B). The motivation behind these efforts were often potential applications of such compounds as catalysts or reagents in organic synthesis.

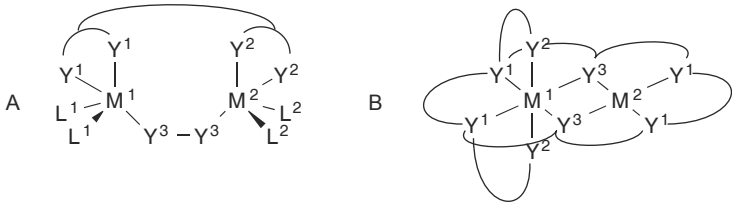


**Figure 1.2:** Suitable polydentate ligands (A) or more complex dinucleating ligands (B) give access to heterobimetallic complexes.

Although considerable progress has been made in the design and preparation of polynuclear compounds[1], synthetically useful candidates are still rare [12–17]. A reason for this is probably the difficult syntheses of the ligands, which strongly limits the rate at which these compounds are developed and assayed. We will see in the following subsection

1. For some recent reviews see [4–11].

that the use of halogeno-bridged complexes provides synthetic routes to heterobimetallic complexes, which are, on the contrary, remarkably fast and easy.

### 1.1.2 Synthesis

The exchange of the metal fragments of two symmetrical, halogeno-bridged dimers in a metathesis reaction represents the most general and easy way to obtain mixed complexes (Scheme 1.7, Method A). F. G. A. Stone *et al.* were among the first to report a reaction of this kind. In 1972, they observed that the *ortho*-metallated Rh(III) complex **1** reacts with the Rh(I) complex **2** to afford the mixed valence Rh(I)-Rh(III) complex **3** (Scheme 1.1) [18].

**Scheme 1.1**

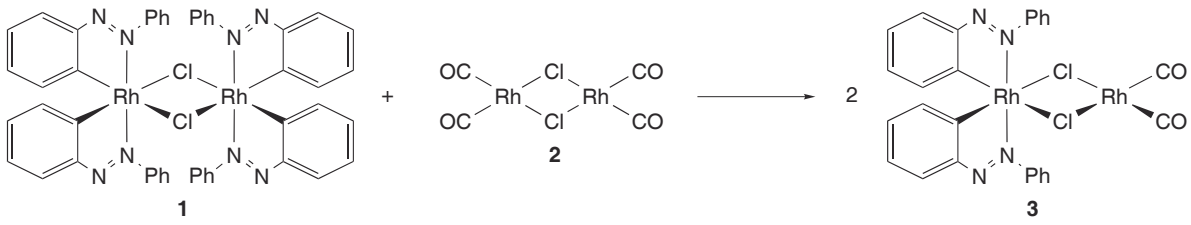


Other synthetic strategies, which allow the easy preparation of such complexes in excellent yields, have emerged. In 1986, for instance, G. Lopez *et al.* described the synthesis of bimetallic, chloro-bridged pentafluorophenyl Pd(II) complexes containing $\{ML_2\}$ fragments (**4**) (M = Ni, Pd, or Pt and LL = dpe or 2 × $PEt_3$). These compounds were obtained upon reaction of $[(C_6F_5)_2Pd(NCPh)_2]$ (**5**) with different mononuclear chloro complexes of nickel, palladium, or platinum (**6**) (Scheme 1.2) [19]. The palladium complex **5** possesses two weakly bound benzonitrile ligands, which are lost during the reaction. The bimetallic product is thus thermodynamically favored due to entropic reasons. Complexes having two terminal halogeno ligands available for bridging coordination seem to be generally suited reaction partners (Scheme 1.7, Method B).

**Scheme 1.2**

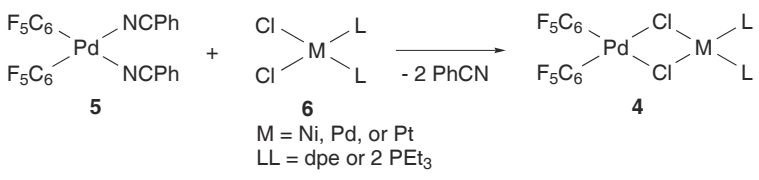


A few years later, G. van Koten *et al.* described a different synthetic method to obtain

mixed complexes. They used a mononuclear complex having only one weakly bound ligand. In this case, dimeric, monohalogeno complexes are appropriate reaction partners (Scheme 1.7, Method C) [20]. The binuclear complexes **7** were synthesized by mixing *trans*-[(N-C-N)$RhCl_2(H_2O)$] (**8**) with $[IrCl(cod)]_2$ (**9**) or $[RhCl(cod)]_2$ (**10**) (Scheme 1.3). Again, the loss of solvent molecules increases the entropy, which makes the resulting mixed complex thermodynamically favored.

**Scheme 1.3**

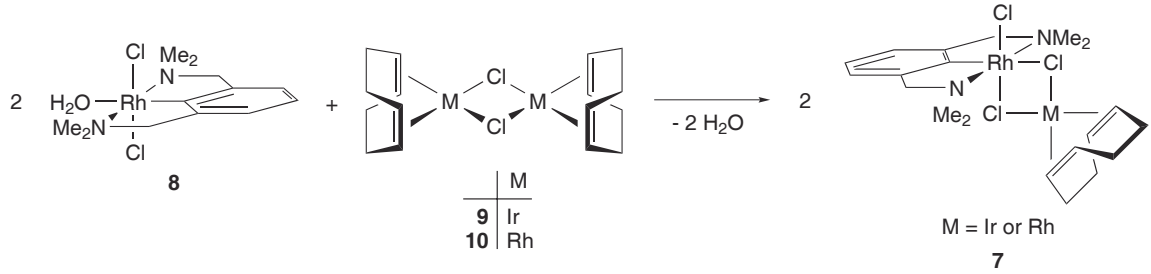


In 1999, R. H. Grubbs *et al.* reported the formation of mixed complexes based on a ligand transfer reaction between a mononuclear carbene complex and halogeno-bridged half-sandwich complexes (Scheme 1.7, Method D).

**Scheme 1.4**

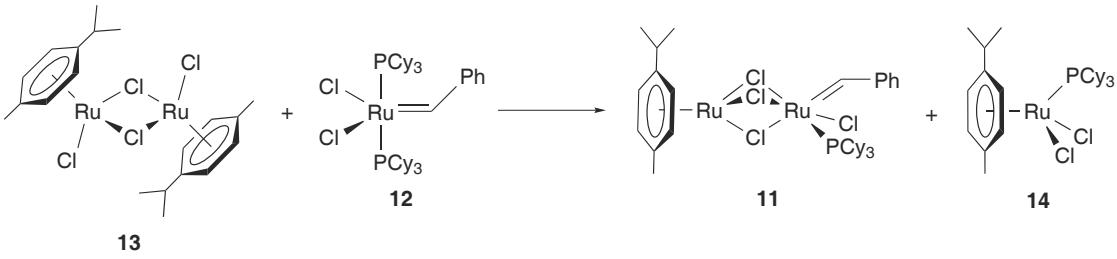


The bimetallic Ru complex [(cymene)Ru($\mu$-Cl)$_3$RuCl(CHPh)($PCy_3$)] (**11**)[2], for example, has been obtained by reaction of $[RuCl_2(CHPh)(PCy_3)_2]$ (**12**) (the "Grubbs catalyst") with $[(cymene)RuCl_2]_2$ (**13**) (Scheme 1.4) [22]. The obvious drawback of this reaction is

2. Although this type of complex is known for several years, no structural characterization has so far been achieved. They are generally depicted with two chloro-bridges with the molecular structure [LClM($\mu$-Cl)$_2$RuCl(CHPh)($PCy_3$)] [21, 22]. The unsaturated 16-electron Ru(II) metal center of the carbene fragment and the non-bridging chloro ligand of the {$LMCl_2$} fragment, available for the formation of a third bridge, however, suggest that these complexes most likely show a triply-bridged {M($\mu$-Cl)$_3$Ru} structural motif.

the formation of one equivalent of the undesired side product **14**, which has to be separated during workup.

Although chloro-bridge metathesis reactions are applicable to a wide range of halogeno-bridged complexes of the late transition metals, it is important to note that these reactions are often dynamic equilibria, in which the mixed complexes are in equilibrium with the symmetrical starting materials. Recent investigations, however, suggest that the use of particular starting materials allows the quantitative formation of mixed complexes [23–30]. This is the case when one of the dimeric starting materials is sterically crowded or charged. The dicationic platinum complex $[PtCl(PEt_3)_2]_2(BF_4)_2$ (**15**), for example, can be combined with the neutral bimetallic complex $[(allyl)PdCl]_2$ (**17**) to give the heterobimetallic complex $[(PEt_3)_2Pt(\mu\text{-}Cl)_2Pd(allyl)]BF_4$ (**16**) in quantitative yield [29]. The separation of the two positively charged $\{PtCl(PEt_3)_2\}^+$ fragments is the thermodynamic driving force of the reaction. The reaction depicted in Scheme 1.1 is a good example of a quasi-irreversible metathesis reaction due to steric congestion of one of the reaction partners. The starting complex **1** is composed of two rhodium(III) fragments, each of which bears two large azobenzene ligands, which gives rise to unfavorable interactions. The metathesis reaction with complex **2**, composed of two small $\{RhCl(CO)_2\}$ fragments, allows the formation of the mixed complex **3** of lower energy.

**Scheme 1.5**

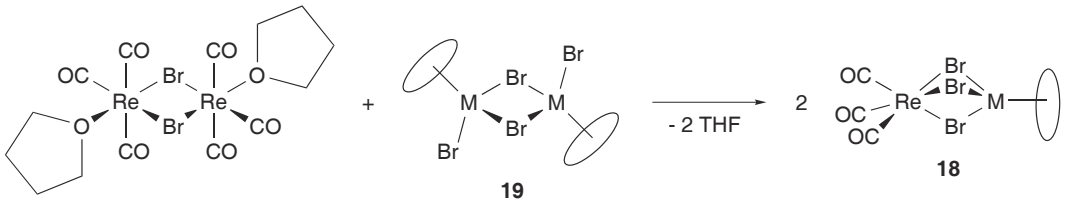


**20** **19** **18**

(π-ligand)M = (benzene)Ru, $(C_6H_3Et_3)$Ru, (cymene)Ru, Cp*Ir, or Cp*Rh

Another method to shift the equilibrium in favor of the mixed complex is to combine the metathesis reaction with a loss of one or several weakly bound ligands (Scheme 1.7, Method E). In that case, as observed for Methods B and C, the increase in entropy is the driving force. K. Severin *et al.* reported recently that heterobimetallic complexes, in which Ru(II), Rh(III), and Ir(III) half-sandwich fragments are connected by three bromo-bridges to a $\{Re(CO)_3\}$ fragment, can be obtained in metathesis reactions of complex $[ReBr(CO)_3(THF)]_2$ (**20**) and the bromo-bridged dimers **19** (Scheme 1.5) [28].

The reaction between the trichloro-bridged complex $[(PPh_3)_2ClRu(\mu\text{-}Cl)_3Ru(PPh_3)_2$-

**Scheme 1.6**

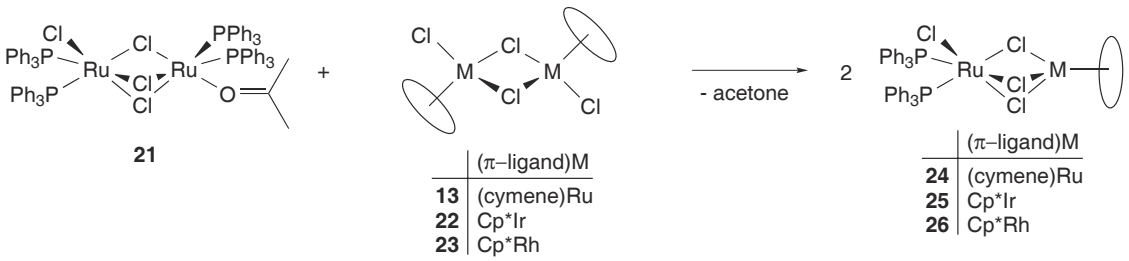


(acetone)] (**21**), which contains a weakly bound acetone ligand, and bimetallic half-sandwich complexes of Ru(II), Rh(III), and Ir(III) represents another route to mixed complexes with three halogeno-bridges (Scheme 1.7, Method F) (Scheme 1.6) [26].

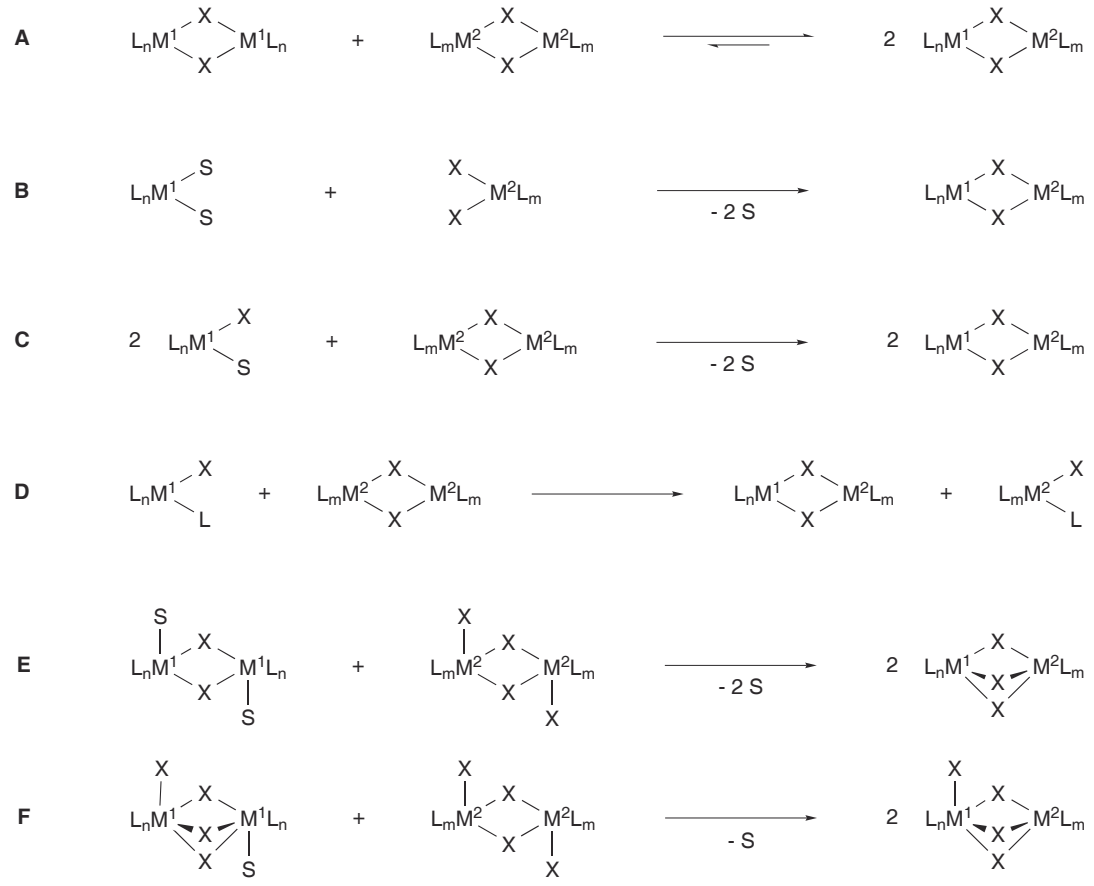


**Scheme 1.7:** Methods for the synthesis of mixed, halogeno-bridged complexes (S = solvent molecule or weakly bound ligand).

### 1.1.3 Properties and reactivity

Halogeno-bridged complexes are intrinsically very reactive. The fast metathesis reactions that they undergo are a manifestation of their low kinetic stability. In the presence of good donor ligands such as phosphines, the halogeno-bridges are rapidly cleaved to give the respective monomeric adducts (Scheme 1.8).

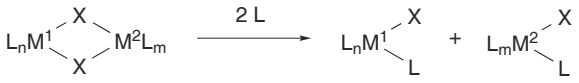


**Scheme 1.8:** Halogeno-bridged bimetallic complexes react with donor ligands (L) to give the corresponding monomeric species.

First evidence that there is some electronic communication between the metal fragments of mixed, halogeno-bridged complexes was provided by J. Halpern *et al.* in 1982 [31]. While studying catalytic intermediates and derivatives of the Wilkinson's catalyst, they observed that the rate of dihydrogen addition to the first rhodium center of the chloro-bridged complex $[RhCl(PPh_3)_2]_2$ (**27**), to form the mixed valence complex $[(PPh_3)_2H_2Rh(\mu\text{-}Cl)_2Rh(PPh_3)_2]$ (**28**), was almost identical to that observed for the monomeric analogue $[RhCl(PPh_3)_3]$ (**29**). The remaining Rh(I) site of complex **28**, on the other hand, did not add dihydrogen, even under higher pressure (Scheme 1.9). The reduced electronic density on the Rh(I) center, due to the close proximity of the Rh(III) cation, may be the origin of this deactivation. More recently, theoretical investigations have shown that the electron density of the allyl ligand in complexes $[(PEt_3)_2M(\mu\text{-}Cl)_2Pd(allyl)]BF_4$ (M = Pt (**16**) or Pd (**30**)) was significantly reduced compared to that of the symmetric complex **17** [27].

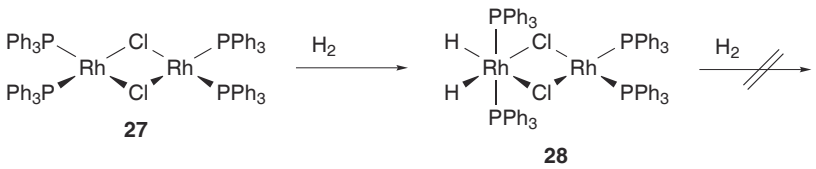


**Scheme 1.9:** Example of deactivation in a halogeno-bridged complex: The binuclear complex **27** adds one $H_2$ molecule at approximatively the same rate as its mononuclear analogue. A second oxidative addition of $H_2$, however, is not observed.

Modification of one metal center in a bimetallic complex can dramatically affect the solubility of the latter. The Ru(IV) complexes $[(C_{10}H_{14})ClRu(\mu\text{-}Cl)_2Pd(C_9H_{12}N)]$ (**31**)

and $[(C_{10}H_{14})ClRu(\mu\text{-}Cl)_2RhClCp^\star]$ (**32**), for example, display a good solubility in a variety of organic solvents, whereas the corresponding homo-dimer $[(C_{10}H_{16})RuCl_2]_2$ (**33**) is only sparingly soluble [32].

### 1.1.4 Catalysis

As outlined in Subsection 1.1.2, complexes of the late transition metals, in which two different metal fragments are connected by halogeno-bridges, can be synthesized from simple starting materials. Furthermore, due to their high intrinsic reactivity, they are well suited as catalyst precursors.

First convincing evidence that highly active catalysts can be found within this class of compounds was provided by R. H. Grubbs *et al.* [22]. They have reported the synthesis of the homo- and heterobimetallic complexes $[(\pi\text{-ligand})M(\mu\text{-}Cl)_3RuCl(PCy_3)(CHPh)]$ ($(\pi$-ligand)M = (cymene)Ru (**11**), (cymene)Os (**34**), and ($^t$Bu$_2$Cp)Rh (**35**)). In ring-closing and ring-opening olefin metathesis reactions, these complexes proved to be significantly more active (up to 70 times) than the widely used carbene complex **12**, which was developed by the same group. With the catalyst precursor **35**, even hexafluorodimethylnorbornadiene could be polymerized, a reaction that proved to be difficult with the standard catalyst **12**. Soon after, W. A. Hermann *et al.* described the structurally related complexes $[(\pi\text{-ligand})M(\mu\text{-}Cl)_3RuCl(NN\text{-}Cy_2Imi)(CHPh)]$ ($(\pi$-ligand)M = (cymene)Ru (**36**) and Cp$^\star$Rh (**37**)), which displayed even higher activities (Scheme 1.10) [21].

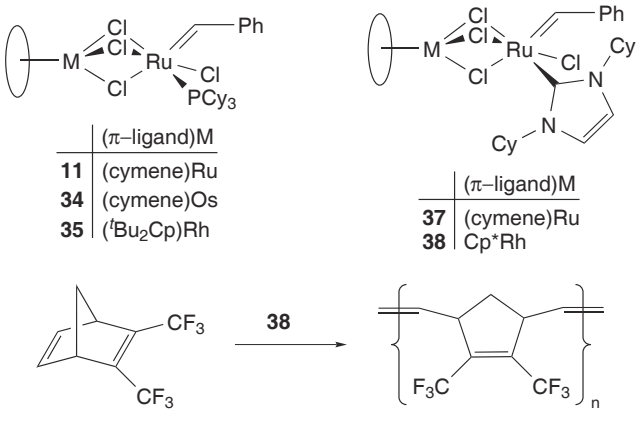


**Scheme 1.10:** Efficient olefin metathesis catalysts are found within homo- and heterobimetallic complexes.

More recently, K. Severin and coworkers have reported the Rh(III)-Ru(II) complex $[Cp^\star Rh(\mu\text{-}Cl)_3RuCl(PPh_3)_2]$ (**26**), which displays an exceptional catalytic activity for the Oppenauer-type oxidation of alcohols, surpassing that of complex $[RuCl_2(PPh_3)_3]$

(**38**), one of the most successful catalyst precursors for this reaction (Scheme 1.11) [26]. This catalyst was identified by a screening of the mixed complexes with three halogeno-bridges depicted in Scheme 1.6. For these reactions, the half-sandwich complexes can be regarded as labile ligands, which solubilize and stabilize the catalytically important fragment $\{RuCl_2(PPh_3)_2\}$.

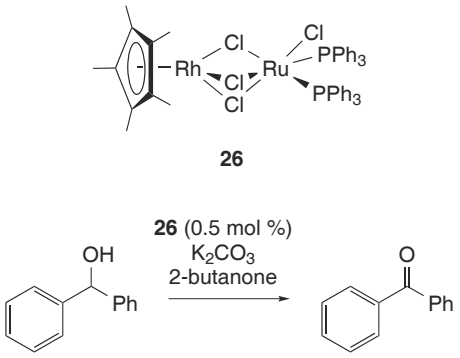


**Scheme 1.11:** The heterobimetallic complex **26** allows the efficient catalytic oxidation of diphenylmethanol.

Although there are numerous halogeno complexes, which could be used for this purpose, it would be difficult to determine a priori which candidate would provide the most suited structural and electronic effects in order to increase the activity of the $\{RuCl_2(PPh_3)_2\}$ fragment. To compensate for this lack of understanding, methods that would allow the testing of a large number of combinations in a short period of time would be welcome. This leads us to the method of combinatorial catalysis.

## 1.2 Combinatorial Catalysis

### 1.2.1 The method of combinatorial chemistry

In combinatorial chemistry[3], a recurrent three steps process is often employed: First, a library of compounds is synthesized. These compounds are then tested for a desired property, and finally, the compounds that show the best performance (hits) are identified. A new library may then be constructed that probes a smaller region of the diversity space around the initial hit. Combinatorial chemistry can therefore be considered as an artificial accelerated evolution process with human rather than natural selection as its motor.

Merrifield's solid phase synthesis of polypeptides on polystyrene beads was a first step on the road to this new concept [34]. In a Merrifield synthesis, the growing polypeptide chain is anchored to a polystyrene bead and extended one amino acid residue at a time using appropriate reagents; final cleavage gives the desired polypeptide. The method could readily be automated. The advantage of the solid phase is that the steps can be pushed to high yields using an excess of reagents and the growing polypeptide can be separated at each step simply by filtering the beads and washing. In order to create a library of polypeptides, a specific amino acid residue reagent, as is normally used in a chain extension step, is replaced by a mixture of reagents, leading to a mixture of compounds in the final product. By fixing amino acids at most sites and incorporating variable residues at a few sites, a large degree of diversity can be obtained rather easily. The next conceptual step was the recognition by J. A. Ellman that the same sort of diversity can be created by solid phase organic synthesis (SPOS) for non-peptidic compounds, where the substituents on a central motif are permuted [35].

From this, it has been a short step to the idea of creating a library of potential ligands on beads, binding a reactive metal complex to the supported ligands, and assaying the resulting beads for catalytic activity. Further development of methods, which allow the combinatorial synthesis of catalyst libraries, has resulted in the emergence of a new strategy for catalyst discovery: combinatorial catalysis.

### 1.2.2 Combinatorial catalysis

Because structure/function relationships are either obscure or not readily predictable for most catalysts, homogeneous catalyst discovery owes at least as much to empirical

3. For a review of recent applications of combinatorial chemistry see [33].

testing as to mechanistic understanding. The conventional method for catalyst development can be summarized as following: Once an initial lead catalyst has been identified (either in current experimental work in one's laboratory or in the literature), incremental changes in the ligand set, often guided by simple mechanistic considerations, were then made to bring the activity, selectivity or scope of the catalyst up to useful levels. Since each potential catalyst was normally separated and purified, then assayed, progress was relatively slow. With the advent of combinatorial chemistry, a new strategy has emerged: It combines parallel synthesis of a broad range of catalysts (the catalyst library) with a rapid and preferably parallel assay (the rapid screening). This methodology is increasingly being employed and greatly accelerates the rate at which homogeneous transition metal catalysts are discovered and optimized[4]. Another potential advantage of making screening much easier is that complexes that do not appear to be promising candidates can also be assayed. This leads to the possibility that unexpected classes of catalysts may be found[5].

It is important to note that this success owes most to the recent development of sophisticated screening equipment, such as micro-scale parallel reactors, robots, and adapted analytical methods[6]. Appropriate software for data handling and analysis has also been developed for high throughput technologies. Although such equipment can provide a fully integrated workflow from the synthesis of the catalyst libraries to the analysis of the final reaction mixtures, it is only accessible to some specialized groups or companies. More simple devices, such as UV-vis or fluorescence microplate readers and autosamplers for GC, HPLC and NMR analysis, on the other hand, are common in most research centers and also allow valuable savings of time. But high throughput experimentation does not represent the solution to all problems. In many cases, the synthesis of the catalyst library represents the rate determining step in the discovery process. Therefore, methods which allow the fast and easy synthesis of a wide range of structurally related compounds are required.

4. For recent reviews see [36–50].

5. For selected recent examples see [51, 52].

6. For selected recent examples see [51, 53–58].

### 1.2.3 Examples of catalyst libraries

The first report of a combinatorial synthesis of a catalyst library was published by the group of J. A. Ellman. They prepared a number of proline-based amino alcohols by attaching an *N*-ethylcarbamate protected methyl ester of *trans*-4-hydroxy-L-proline to a Merrifield resin. In this system, there were several locations where modifications could be made. The resulting ligands were assayed for their ability to accelerate the addition of diethyl zinc to aldehydes. Several compounds were found to give a good enantiomeric excess (Scheme 1.12) [59].

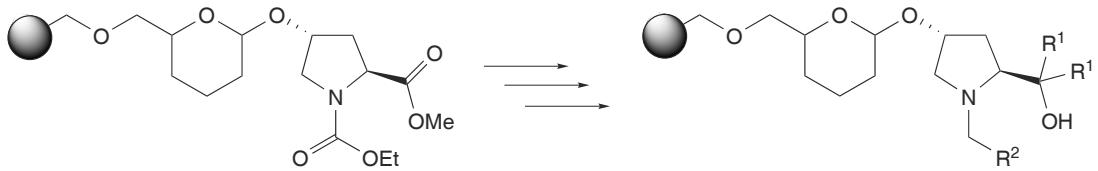


$R^1$ = Ph, Me or Et

$R^2$ = Ph, 3,5-dimethylphenyl, 4-biphenyl, 3,5-dichlorophenyl, 4-(trifluoro□methyl)phenyl, 2-naphthyl

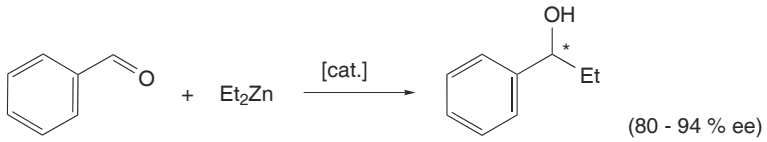


**Scheme 1.12:** A library of proline-based amino alcohols as asymmetric catalysts for the addition of $Et_2Zn$ to aldehydes.

Another example of a combinatorial synthesis of a library of ligands was reported by S. R. Gilbertson *et al.* in 1996 [60]. They used phosphine containing amino acids in combination with a solid-phase peptide synthesis (SPPS) protocol. Rhodium(I) was coordinated to the phosphine ligands and the resulting complexes were evaluated in a parallel manner for their ability to catalyze the asymmetric hydrogenation of enamides (Scheme 1.13). Although the selectivities were found to be low, the results demonstrated the feasibility of such an approach for the combinatorial synthesis of new catalysts.

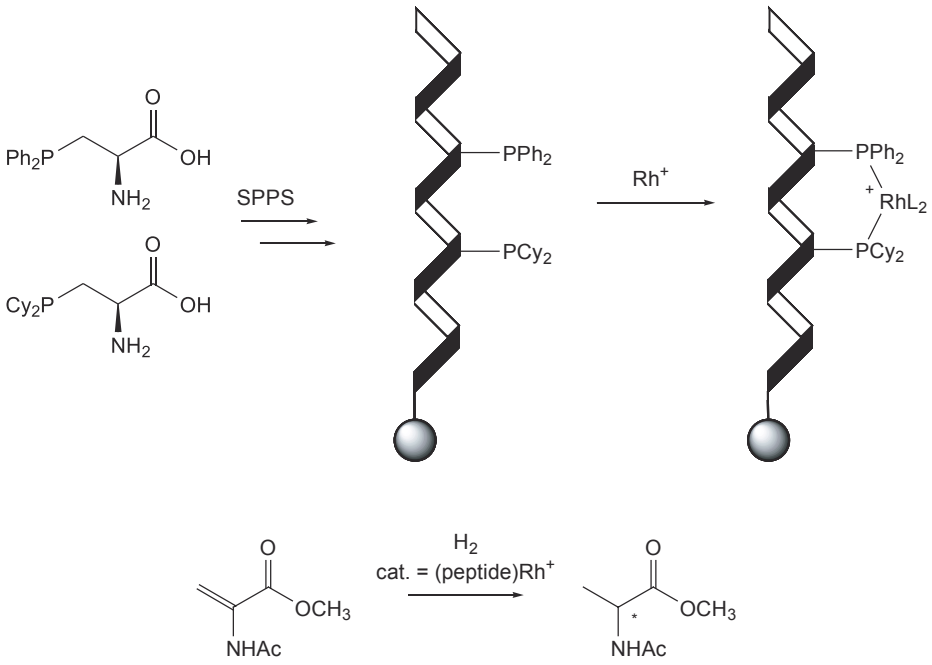


**Scheme 1.13:** Combinatorial synthesis of diphosphine ligands by solid-phase peptide synthesis (SPPS).

### 1.2.4 Combinatorial chemistry with bimetallic complexes ?

In the field of homogeneous combinatorial catalysis, most efforts have focused on mononuclear complexes, with ligands that are preferably built in a modular fashion. The screening of bi- and oligometallic catalysts represents a special challenge since the synthesis of a polynuclear catalyst library is generally more difficult. As outlined in Subsection 1.1.2, complexes of the late transition metals, in which two different metal fragments are connected by halogeno-bridges, can be obtained by fast and easy syntheses and display high structural variability. Moreover, because of their intrinsic reactivity, it was expected that they will give access to new catalysts. This was substantiated by our work about atom-transfer radical addition reactions, which is described in detail in Section 2.2 of this thesis.

## 1.3 Atom-Transfer Radical Addition (ATRA)

### 1.3.1 The Kharasch addition

In the late 1930s, M. S. Kharasch and coworkers investigated the regioselectivity of the addition of hydrobromic acid to olefins. They observed that, in the presence of peroxides, the *anti*-Markovnikov adduct was obtained and explained this result with a free radical mechanism [61]. A few years later, they were able to show that $CCl_4$ and $CHCl_3$ could likewise be added to terminal olefins using radical initiators (Scheme 1.14) [62]. This type of atom-transfer radical addition (ATRA) of polyhalogenated compounds to olefins is nowadays commonly referred to as "Kharasch reaction". The key steps of this reaction are depicted in Scheme 1.15.

With the original system, an important complication was found: The radical formed in step a of the propagation may not only abstract a chloride atom (step b) but also add to another olefin molecule. The result is the telomerization or ultimately the polymerization of the olefin.

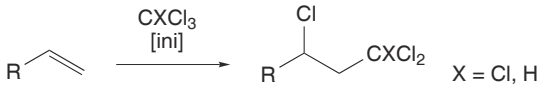


**Scheme 1.14:** *Anti*-Markovnikov addition of $CCl_4$ or $CHCl_3$ to terminal olefins.

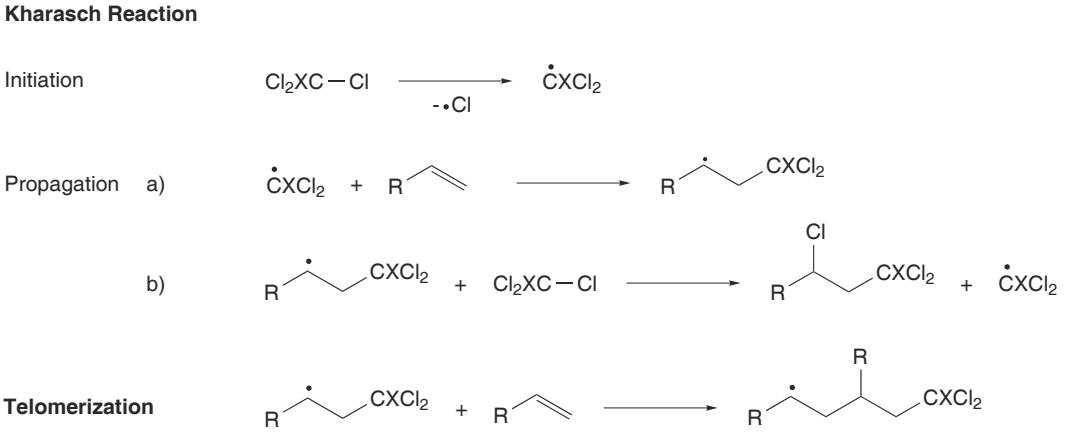


**Scheme 1.15:** Free radical mechanism for the Kharasch reaction.

### 1.3.2 First transition metal complexes as Kharasch catalysts

The first observation that transition metals could catalyze the addition of $CCl_4$ or $CHCl_3$ to terminal olefin was reported by F. Minisci and co-workers in the mid-1950s [63]. During attempts to thermally polymerize acrylonitrile in $CCl_4$ or $CHCl_3$ in a steel

autoclave, they observed that considerable amounts of the monoadduct between $CCl_4$ or $CHCl_3$ and acrylonitrile was produced. Further investigation of the phenomena revealed that some $FeCl_2$ had formed from the corrosion of the autoclave and acted as catalyst.

This discovery represented a major breakthrough, and a number of transition metal complexes were subsequently developed in order to catalyze the reaction with more ease and higher selectivity for the 1:1 adduct. They can mainly be classified in two groups: metal halides [64–70] and metal carbonyls [71–77].

### 1.3.3 $[RuCl_2(PPh_3)_3]$ as ATRA catalyst

In 1973, Y. Nagai *et al.* investigated the possibility of using transition metal phosphine complexes—commonly used for homogeneous hydrogenation [78, 79]—as Kharasch catalysts [80]. Among them, the ruthenium complex $[RuCl_2(PPh_3)_3]$ (**38**) was found to catalyze the addition of $CCl_4$ and $CHCl_3$ to 1-olefins under mild conditions with an increased selectivity for the 1:1 adduct.

Mechanistic investigations of the addition of $CCl_4$ to alkenes in the presence of complex **38** have been reported by J. L. A. Durrant *et al.* (Scheme 1.16) [81,82]. The reaction rates decreased when triphenylphosphine was added, which indicates that an initial dissociation of a $PPh_3$ ligand has to take place. The fourteen-electron fragment $\{RuCl_2(PPh_3)_2\}$ was suggested to be the catalytically active species, which reacts with $CCl_4$ to give the oxidized Ru(III) fragment $\{RuCl_3(PPh_3)_2\}$ and the radical $\dot{C}Cl_3$. Further reaction of the $\dot{C}Cl_3$ radical with the alkene yields the radical $Ph\dot{C}HCH_2CCl_3$. Final elimination of the 1:1 adduct, with the abstraction of one chlorine atom from the oxidized form of the catalyst, recycles the active Ru(II) fragment. In addition, the reaction between complex **38** and $CCl_4$ in refluxing ethanol was shown to yield hexachloroethane and a paramagnetic material, most likely the oxidized ruthenium complex $[RuCl_3(PPh_3)_3]$.

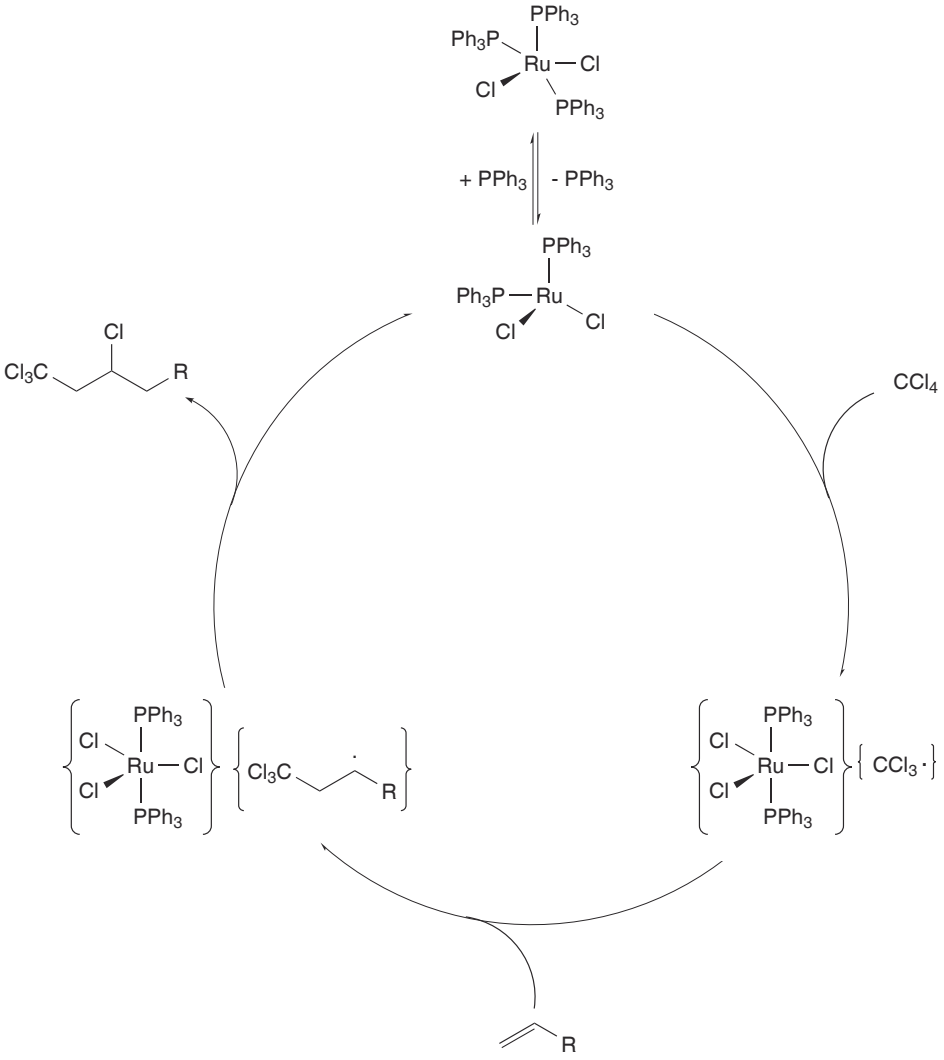


**Scheme 1.16:** Presumed catalytic cycle for the addition of $CCl_4$ to terminal olefins catalyzed by $[RuCl_2(PPh_3)_3]$ (**38**).

### 1.3.4 New organic reactions based on ATRA

The availability of efficient ATRA catalysts has enabled the development of new synthetically useful reactions. The bimolecular reaction was found to be possible using a wide range of polyhalogenated and olefinic substrates (Scheme 1.17). A major application of ATRA reactions, however, is the formation of cyclic compounds [65, 71, 72, 83–86]. Based on the observation that di- and trichloroacetic esters undergo additions reactions with 1-olefins [69,75,87], S. M. Weinreb and co-workers have developed an intramolecular variant, in which unsaturated dichloroesters cyclize in the presence of complex **38** [72, 86]. In the year 1990, the same group demonstrated that trichloromethylalkenes could likewise undergo a radical cyclization [71]. The concept was applied by K. Ito *et al.* for the construction of trichlorinated $\gamma$-lactams by cyclization of *N*-allyltrichloroacetamides [83–85, 88]. The lactams were then reduced into bicyclic pyrrolidines, which could be used as components of alkaloid or amino acid derivatives with potent physiological activities. Another remarkable application of ATRA in organic synthesis was the double cyclization of *N*-linalyl- and *N*-geranyltrichloroacetamides, catalyzed by complex **38** (Scheme 1.18) [83].

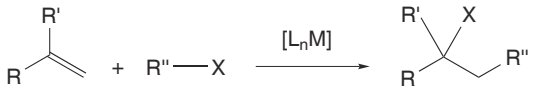


**Scheme 1.17:** Various polyhalogenated compounds can be added to olefins with the help of transition metal complexes [$L_nM$].

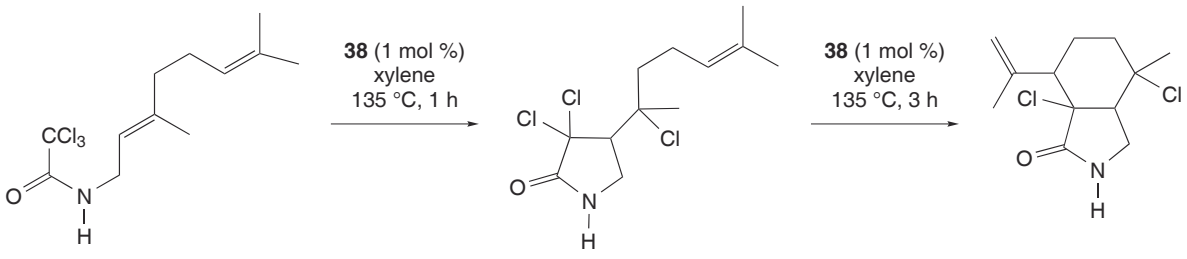


**Scheme 1.18:** Double cyclization of *N*-geranyltrichloroacetamide catalyzed by complex **38**.

So far, there are only few reports on enantioselective Kharasch additions [85, 89–92]. The complex $[Ru_2Cl_4((+/-)\text{-diop})_3]$ (**39**), for example, has been employed for the asymmetric addition of sulfonyl chlorides to styrene and derivatives, but the enantiomeric excess and the yields were relatively modest [90, 91].

### 1.3.5 From atom-transfer radical addition to controlled radical polymerization

Radical polymerization has long been—and still is—one of the most important methods for the synthesis of polymers. The reason for its success is mainly the convenient temperature range, which can be employed, and the minimal requirements for the purification of the monomers and solvents. Furthermore, the process displays a high tolerance to functional groups and a wide range of alkenes can be polymerized. The radical polymerization, however, suffers from a severe limitation when compared to an ionic polymerization process: The growing radical chains are electrically neutral and tend to react with each other, causing the annihilation of two radical centers at a time. This stops the growth of the polymers, resulting in a broad molecular weight distribution.

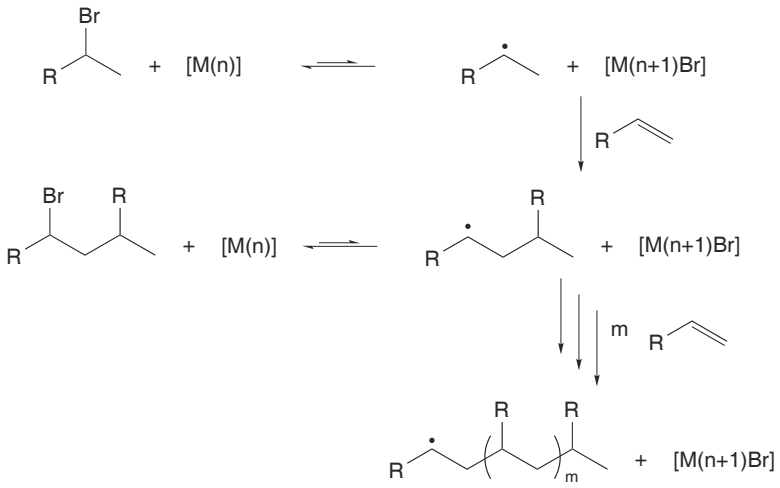


**Scheme 1.19:** Radical polymerization can be controlled by transition-metal redox systems.

M. Sawamoto [93] and K. Matyjaszewski [94] simultaneously and independently reported in the mid-1990s the first examples of radical polymerizations proceeding in a controlled fashion. The so-called atom-transfer radical polymerization (ATRP) can be seen as an extension of the original addition reaction, in which the polyhaloalkane is not used as a substrate, but as an initiator. In ATRP, a high olefin/polyhaloalkane ratio is thus employed (Scheme 1.19). Since the initiation is practically instantaneous with subsequent uniform propagation of the growing chains, the polymerization can proceed with a precise control of the chain lengths, resulting in a very narrow molecular weight distribution. The growing radical chain is in a dynamic equilibrium with its covalent counterpart. The latter is the so-called dormant species, which acts as a reservoir for the growing end. The dynamic equilibrium is on the side of the dormant species. As a

consequence, the concentration of the free radicals is much lower than in the conventional uncontrolled polymerization. The undesirable bimolecular termination reactions are thus less likely.

Many redox systems have found application in ATRP catalysis, among which the Cu(I)/Cu(II) pair plays a prominent role [95, 96]. The most efficient Ru-based catalysts are generated in-situ from $[(\text{arene})RuCl_2]_2$ and tricyclohexylphosphine (arene = cymene [97–100] or $C_6H_3{}^{i}Pr_3$ [101]).

### 1.3.6 New ruthenium catalysts for ATRA

For 25 years, modifications of ATRA catalysts by ligand variation were hardly investigated [102]. In the late 1990s, the interest in ruthenium catalyzed radical reactions grew, mainly because complex **38** was found to be a quite effective catalyst for the controlled polymerization of olefins (see above). In fact, most ruthenium catalysts, which were recently developed for atom-transfer radical polymerizations, are also able to catalyze the Kharasch reaction and vice versa. Another aspect, which has stimulated the field of ruthenium-catalyzed radical reactions, is the pronounced current interest in synthetic organometallic chemistry of ruthenium due to the tremendous success of alkylidene complexes in olefin metathesis reactions [103,104]. Again, several of the complexes which were initially used for metathesis reactions turned out to catalyze ATRP and ATRA reactions.

Since 1999, a number of new ruthenium catalysts, with in some cases significantly increased activity, were reported[7]. These recent contributions are summarized in the following paragraphs.

**Figure 1.3**

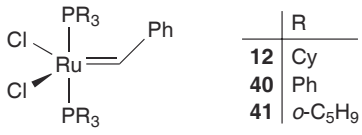


| | R |
|---|---|
| **12** | Cy |
| **40** | Ph |
| **41** | *o*-$C_5H_9$ |

**1999:** Two research groups independently reported a new reactivity of the complex $[RuCl_2(CHPh)(PCy_3)_2]$ (**12**). Investigating olefin metathesis reactions with ruthenium catalysts, M. L. Snapper *et al.* unexpectedly isolated a product derived not from olefin metathesis but from a metal-catalyzed addition of $CHCl_3$ to the alkene. Further investigations revealed that complex **12** can act as an efficient catalyst for the Kharasch addition of

7. For reviews see [105, 106].

$CHCl_3$ [107]. While temperatures of around 120 °C had usually been required to perform this reaction with catalyst **38**, the use of complex **12** enables the Kharasch addition of $CHCl_3$ across various olefins at a temperature as low as 65 °C. Complex **12** still ranges among the best ruthenium catalysts for the addition of $CHCl_3$ to olefins. In parallel, A. Demonceau and coworkers reported the ability of complex **12** and the related compounds **40** and **41** (Figure 1.3) to catalyze the Kharasch addition of $CCl_4$ and to promote the ATRP of vinyl monomers [108].

**2000:** With the catalysts **38** and **12**, the formation of unsaturated 14-electron ruthenium species (through phosphine dissociation) takes place prior to halocarbon activation [81,82,107]. It was therefore expected that well-defined 14-electron complexes would give a direct access to these catalytic species. The group of A. Demonceau investigated the catalytic activity of the complexes **42**, **43**, and **44**, which bear one or two *nido*-diphosphinocarborane ligands of the formula [7,8-$(PPh_2)_2$-7,8-$C_2B_9H_{10}$]$^-$ (Figure 1.4) [109]. For these complexes, the steric crowding of the bulky tertiary phosphines forces agostic interactions between C–H bonds and the metal cations, thus preventing dimerization or solvent coordination. Among them, the hydride complex **42** gave the best results with activities, which compare favorable with that of complex **38** for reactions with $CCl_4$. In the same year, they reported on the ATRA activity of half-sandwich complexes of the general formula [Cp*RuCl$(PR_3)_2$]. For the addition of $CCl_4$ and $CHCl_3$ to olefins, complex [Cp*RuCl$(PPh_3)_2$] (**45**) turned out to be superior to all catalysts known at that time [110]. Variation of the ligand led to reduced activity: Upon substitution of the $PPh_3$ ligands of **45** with either *tris*(4-trifluoromethylphenyl)phosphine (**46**) or *tris*(4-methoxyphenyl)phosphine (**47**), the yields dropped significantly.

**Figure 1.4**

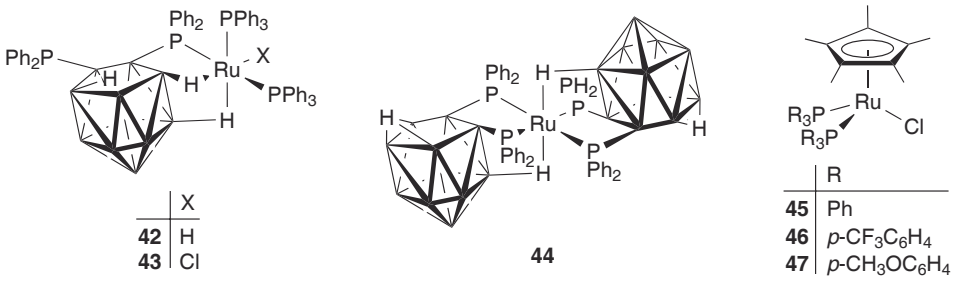


**2001:** In addition to {Cp*Ru} complexes, the isoelectronic complexes **48** and **49**[8]

8. These complexes were reported one year before by M. Sawamoto *et al.* to catalyze living radical

(Figure 1.5) were shown to display good to excellent ATRA activity [112]. For all the reactions investigated, the {CpRu} complex **48** gave lower yields than complexes **45** and **49**. The latter, however, are among the most active catalysts for the addition of $CCl_4$ and $CHCl_3$ to olefins described so far. Complex **45** allows the Kharasch addition of $CCl_4$ to olefins to be carried out at ambient temperature, a property shared by only a few catalysts[9].

F. Verpoort *et al.* reported the synthesis and the catalytic activity of half-sandwich ruthenium(II) complexes, which contain neither phosphine nor *N*-heterocyclic carbene (NHC) ligands but bidentate Schiff base ligands (**50**) [114]. The advantage of using Schiff base ligands is that their steric and electronic properties can be modified easily.

**Figure 1.5**

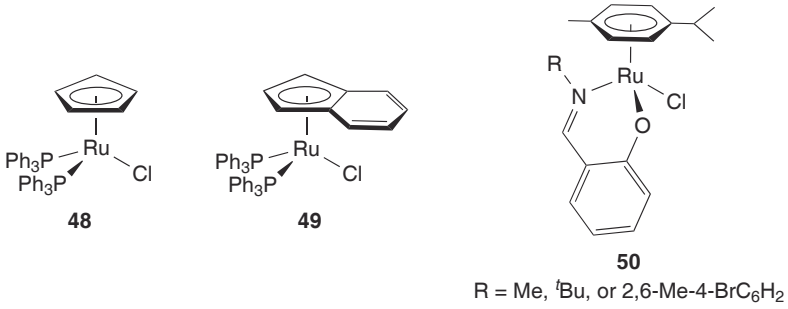


**2002:** The group of Verpoort also developed various other ruthenium complexes, which were used as ATRA catalysts. The vinylidene complexes **51** and **52** [115] and the mixed carbene complexes **53** [116] (Figure 1.6) were found to be particularly active. One of the latter was even able to compete the highly active catalyst **45**.

**2003:** Half-sandwich ruthenium complexes with anionic $\eta^5$-carboranyl (Dcb) ligands (**54**) (Figure 1.7) were tested by the group of A. Demonceau *et al.* [117, 118]. These complexes can be regarded as analogues of the catalyst **45**, in which the chloro ligand is replaced by a hydrido ligand and the Cp$^\star$ ligand by a Dcb ligand. The advantage of the Dcb ligands is that they offer numerous sites for substitution. After testing complexes with different ligands of the general formula 10-$R^1R^2$S-7-R-7,8-$C_2B_9H_{10}$, the candidate with R = H, $R^1$ = Et, and $R^2$ = Ph was found to show an outstanding activity for

polymerizations [111].

9. Unless the very reactive substrate $CBrCl_3$ is employed [113], the only catalyst, which has been reported to allow Kharasch reactions at room temperature, is a bimetallic ruthenium ethylene complex, which will be introduced and discussed in Subsection 2.5.3.

**Figure 1.6**

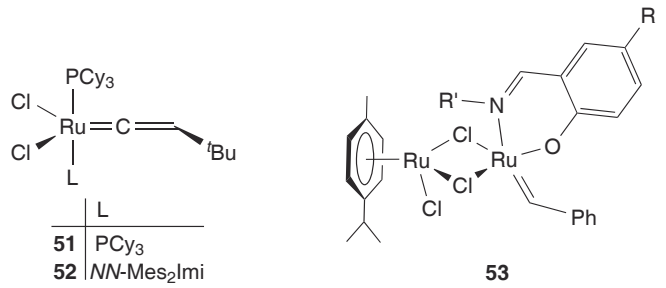


the Kharasch addition of $CCl_4$ under mild conditions. At 40 °C, total turnover numbers (TONs) of 4200 and 9000 and initial turnover frequencies (TOFs) of 1880 and 1500 $h^{-1}$ were obtained for reactions with methyl methacrylate and styrene, respectively. These values are the highest ever reported for a ruthenium catalyzed Kharasch reaction. Despite their exceptional performances in addition reactions with $CCl_4$, complexes **54** were found to be rather poor catalysts for the addition of $CHCl_3$ to olefins [118].

The same group also described a half-sandwich complex with a *N*-heterocyclic (NHC) ligand (**55**), which was active for the ATRA of $CCl_4$ to styrene [119][10]. A precise control of the steric and electronic properties of the NHC ligand, however, was necessary to observe catalytic activity. When the chloro atoms in complex **55** were substituted with hydrogen atoms, for example, the catalytic activity was strongly decreased.

Two new classes of ATRA catalysts were synthesized by F. Verpoort *et al.*: the carbene complexes with Schiff base and phosphine/NHC ligands **56** [120] and the indenylidene complexes **57** and **58** [121]. The latter have the advantage to be synthetically easy to access. The {Cp*Ru(II)} amidinate complexes **59** and **60** were shown by H. Nagashima *et al.* to be able to catalyze the atom-transfer radical cyclization of *N*-allyltrichloroacetamides under mild conditions [122]. The reactions were performed at room temperature, which is clearly superior to the 140 °C required for catalyst **38** [83–85, 88].

10. The corresponding $PCy_3$ complex [(cymene)$RuCl_2(PCy_3)$] (**14**) was found to be inactive for this transformation [108], but proved to be very efficient in ATRP [97–100].

**Figure 1.7**

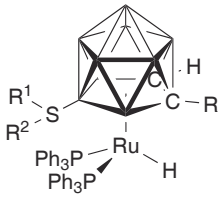

**54**

R = H or Me
$R^1$, $R^2$ = Me, Et, Ph, or $(CH_2)_2$

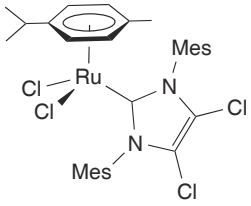

**55**

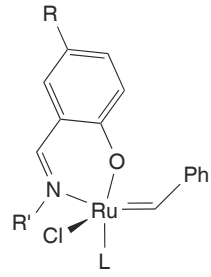

**56**

L = $PCy_3$ or *NN*-$Me_2H_2Imi$
R = H or $NO_2$
R' = Me, 2,6-Me-4-$BrC_6H_2$, or 2,6-$^i$Pr$C_6H_3$

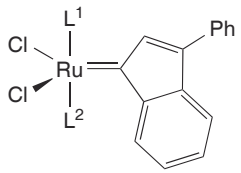

**57**

$L^1$ = $PPh_3$ or $PCy_3$
$L^2$ = $PCy_3$, $PCy_3$, or *NN*-$Mes_2H_2Imi$

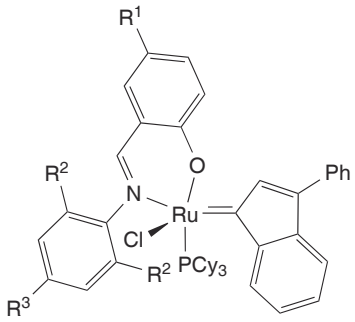

**58**

$R^1$ = H or $NO_2$
$R^2$ = $^i$Pr or Me
$R^3$ = H or Br

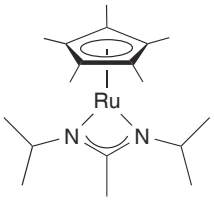

**59**

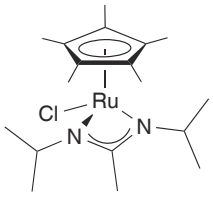

**60**

# Chapter 2

# Results and Discussion

## 2.1 Synthesis and Structure of Bimetallic Complexes of the General Formula [LM(μ-Cl)$_3$RuCl(PPh$_3$)$_2$] (LM = (arene)Ru or Cp*Rh)[1]

In a previous publication [26], K. Severin and co-workers reported that the reaction of the complex [(PPh$_3$)$_2$ClRu(μ-Cl)$_3$Ru(PPh$_3$)$_2$(acetone)] (**21**) with an equimolar amount of a half-sandwich chloro complex, in dichloromethane, quantitatively affords complexes of the general formula [LM(μ-Cl)$_3$RuCl(PPh$_3$)$_2$] (LM = (arene)Ru or Cp*Rh) (see Introduction, Scheme 1.6, p. 8). For the Oppenauer type oxidation, these homo- and heterobimetallic complexes displayed superior activities than the commonly employed catalyst [RuCl$_2$(PPh$_3$)$_3$] (**38**) (see Introduction, Subsection 1.1.2). However, only three complexes of this family were synthesized and assayed and no structural characterization was achieved. For a combinatorial approach, the first requirement was to increase the number of candidates.

We followed a similar procedure to synthesize the complexes [(cymene)Ru(μ-Cl)$_3$RuCl(PPh$_3$)$_2$] (**24**), [(C$_3$H$_3$Me$_3$)Ru(μ-Cl)$_3$RuCl(PPh$_3$)$_2$] (**61**), [(C$_6$H$_3$Et$_3$)Ru(μ-Cl)$_3$RuCl(PPh$_3$)$_2$] (**62**), [(C$_6$H$_3$$^i$Pr$_3$)Ru(μ-Cl)$_3$RuCl(PPh$_3$)$_2$] (**63**), [(C$_6$Me$_6$)Ru(μ-Cl)$_3$RuCl(PPh$_3$)$_2$] (**64**), and [Cp*Rh(μ-Cl)$_3$RuCl(PPh$_3$)$_2$] (**26**), which were rapidly obtained in high yields (Scheme 2.1). All complexes were characterized by $^1$H, $^{13}$C, and $^{31}$P NMR spectroscopy. In addition, single crystal X-ray analyses of the complexes **24**, **62**, **63**, **64**, and **26** were performed (Figure 2.1, for structural data see Table 2.1).

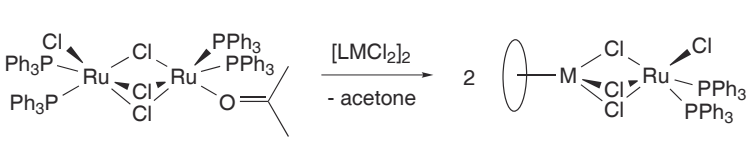


| | (π-ligand)M |
|---|---|
| **24** | (cymene)Ru |
| **61** | (C$_6$H$_3$Me$_3$)Ru |
| **62** | (C$_6$H$_3$Et$_3$)Ru |
| **63** | (C$_3$H$_3$$^i$Pr$_3$)Ru |
| **64** | (C$_6$Me$_6$)Ru |
| **26** | Cp*Rh |

**Scheme 2.1:** Synthesis of homo- and heterobimetallic complexes with the {RuCl$_2$(PPh$_3$)$_2$} fragment.

In the five complexes, the {LM} fragment is coordinated via three chloro-bridges to the Ru-phosphine fragment. The Ru–Cl bond lengths of the terminal chloro ligands (2.363(3) – 2.3890(14) Å) are shorter than those found for the bridging chloro ligands (2.395(3) – 2.5334(14) Å), which is consistent with what was reported for similar complexes having a

1. Part of the work described in this section has been published, see ref. [23].

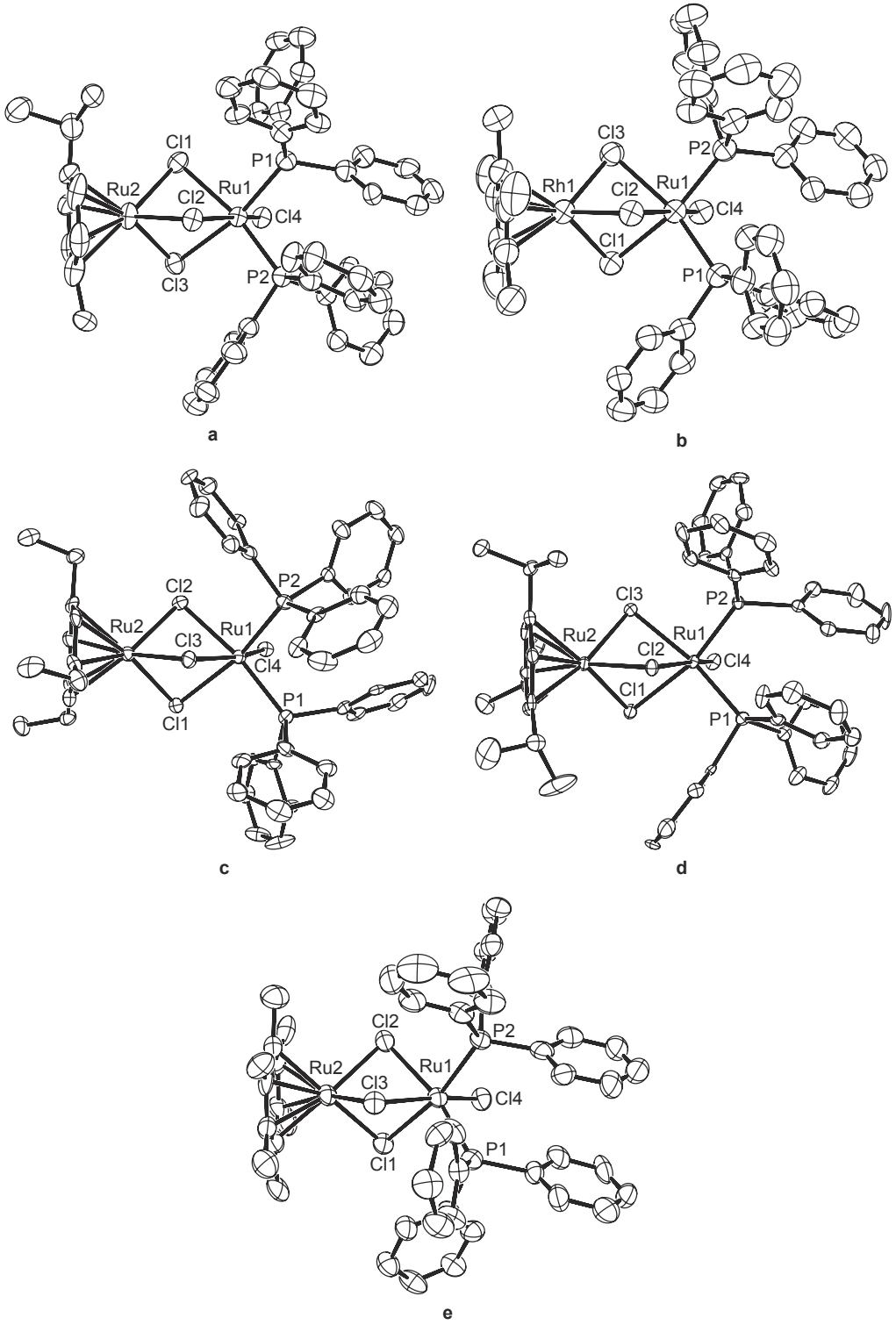


**Figure 2.1:** ORTEP drawings of the molecular structure of **24** (a), **26** (b), **62** (c), **63** (d) and **64** (e). The hydrogen atoms and solvent molecules are not shown for clarity.

dppb (2.387(2) and 2.407(2) – 2.534(2) Å) or a cod (2.388(1) and 2.422(1) – 2.485(1) Å) bidentate ligand instead of the two $PPh_3$ ligands [26]. As expected, the angles between the sterically demanding $PPh_3$ groups and the ruthenium atoms are enlarged (P–Ru–P =

97.31(9) – 103.71(16) °), which results in a distorted octahedral geometry around the Ru atoms. The plane defined by the Cp* or arene ligand is almost parallel to that defined by the bridging chloro ligands. The Ru–Cl and Ru–P distances in the mixed complexes are very similar to what was observed for the starting material **21** [26].

**Table 2.1:** Selected bond lengths (Å) and angles (°) for **24**, **26**, and **62** – **64**.

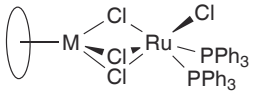


| Complex | Ru/M–Cl$^{b[a]}$ | Ru–Cl$^{t}$ | Ru–P$^{[a]}$ | P–Ru–P' | P–Ru–Cl$^{t[a]}$ | M···Ru |
|---|---|---|---|---|---|---|
| **24** | 2.49 | 2.364(3) | 2.29 | 98.90(12) | 91.68 | 3.330 |
| **26** | 2.48 | 2.3752(16) | 2.29 | 103.71(6) | 90.81 | 3.232 |
| **62** | 2.49 | 2.382(3) | 2.30 | 97.31(9) | 93.40 | 3.320 |
| **63** | 2.50 | 2.3890(14) | 2.28 | 99.49(5) | 91.45 | 3.360 |
| **64** | 2.48 | 2.363(3) | 2.27 | 99.75(11) | 93.67 | 3.291 |

[a] Average values; $b$ = bridging, $t$ = terminal.

Interestingly, these complexes react with chloroform: A solution of complex **24** in chloroform, for example, to which pentane was slowly added by diffusion over several weeks, led to the formation of dark red crystals of the mixed valence complex [(cymene)Ru(μ-Cl)$_3$RuCl$_2$(PPh$_3$)] (**65**) (Scheme 2.2), which was structurally characterized (Figure 2.2).

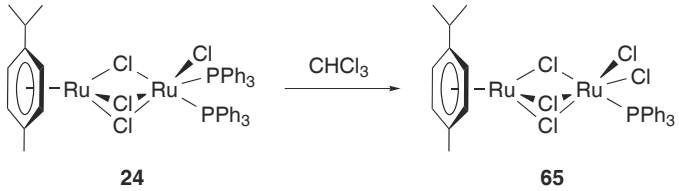


**24** **65**

**Scheme 2.2:** Oxidation of complex **24** in presence of $CHCl_3$.

In the Ru(II)-Ru(III) complex **65**, the Ru–Cl bond lengths of the terminal chloro ligands were found to be slightly shorter (2.2964(18) and 2.3169(16) Å) than those of the non oxidized M-Ru(II) complexes (2.363(3) – 2.3890(14) Å). This highlights stronger electrostatic interactions between the negatively charged chloro ligands and the Ru(III) cation. The Ru–P bond length, on the other hand, remained almost unchanged.

The loss of a triphenylphosphine ligand, followed by the abstraction of a chlorine atom from the polychlorocarbon, can be regarded as the first step of the catalytic cycle of a

Kharasch addition catalyzed by complex **24** (see Introduction, Scheme 1.16, p. 18). This observation reinforced our expectations to find efficient catalysts within this particular family of bimetallic complexes.

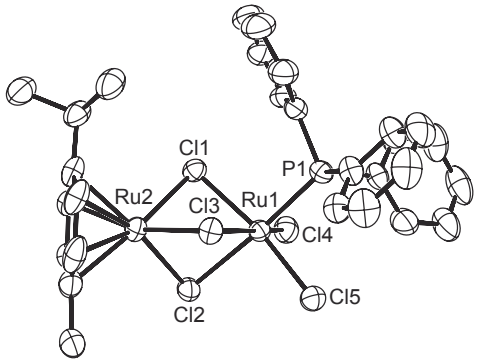


**Figure 2.2:** ORTEP drawing of the molecular structure of **65**. The hydrogen atoms and solvent molecules are not shown for clarity. Selected bond lengths (Å) and angles (°): Ru1–$Cl^{b[a]}$ 2.46, Ru1–$Cl^{t[a]}$ 2.30, Ru1–P1 2.2807(16); Cl–Ru1–$P1^{[a]}$ 90.19, Cl4–Ru1–Cl5 94.79; [a] Average values; $b$ = bridging, $t$ = terminal.

## 2.2 Combinatorial Catalysis with Bimetallic Complexes: Robust and Efficient Catalysts for Atom-Transfer Radical Additions[2]

### 2.2.1 Screening of a library of bimetallic ATRA catalysts

In addition to the complexes of the general formula $[LM(\mu\text{-}Cl)_3RuCl_2(PPh_3)_2]$, we have found that structurally related complexes with chelating 1,4-*bis*(diphenylphosphino)butane (dppb) or 1,4-*bis*(dicyclohexylphosphino)butane (dcypb) ligands instead of the two $PPh_3$ ligands can be synthesized using the aqua complex $[(dppb)ClRu(\mu\text{-}Cl)_2(\mu\text{-}OH_2)\text{-}RuCl(dppb)]$ (**66**) [124] or the dinitrogen complex $[(dcypb)(N_2)Ru(\mu\text{-}Cl)_3RuCl(dcypb)]$ (**67**) [125] instead of the acetone complex **21** (Scheme 2.3).

**Scheme 2.3**

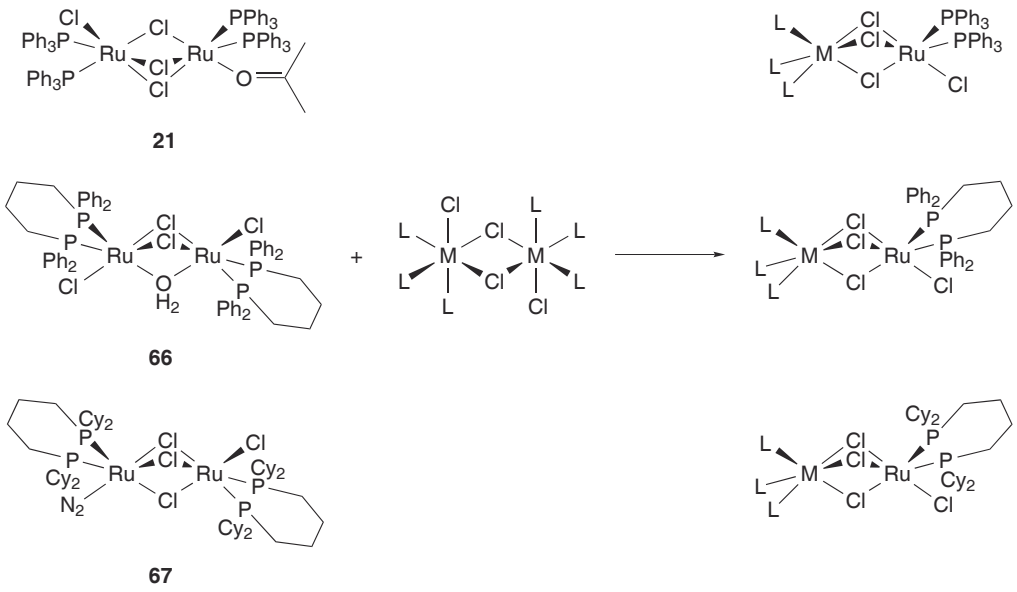


In order to investigate whether compounds of this type can be useful catalyst precursors for ATRA reactions, we have tested 69 different combinations in a parallel fashion. Assuming that reactions similar to those depicted in Scheme 2.3 would occur with other chloro-bridged complexes of the late transition metals, we have prepared mixtures of **21**, **66**, or **67** with various dimeric $[L_nM(\mu\text{-}Cl)]_2$ complexes of Ru(II), Ru(III), Ru(IV), Rh(I), Rh(III), Ir(I), Ir(III), Pd(II), and Pt(II) (Figure 2.3). For several combinations it is likely that doubly bridged, instead of triply bridged, complexes $M(\mu\text{-}Cl)_2Ru$ are formed[3].

2. Part of the work described in this section has been published, see ref. [123].

3. The structure of the complexes, which could be obtained by reaction of complex **21** and chloro com-

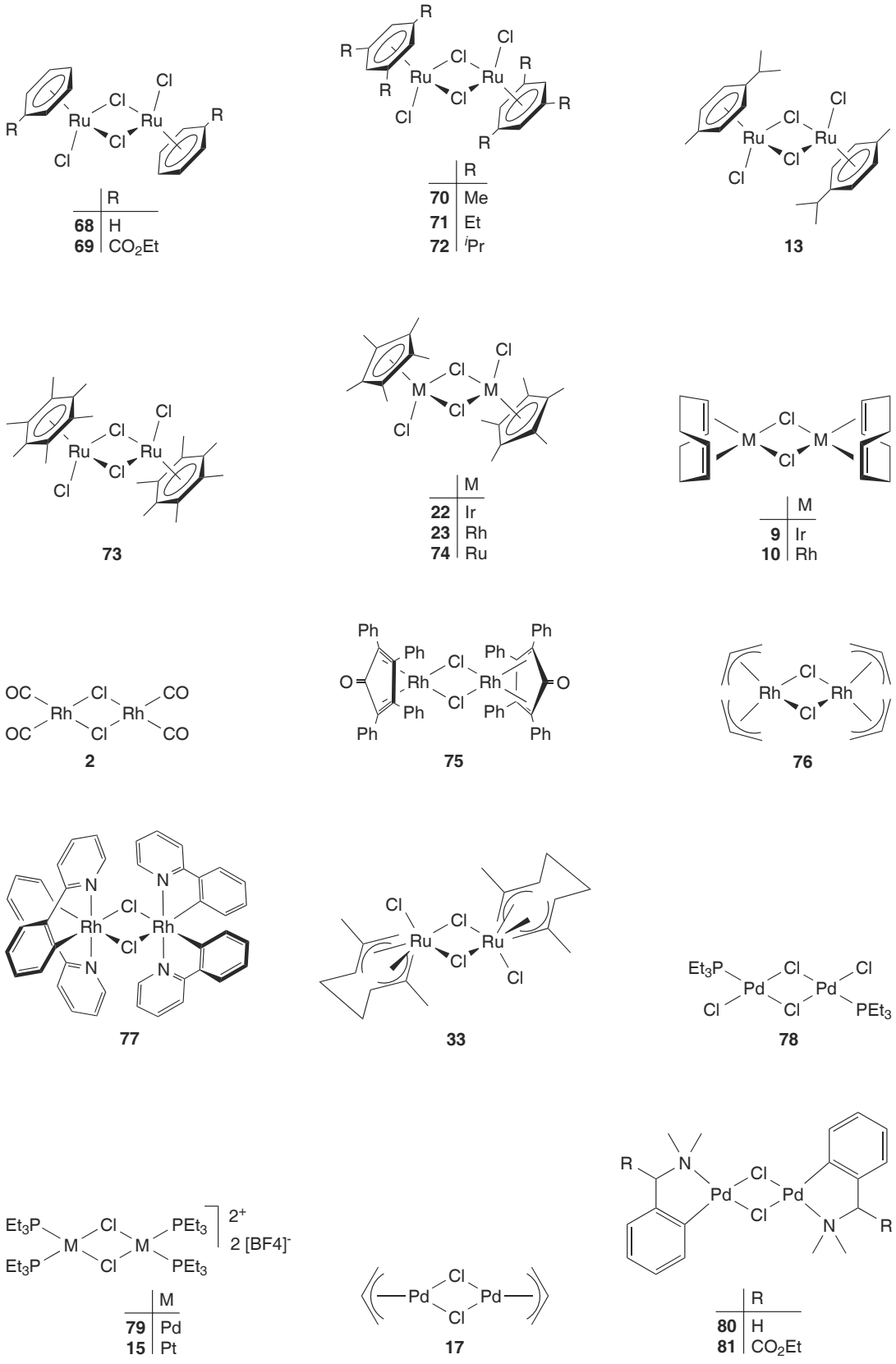


**Figure 2.3:** List of the 23 bimetallic complexes, which were combined with **21**, **66**, and **67** in the screening experiment.

plexes of square planar transition metal ions, will be discussed in Section 2.7.

The reactions were carried out simultaneously on a small scale and the resulting products were immediately tested in a parallel fashion for catalytic activity without purification. The chloro-bridged complexes $[L_nM(\mu\text{-Cl})]_2$ were added in excess (Ru/M = 1:2) to enforce the formation of the mixed complexes. As a benchmark reaction we have employed the addition of $CCl_4$ to styrene, which was analyzed by gas chromatography using an autosampler (Figure 2.4).

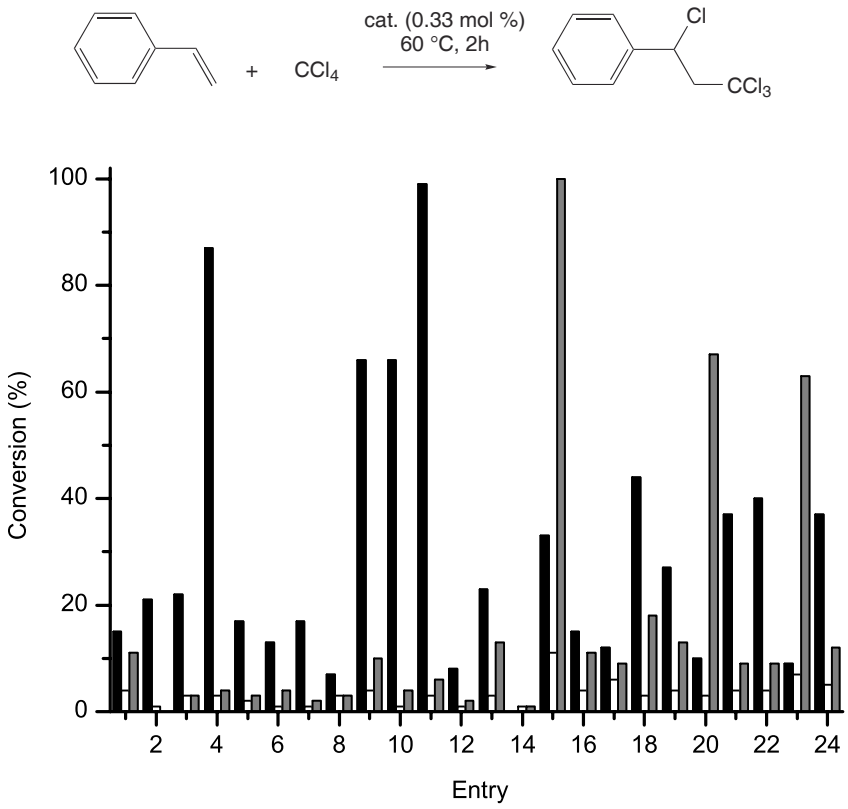


**Figure 2.4:** Parallel screening of catalyst activity using the addition of $CCl_4$ to styrene as a benchmark reaction. The catalysts were prepared in situ by mixing complex **21** (black), **66** (white), or **67** (grey) with: 1) no additional complex, 2) **69**, 3) **68**, 4) **70**, 5) **71**, 6) **13**, 7) **73**, 8) **72**, 9) **74**, 10) **22**, 11) **23**, 12) **9**, 13) **10**, 14) **2**, 15) **75**, 16) **76**, 17) **77**, 18) **33**, 19) **78**, 20) **79**, 21) **17**, 22) **80**, 23) **15**, 24) **81**. Reaction conditions: **21**, **66**, or **67**/additional complex/styrene/$CCl_4$ = 0.5:1:300:432, [**21**, **66**, or **67**] = 2.3 mM, solvent = chloroform, reaction volume = 1 mL, $T$ = 60 °C. The conversion after 2 hours is based on the consumption of styrene as determined by gas chromatography.

For reactions with the $\{RuCl_2(PPh_3)_2\}$ complex **21**, several of the in-situ generated homo- and heterobimetallic complexes display a substantial catalytic activity (Figure 2.4, black bars). The highest activity is observed for reactions with a mixture of **21** and the

Rh(III) complex $[Cp^{\star}RhCl_2]_2$ (**23**) (Figure 2.4, Entry 11a; a = black, b = white, c = grey). The Rh(I) complex $[RhCl(CO)_2]_2$ (**2**), on the other hand, seems to inhibit the reaction completely (Entry 14a). For mixtures containing the $\{RuCl_2(dppb)\}$ complex **66** (white bars), consistently low conversions were observed (1 – 11 %). This pointed to an intrinsic advantage of two monodentate $PPh_3$ ligands as compared to a chelating dppb co-ligand. Similarly, reactions with the $\{RuCl_2(dcypb)\}$ complex **67** gave low or moderate conversions with three notable exceptions: For mixtures with the cationic complexes $[PdCl(PEt_3)_2]_2(BF_4)_2$ (**79**) (Entry 20c) and $[PtCl(PEt_3)_2]_2(BF_4)_2$ (**15**) (Entry 23c) conversions of 67 % and 63 % were observed whereas a quantitative conversion was found for mixtures with the Rh(I) complex $[RhCl(tpc)]_2$ (**75**) (Entry 15c).

In a second set of experiments, we have tested the catalytic activity of all symmetrical complexes $[L_nM(\mu\text{-}Cl)]_2$ without the addition of the ruthenium complexes **21**, **66**, or **67**. None of the complexes displayed any significant activity (conversion $< 1$ %). This indicates that the ruthenium-phosphine fragments are responsible for catalysis. The overall activity, however, is clearly modulated by the second metal fragment $\{L_nMCl\}$.

From the parallel screening, two promising catalyst precursors emerged. The first is formed by reaction of **21** with $[Cp^{\star}RhCl_2]_2$ (**23**) and the second is formed by reaction of **67** with $[RhCl(tpc)]_2$ (**75**). The synthesis and the characterization of the first one has been described in the previous section. For the second catalyst, the reaction was repeated on a preparative scale, from which we were able to isolate the heterometallic complex $[\{(tpc)Rh(\mu\text{-}Cl)_3Ru(dcypb)\}_2(\mu\text{-}N_2)]$ (**82**), which was characterized by single crystal X-ray analysis (Figure 2.5).

Similar to what was found for the complexes **24**, **62**, **63**, **64**, and **26**, the $\{(tpc)Rh\}$ fragment in **82** is coordinated through three chloro-bridges to the Ru-phosphine fragment. Consequently, the Rh center exhibits a five-coordinate, electronically saturated configuration. This is in agreement with the known tendency of cyclopentadienone-rhodium complexes to form piano-stool-type complexes [126–128]. The ruthenium atom shows a distorted octahedral geometry with one coordination site being occupied by a dinitrogen ligand. The latter acts as an end-on bridging ligand that connects two heterobimetallic Rh(I)-Ru(II) complexes. The bond lengths and angles found for the $Ru(\mu^2\text{-}N_2)Ru$ moiety are comparable to those observed for other ruthenium complexes with bridging $N_2$ ligands [129–133].

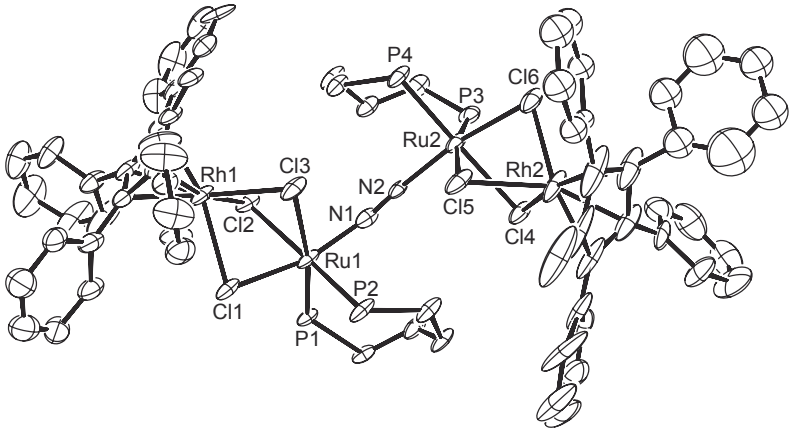


**Figure 2.5:** ORTEP drawing of the molecular structure of **82** in the crystal. The hydrogen atoms, the cyclohexyl side chains, and the solvent molecules are not shown for clarity. Selected bond lengths (Å) and angles ( $^\circ$ ): Ru1–N1 1.963(10), Ru2–N2 1.985(9), N1–N2 1.118(12), Ru–$Cl^{b[a]}$ 2.47, Ru–$P^{[a]}$ 2.33; P1–Ru1–P2 93.53(9), P3–Ru2–P4 94.14(11), P–Ru–$N^{[a]}$ 94.8, N2–N1–Ru1 164.6(8), N1–N2–Ru2 164.2(8); [a] Average values; $b$ = bridging.

### 2.2.2 Scope and limitation of the new catalysts

With the isolated complexes **26** and **82**, we have carried out a more detailed analysis of the catalytic performance using again the benchmark reaction between styrene and $CCl_4$. In addition to chloroform, toluene was employed as a solvent. The results are summarized in Table 2.2.

**Table 2.2:** Addition of $CCl_4$ to styrene, catalyzed by the complexes [Cp*Rh($\mu$-Cl)$_3$RuCl-($PPh_3$)$_2$] (**26**), [{(tpc)Rh($\mu$-Cl)$_3$Ru(dcypb)}$_2$($\mu$-$N_2$)] (**82**), [$RuCl_2(PPh_3)_3$] (**38**), or [Cp*Ru-Cl($PPh_3$)$_2$] (**45**), in different solvents.[a]

| Entry | Catalyst | Solvent | Conv. (%) | |
|---|---|---|---|---|
| | | | a. dry | b. wet[b] |
| 1 | **26** | toluene | 23 | 36 |
| 2 | **26** | chloroform | 20 | 37 |
| 3 | **82** | toluene | 78 | 76 |
| 4 | **82** | chloroform | 94 | 96 |
| 5 | **38** | toluene | 28 | 15 |
| 6 | **38** | chloroform | 14 | 7 |
| 7 | **45** | toluene | 48 | 44 |
| 8 | **45** | chloroform | 51 | 29 |

[a] Reaction conditions: cat./styrene/$CCl_4$ = 1:300:432, [cat.] = 4.6 mM, reaction volume = 1 mL, $T = 60\,^{\circ}$C. [b] solvent saturated with $H_2O$. The conversion after 1 hour is based on the consumption of styrene as determined by GC.

After 1 h reaction, with toluene as the solvent, the Rh(I)-Ru(II) complex **82** was found to display a very high activity surpassing not only that of the Rh(III)-Ru(II) complex **26**, but also that of the previously described catalyst precursors [$RuCl_2(PPh_3)_3$] (**38**) and [Cp*RuCl($PPh_3$)$_2$] (**45**) (Entries 1a, 3a, 5a, and 7a). When the solvent was changed to chloroform, the activity of catalyst **82** was even higher. A surprising discovery was that for catalyst **26**, reactions performed in "wet" chloroform and toluene gave better results than those performed in thoroughly dried solvents (Entries 1 and 2). For the catalyst **82**, the presence of water did not affect the catalytic activity (Entries 3 and 4). This is in sharp contrast to the reactions catalyzed by [$RuCl_2(PPh_3)_3$] (**38**) or by the very sensitive [Cp*RuCl($PPh_3$)$_2$] (**45**) [134], for which traces of water were found to reduce the catalytic activity significantly (Entries 5 – 8).

Next, we investigated the influence of the $CCl_4$ concentration on the activity of the new catalysts using "wet" chloroform as the solvent (Table 2.3). As expected, higher $CCl_4$ concentration resulted in faster reaction rates. The two complexes were found to tolerate four equivalents of $CCl_4$, with regard to the substrate, which corresponds to a concentration of about 5.5 M (cat./substrate/$CCl_4$ = 1:300:1200).

**Table 2.3:** Addition of $CCl_4$ to styrene, catalyzed by the complexes [Cp*Rh($\mu$-Cl)$_3$RuCl-($PPh_3$)$_2$] (**26**) or [{(tpc)Rh($\mu$-Cl)$_3$Ru(dcypb)}$_2$($\mu$-$N_2$)] (**82**), with different concentrations of $CCl_4$.[a]

| Entry | Styrene/$CCl_4$ | Conv. (%) | |
|---|---|---|---|
| | | a. Cat. = **26** | b. Cat. = **82** |
| 1 | 1:1 | 33 | 86 |
| 2 | 1:2 | 53 | 96 |
| 3 | 1:3 | 66 | 97 |
| 4 | 1:4 | 73 | 99 |

[a] Reaction conditions: cat./styrene = 1:300, [cat.] = 4.6 mM, solvent = $CHCl_3$ saturated with $H_2O$, reaction volume = 1 mL, $T = 60\,^{\circ}$C. The conversion after 1 hour is based on the consumption of styrene as determined by GC.

Using these optimized conditions, the scope of the new heterobimetallic catalyst precursors **26** and **82** was tested in reactions with various olefinic substrates (Table 2.4). For styrene and methyl acrylates, a nearly total conversion of the substrate was observed after only 1 h for catalyst **82** and after 4 h for catalyst **26** (Entries 1 – 6). The yields were slightly lower than the conversions due to the formation of oligomers, a problem generally encountered for these types of addition reactions. Longer reaction times were required for 1-octene and 1-decene, two notoriously bad substrates for Kharasch reactions. It is interesting to note that for these substrates it is the Rh(III)-Ru(II) complex **26** that gives the best results: After 10 h, a yield of 88 and 90 %, respectively, was found together with a nearly quantitative conversion (Entry 7 and 9). These values are clearly superior to what was observed for other catalysts precursors. With [Cp*RuCl($PPh_3$)$_2$] (**45**), for example, a yield of 27 % and a conversion of 46 % was observed after 24 h under nearly identical conditions [110, 112].

The potential of the catalyst precursor **82** is further underlined by the high turnover frequencies and numbers, which can be achieved. For the addition of $CCl_4$ to styrene, for

**Table 2.4:** Atom-transfer radical additions, catalyzed by the heterobimetallic complexes [Cp*-Rh($\mu$-Cl)$_3$RuCl(PPh$_3$)$_2$] (**26**) and [{(tpc)Rh($\mu$-Cl)$_3$Ru(dcypb)}$_2$($\mu$-N$_2$)] (**82**).[a]

| Entry | Cat. | Substrate | Product | $t$ (h) | Conv./Yield (%) |
|---|---|---|---|---|---|
| 1 | **26** |  | 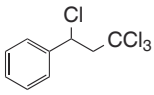 | 4 | 88/86 |
| 2 | **82** | | | 1 | 99/98 |
| 3 | **26** |  | 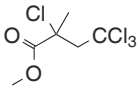 | 4 | 99/84 |
| 4 | **82** | | | 1 | 98/93 |
| 5 | **26** |  | 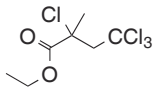 | 4 | 99/79 |
| 6 | **82** | | | 1 | 98/92 |
| 7 | **26** | 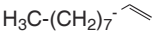 | 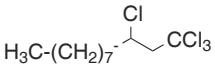 | 10 | 97/88 |
| 8 | **82** | | | 24 | 80/75 |
| 9 | **26** | 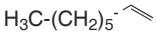 | 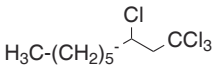 | 10 | 98/90 |
| 10 | **82** | | | 24 | 80/74 |

[a] Reaction conditions: cat./styrene/$CCl_4$ = 1:300:1200, [cat.] = 4.6 mM, solvent = $CDCl_3$ saturated with $D_2O$, reaction volume = 1 ml, $T$ = 60 °C. The conversion is based on the consumption of the substrate and the yield is based on the formation of product as determined by GC or by $^1$H NMR spectroscopy.

example, an initial TOF of 1200 h$^{-1}$ [4] and a total TON of 4500[5] was determined. These are among the highest values that have been reported for an ATRA catalyst. To the best of our knowledge, there is only one catalyst for which slightly higher values have been reported (TOF = 1500 h$^{-1}$ and TON = 9000 for the addition of $CCl_4$ to styrene; see ref. [117,118]). The unique tetrameric structure of **82** points to a possible explanation of its exceptionally high catalytic activity: As for the starting material [(dcypb)($N_2$)Ru($\mu$-Cl)$_3$RuCl(dcypb)] (**67**), the dinitrogen ligand is expected to be labile. Upon liberation

4. A yield of 20 % was measured after 30 min with the reaction conditions: **82**/styrene/$CCl_4$ = 1:3000:12000, [**82**] = 0.46 mM, solvent = $CDCl_3$ saturated with $D_2O$, reaction volume = 1 mL, $T$ = 60 °C.

5. A yield of 75 % was measured after 3 weeks with the reaction conditions: **82**/styrene/$CCl_4$ = 1:6000:12000, [**82**] = 0.23 mM, solvent = $CDCl_3$ saturated with $D_2O$, reaction volume = 1 mL, $T$ = 60 °C.

of this ligand, an unsaturated 16-electron ruthenium complex would be generated, which is then stabilized by the sterically demanding {(tpc)Rh} fragment and the large dcypb ligand. For complex **26**, the mode of activation is less evident. A plausible mechanism involves the cleavage of one or several chloro-bridges, as it was mentioned for a chloro-bridged Rh(III)-Ru(II) metathesis catalyst [21], but the decomposition of the complex [(cymene)Ru($\mu$-Cl)$_3$RuCl(PPh$_3$)$_2$] (**24**) in CHCl$_3$ suggests a loss of one PPh$_3$ ligand as the initial activation for this type of complexes (Scheme 2.2, p. 31). It is clear, however, that both the {Cp*Rh(III)} and the {Ru(II)(PPh$_3$)$_2$} fragments are essential constituents of this new catalyst.

We finally wanted to establish whether our bimetallic catalysts would also display high catalytic activity for the addition of the notoriously more difficult substrate CHCl$_3$. The addition reactions of chloroform to styrene were performed at a temperature of 60 °C, with 0.33 mol % of the respective catalyst. For comparison, the known catalysts **38**, **12**, and **45** were tested in parallel under the same reaction conditions (Table 2.5).

**Table 2.5:** Addition of chloroform to styrene, catalyzed by the complexes [Cp*Rh($\mu$-Cl)$_3$RuCl(PPh$_3$)$_2$] (**26**), [{(tpc)Rh($\mu$-Cl)$_3$Ru(dcypb)}$_2$($\mu$-N$_2$)] (**82**), [RuCl$_2$(PPh$_3$)$_3$] (**38**), [RuCl$_2$(CHPh)(PCy$_3$)$_2$] (**12**), and [Cp*RuCl(PPh$_3$)$_2$] (**45**).[a]

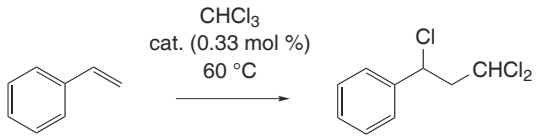


| Entry | Catalyst | Conv. (%) |
|---|---|---|
| 1 | **26** | 9 |
| 2 | **82** | 20 |
| 3 | **38** | 2 |
| 4 | **12** | 50 |
| 5 | **45** | 53 |

[a] Reaction conditions: cat./styrene = 1:300, [cat.] = 4.6 mM, solvent-substrate = CHCl$_3$, reaction volume = 1 mL, $T$ = 60 °C. The conversion, measured after 5 h reaction, is based on the consumption of the styrene as determined by GC.

With the catalysts **26** and **82**, conversions of 9 and 20 %, respectively, were measured after 5 h reaction (Entries 1 and 2). This is superior to what was found for catalyst **38** (2 %, Entry 3), but less than what was observed for the catalysts **12** and **45**, which were

able to convert about 50 % of styrene over the same period of time.

### 2.2.3 Discussion about the lability of the dinitrogen ligand in the complex [{(tpc)Rh($\mu$-Cl)$_3$Ru(dcypb)}$_2$($\mu$-N$_2$)] (82)

When the reaction between the complexes [(dcypb)(N$_2$)Ru($\mu$-Cl)$_3$RuCl(dcypb)] (**67**) and [RhCl(tpc)]$_2$ (**75**) was performed in a mixture of $CH_2Cl_2$ and acetone instead of pure $CH_2Cl_2$, the bimetallic complex [(tcp)Rh($\mu$-Cl)$_3$Ru(dcypb)(acetone)] (**83**) was obtained (Scheme 2.4) [126].

**Scheme 2.4**

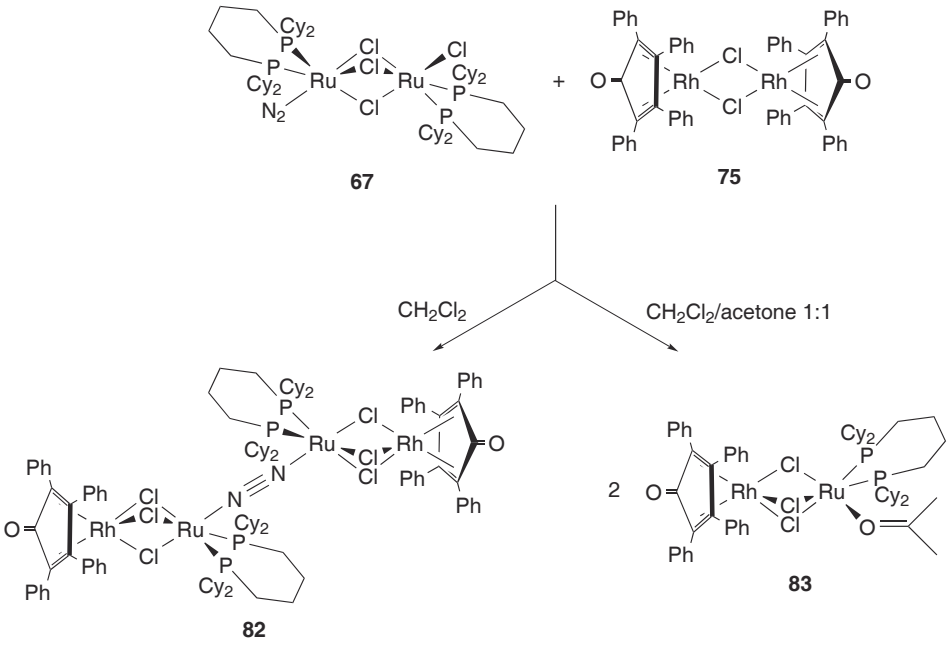


The acetone, however, was found to be a weakly coordinated ligand: When complex **83** was dissolved in $CH_2Cl_2$, partial exchange of the acetone ligand for a dinitrogen ligand was observed. This was supported by $^{31}$P NMR spectroscopy, which revealed the presence of the two species in solution. Regarding catalysis, experiments demonstrated that the ATRA activity of the acetone complex **83** was similar to that of the dinitrogen complex **82**[6].

When the complex [(PPh$_3$)$_2$ClRu($\mu$-Cl)$_3$Ru(PPh$_3$)$_2$(acetone)] (**21**) was employed instead of **67**, a similar reaction was observed: In a mixture of acetone and $CH_2Cl_2$, after

6. With styrene and $CCl_4$ as the substrates, conversions of 84 (**83**) and 89 % (**82**) were obtained after 30 min reaction using 0.33 % of the catalysts (Reaction conditions: styrene/$CCl_4$ = 300:432, solvent = $CHCl_3$, reaction volume = 1 mL, $T$ = 60 °C.

20 min stirring at room temperature, followed by removal of the solvent under vacuum, the bimetallic acetone complex [(tcp)Rh($\mu$-Cl)$_3$Ru(PPh$_3$)$_2$(acetone)] (**84**) was obtained in quantitative yield [135]. Again, the catalytic activity of the acetone complex towards the Kharasch addition of $CCl_4$ to styrene was found to be similar to that of the corresponding catalyst obtained in absence of this ligand[7,8].

### 2.2.4 Crystal structure of the complex [(dcypb)(N$_2$)Ru($\mu$-Cl)$_3$RuCl(dcypb)]

The starting material **67** was reported to exist in the form of a non symmetric dimer, in which a {RuCl(dcypb)} and a {Ru(dcypb)(N$_2$)} fragments are connected by three chloro-bridges [125]. This molecular structure differs from that of the above-described catalyst **82**, for which the dinitrogen molecule acts as an end-on bridging ligand. The presence of a $N_2$ ligand in complex **67** was confirmed by IR, mass spectroscopy, and by elemental analysis [125]. Here, we report the molecular structure of complex [(dcypb)(N$_2$)Ru($\mu$-Cl)$_3$RuCl(dcypb)] (**67**), which supplements these observations (Figure 2.6). Crystals of complex **67** were grown by a slow diffusion of pentane in a solution of complex **67** in a 1:1 mixture of benzene and dichloromethane. The interatomic distances and angles for the {RuCl$_2$(dcypb)(N$_2$)} fragment of complex **67** are very similar to those found for complex **82**.

7. With styrene and $CCl_4$ as the substrates, a conversion of 28 % was measured after 2 h with complex **84** as the catalyst. In the screening experiment the mixture of **21** and **75** afforded a conversion of 33 % under strictly identical reaction conditions.

8. It is important to note that a small amount of acetone is inevitably present in the solution, brought by the starting material **21**.

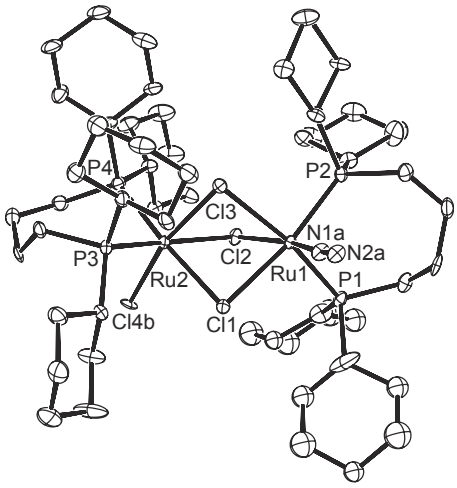


**Figure 2.6:** ORTEP drawing of the molecular structure of **67** in the crystal. The hydrogen atoms and the solvent molecules are not shown for clarity. Selected bond lengths (Å) and angles ($^\circ$): Ru1–N1a 1.848(15), N1a–N2a 1.122(16), Ru–Cl$^{b[a]}$ 2.47, Ru2–Cl$^{t}$ 2.429(5), Ru–P$^{[a]}$ 2.30; P1–Ru1–P2 95.55(7), P3–Ru2–P4 93.53(8), P–Ru1–N1a$^{[a]}$ 92.6, P–Ru2–Cl4b$^{[a]}$ 94.4; [a] Average values; $b$ = bridging, $t$ = terminal.

## 2.3 Additional ATRA Catalysis Screening Assays

### 2.3.1 Combination of the complexes $[RuCl_2(CHPh)(PCy_3)_2]$ and $[Cp^*RuCl(PPh_3)_2]$ with various chloro-bridged dimers for the ATRA of $CCl_4$

The complexes $[(PPh_3)_2ClRu(\mu\text{-}Cl)_3Ru(PPh_3)_2(acetone)]$ (**21**), $[(dppb)ClRu(\mu\text{-}Cl)_2(\mu\text{-}OH_2)RuCl(dppb)]$ (**66**), and $[(dcypb)(N_2)Ru(\mu\text{-}Cl)_3RuCl(dcypb)]$ (**67**) easily undergo chloro-bridge metathesis reactions with half-sandwich bimetallic complexes (Scheme 2.3, p. 33). The products of these reactions are mostly triply bridged bimetallic complexes of the general formula $[LM(\mu\text{-}Cl)_3RuCl(PP)]$ (LM = (arene)Ru, Cp*Ir, Cp*Rh, or Cp*Ru; PP = 2 $PPh_3$, dppb, or dcypb) and several of these were found to be excellent catalysts for ATRA reactions. The Grubbs catalyst $[RuCl_2(CHPh)(PCy_3)_2]$ (**12**) represents another complex, which can be employed for the synthesis of ATRA active mixed complexes (see Introduction, Scheme 1.4, p. 6). The reaction, however, proceeds with the transfer of one $PCy_3$ ligand and the formation of one equivalent of a mononuclear side product (Scheme 2.5). If the bimetallic catalysts are generated in-situ, the resulting solution will be a mixture of the two complexes. Because both complexes can display a catalytic activity, the identification of the best candidates will be more difficult. Regarding the catalyst $[Cp^*RuCl(PPh_3)_2]$ (**45**), there was no indication that an analogous reaction can occur, although the dissociation of one phosphine ligand was known to be relatively easy [112]. Nevertheless, we decided to perform a screening assay with the two complexes **12** and **45**. They were thus combined with the 23 dimeric transition metal complexes shown in Figure 2.3, p. 34. The mixtures were tested in a parallel fashion for their ability to catalyze the addition of $CCl_4$ to styrene. The results are displayed in Figure 2.7.

**Scheme 2.5**

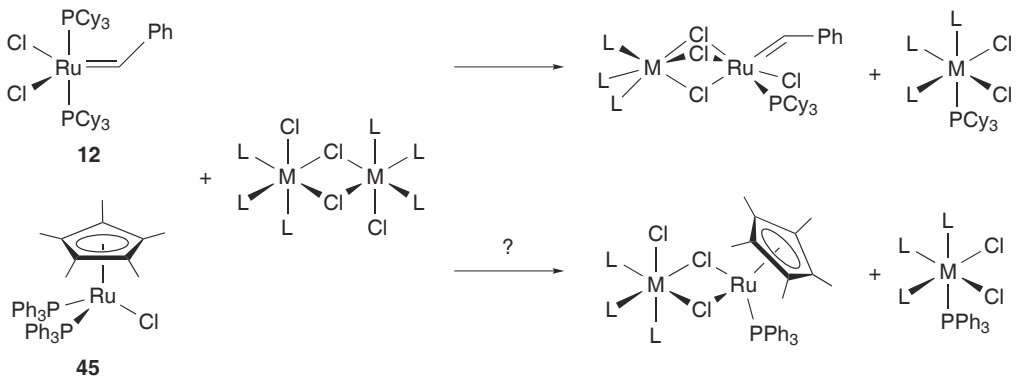


The activity of complex **12** (white bars) was found to be strongly dependent on the na-

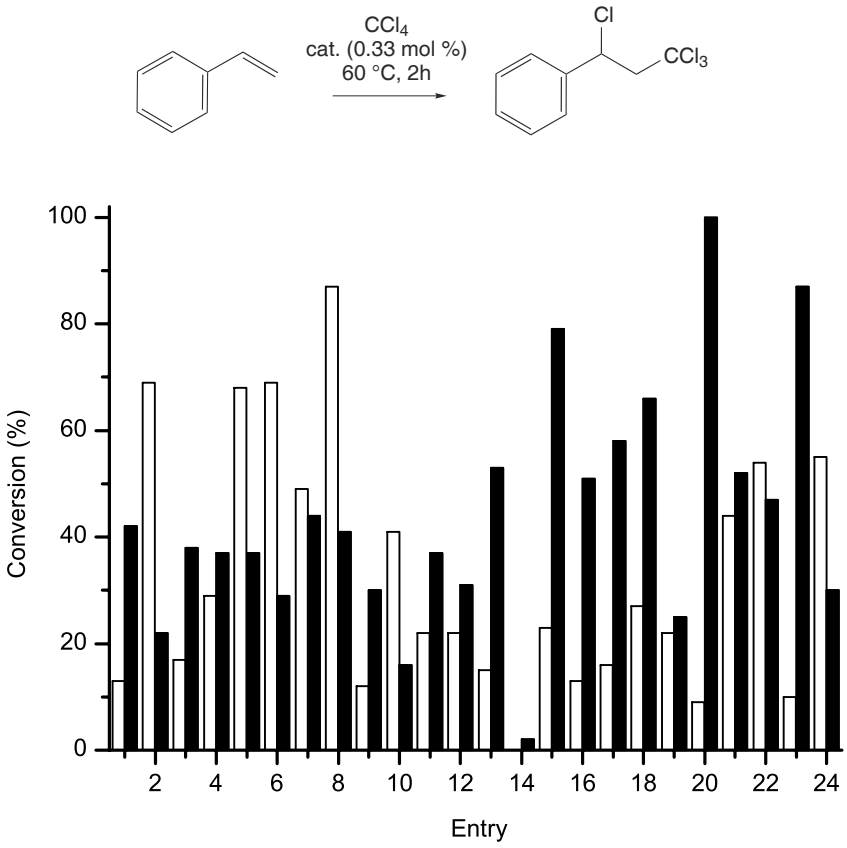


**Figure 2.7:** Parallel screening of catalyst activity using the addition of $CCl_4$ to styrene as a benchmark reaction. The catalysts were prepared in-situ by mixing complex **12** (white bars) or **45** (black bars) with: 1) no additional complex, 2) **69**, 3) **68**, 4) **70**, 5) **71**, 6) **13**, 7) **73**, 8) **72**, 9) **74**, 10) **22**, 11) **23**, 12) **9**, 13) **10**, 14) **2**, 15) **75**, 16) **76**, 17) **77**, 18) **33**, 19) **78**, 20) **79**, 21) **17**, 22) **80**, 23) **15**, 24) **81**. Reaction conditions: **12** or **45**/additional complex/styrene/$CCl_4$ = 1:1:300:432, [**12** or **45**] = 4.6 mM, solvent = chloroform, reaction volume = 1 mL, $T = 60\,^{\circ}$C. The conversion after 2 hours is based on the consumption of styrene as determined by GC.

ture of the additional complex. Some combinations, notably those with the half-sandwich complexes $[(C_6H_5CO_2Et)RuCl_2]_2$ (**69**), $[(C_6H_3Et_3)RuCl_2]_2$ (**71**), $[(cymene)RuCl_2]_2$ (**13**), and $[(C_6H_3{}^{i}Pr_3)RuCl_2]_2$ (**72**) (Entries 2a, 5a, 6a, and 8a), resulted in a five-fold increase of the conversion, as compared with complex **12** alone.

The combinations, which involve complex **45** (black bars) display more equally distributed activities (22 – 66 % conversion), with two notable exceptions: 1) The complex $[RhCl(CO)_2]_2$ (**2**), as observed for the other catalysts precursors **21**, **66**, **67**, and **12** (Figure 2.4, p. 35 and Figure 2.7, Entries 14), seems to act as a radical trap and inhibits the Kharasch addition; 2) For reactions with the complexes $[PdCl(PEt_3)_2]_2(BF_4)_2$ (**79**) (Entry 20b) and $[PtCl(PEt_3)_2]_2(BF_4)_2$ (**15**) (Entry 23b), very high conversions of 87 and

100 %, respectively, are observed. A plausible explanation for this result will be given in the next section.

### 2.3.2 Combination of the complexes $[RuCl_2(CHPh)(PCy_3)_2]$, $[Cp^*RuCl(PPh_3)_2]$, and $[(PPh_3)_2ClRu(\mu\text{-}Cl)_3Ru(PPh_3)_2(acetone)]$ with various chloro-bridged dimers for the ATRA of $CHCl_3$

As outlined in Table 2.4, p. 40, the catalysts $[Cp^*Rh(\mu\text{-}Cl)_3RuCl(PPh_3)_2]$ (**26**) and $[\{(tpc)Rh(\mu\text{-}Cl)_3Ru(dcypb)\}_2(\mu\text{-}N_2)]$ (**82**) displayed a catalytic activity for the ATRA of $CCl_4$ to styrene, which was superior to what was found for the previously described catalysts **12** and **45**. For the more difficult substrate $CHCl_3$, the situation was reversed (Table 2.5, p. 41). In order to establish whether chloro complexes could activate the $\{RuCl_2(PPh_3)_2\}$ fragment towards the ATRA of $CHCl_3$, we have screened different combinations of complex **21** with the 23 dimeric transition metal complexes. As the benchmark reaction we have employed the addition of $CHCl_3$ to styrene. The reactions were performed at a temperature of 60 °C with a Ru/M/styrene ratio of 1:2:300. In order to limit the undesirable telomerization reactions, the substrate $CHCl_3$ itself was used as the solvent (this corresponds to a styrene/$CHCl_3$ ratio of about 1:10). Because the substrate $CHCl_3$ is less reactive than $CCl_4$, the reaction time was increased to 5 h. The results are depicted in Figure 2.8 (black bars).

Only a single combination displayed slightly more than 20 % conversion (Entry 24a). The catalysts based on the $\{RuCl_2(PPh_3)_2\}$ fragment proved to be less suited for this particular transformation. Most of the bimetallic catalysts, however, displayed higher activities than the mononuclear catalyst $[RuCl_2(PPh_3)_3]$ (**38**), which gave only 2 % conversion under identical reaction conditions (Table 2.5, p. 41, Entry 3).

The catalysts **12** [107] and **45** [112] have been reported to display a high activity for the addition of $CHCl_3$ to various olefins at low temperature. This was confirmed by the results presented in Table 2.5, p. 41 (Entries 4 and 5). The combinations of these complexes with the 23 chloro-bridged dimers were tested as catalyst precursors for the addition of $CHCl_3$ to styrene (Figure 2.8, white and grey bars). As expected, the conversions were higher than those for reactions with complex **21**. Contrary to what was observed for the addition of $CCl_4$, however, the presence of the additional transition metal complex was in most cases detrimental to the catalytic activity and only a few combinations displayed activities, which were superior to those found for the catalysts **12**

and **45** alone.

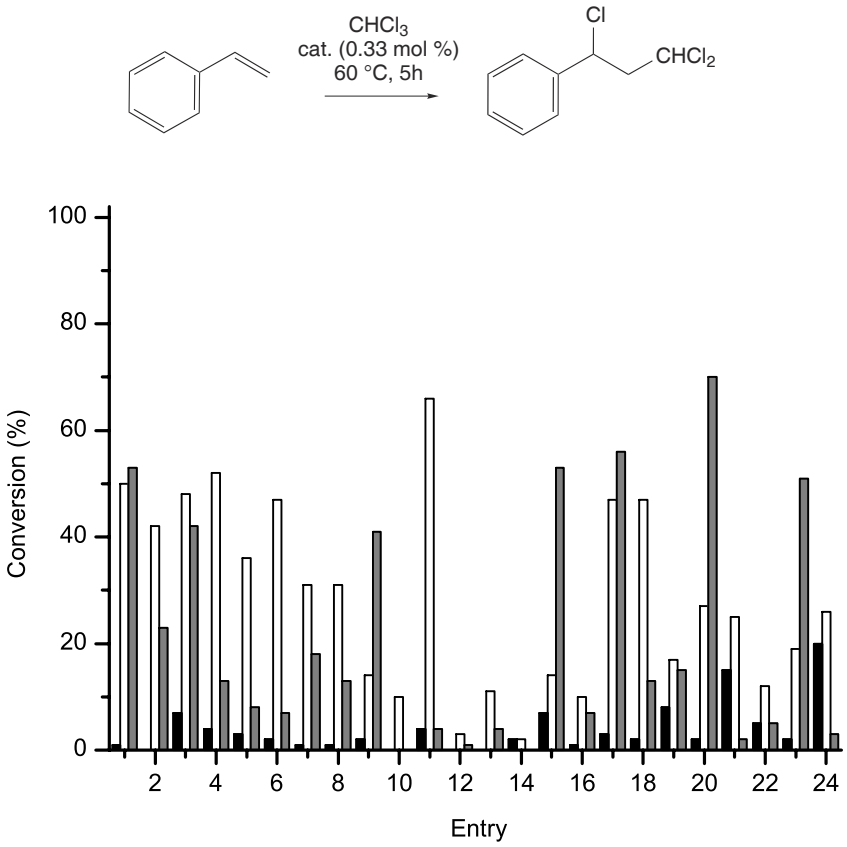


**Figure 2.8:** Parallel screening of catalyst activity using the addition of $CHCl_3$ to styrene as a benchmark reaction. The catalysts were prepared in situ by mixing complexes **21** (black bars), **12** (white bars), or **45** (grey bars) with: 1) no additional complex, 2) **69**, 3) **68**, 4) **70**, 5) **71**, 6) **13**, 7) **73**, 8) **72**, 9) **74**, 10) **22**, 11) **23**, 12) **9**, 13) **10**, 14) **2**, 15) **75**, 16) **76**, 17) **77**, 18) **33**, 19) **78**, 20) **79**, 21) **17**, 22) **80**, 23) **15**, 24) **81**. Reaction conditions: Ru/M/styrene = 1:2:300, [Ru] = 4.6 mM, solvent-substrate = chloroform, reaction volume = 1 mL, $T = 60\,^{\circ}$C. The conversion after 5 h is based on the consumption of styrene as determined by GC.

## 2.4 Atom-Transfer Radical Additions with the Cationic Half-Sandwich Ruthenium Complex [Cp*Ru(PPh$_3$)$_2$(CH$_3$CN)]-OTf [9]

As outlined in the previous section, it is possible to enhance the ATRA catalytic performance of the complex [Cp*RuCl(PPh$_3$)$_2$] (**45**) by adding the complexes [PdCl-(PEt$_3$)$_2$]$_2$(BF$_4$)$_2$ (**79**) or [PtCl(PEt$_3$)$_2$]$_2$(BF$_4$)$_2$ (**15**) to the reaction mixture. A particular feature of those complexes is that the positively charged metal centers can react with chloride anions to transform into the neutral complexes [PdCl$_2$(PEt$_3$)$_2$] (**85**) or [PtCl$_2$-(PEt$_3$)$_2$] (**86**), respectively. A chloride abstraction of **45** with concomitant formation of the positively charged species {Cp*Ru(PPh$_3$)}$^+$ can therefore be an explanation for the superior ATRA performance. This hypothesis was enforced by the observation that the ATRA activity of complex **45** was likewise increased when Me$_3$SiOTf was used as the chloride abstraction agent[10].

A catalyst activation of this kind has already been described in the literature: H. Nagashima *et al.* have recently reported that the activity of the dinuclear complex [Cp*Ru-{$\mu_2$-$^i$PrN=C(Me)N$^i$Pr}RuClCp*] (**87**) towards the atom-transfer radical cyclization of *N*-allyl-trichloroacetamides could be increased by transforming it into a cationic species using NaPF$_6$ or NaBPh$_4$ [137]. Similarly, the activity of ruthenium chloro catalysts for the closely related atom-transfer radical polymerization could be enhanced by chloride abstraction with silver salts [121, 138, 139]. For Ru vinylidene catalysts, on the other hand, it was reported that the abstraction of a chloro ligand lead to a decrease in ATRA activity [115]. We wanted to investigate whether cationic {Cp*Ru-phosphine}$^+$ complexes could be useful ATRA catalysts.

### 2.4.1 Synthesis of new cationic complexes containing the {Cp*Ru} fragment

Cationic complexes of the general formula [Cp*Ru(PR$_3$)$_2$(CH$_3$CN)]X (X$^-$ = weakly coordinating anion) have been obtained by reaction of complex **45** with MX in acetonitrile (M$^+$ = Ag$^+$, NH$_4^+$) [140–142] or by reaction of [Cp*Ru(CH$_3$CN)$_3$]X with PR$_3$ in CH$_2$Cl$_2$ [143] (Scheme 2.6). A new complex, which could display the two advantages—increased catalytic performance and convenient synthesis—would be of great interest.

9. Part of the work described in this section has been published, see ref. [136].

10. When 1 equivalent of Me$_3$SiOTf was added to complex **45**, a conversion of 60 % was obtained after 2 h (reaction conditions: same as in Figure 2.8).

The utilization of complex **45** as an intermediate appeared less suited: From our own experience and as observed by F. Verpoort *et al.* [116], its synthesis has the drawback to be tedious and time consuming, requiring the use of stringent reaction conditions and rigorously dried and purified solvents and reactants [144, 145]. The trisacetonitrile complex $[Cp^{\star}Ru(CH_3CN)_3]X$, on the other hand, is known to be easily accessible by reduction of $[Cp^{\star}RuCl_2]_2$ (**74**) with zinc in acetonitrile in the presence of MX salts [143]. We therefore decided to use the second pathway for the syntheses of new $\{Cp^{\star}Ru(PPh_3)_2\}^+$ complexes.

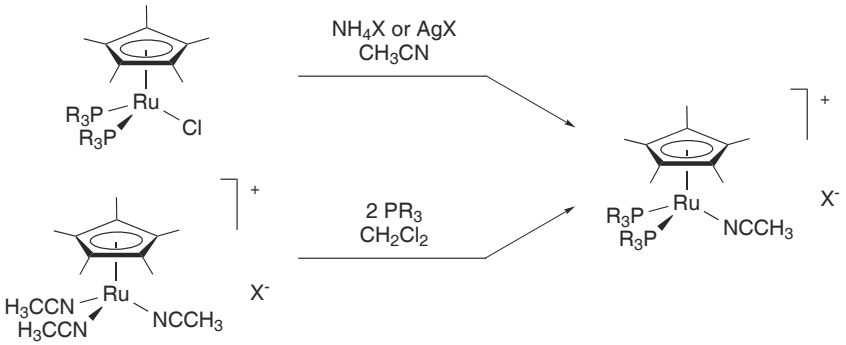


**Scheme 2.6:** Synthesis of cationic complexes of the general formula $[Cp^{\star}Ru(PR_3)_2(CH_3CN)]X$ ($X^-$ = weakly coordinating anion).

We were able to prepare the cationic complex $[Cp^{\star}Ru(PPh_3)_2(CH_3CN)]OTf$ (**88**) in 95 % yield by reaction of **74** with zinc in acetonitrile in the presence of NaOTf and direct conversion of the product with two equivalents of $PPh_3$ (Scheme 2.7). Complex **88** displays a good solubility in polar organic solvents such as THF, dichloromethane and chloroform, and a moderate solubility in toluene. The identity of **88** was confirmed by NMR spectroscopy, elemental analysis and single crystal X-ray analysis (Figure 2.9).

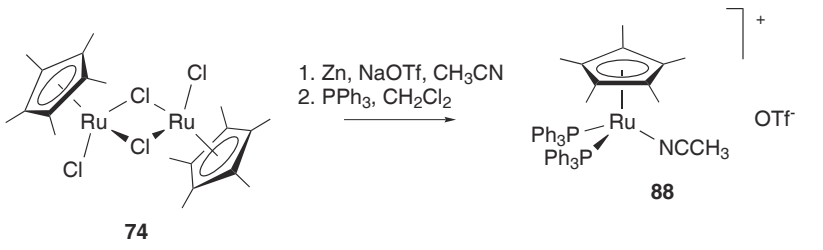


**Scheme 2.7:** Synthesis of complex **88**.

The cation of complex **88** displays the expected piano-stool geometry. As a consequence of the steric demand of the triphenylphosphine ligands, the P–Ru–P angle (99.41(2) ° ) is larger than the N–Ru–P angles (N1–Ru1–P1 = 87.97(5) ° ; N2–Ru1–P2

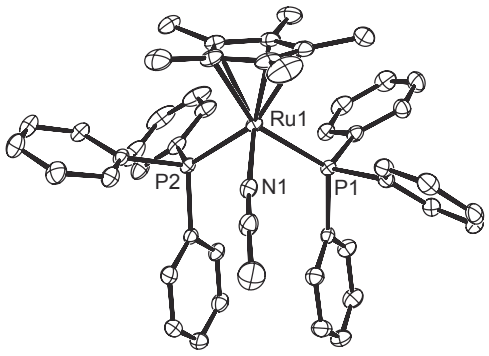


**Figure 2.9:** ORTEP drawing of the molecular structure of **88** in the crystal. The $TfO^-$ anion and the hydrogen atoms are omitted for clarity. Selected bond lengths (Å) and angles ( ° ): Ru1–N1 2.056(2), Ru1–P1 2.3709(6), Ru1–P2 2.3462(7); P2–Ru1–P1 99.41(2), N1–Ru1–P1 87.97(5), N2–Ru1–P2 87.95(6).

= 87.95(6) ° ). The Ru–P bond lengths (Ru1–P1 = 2.3709(6) Å, Ru1–P2 = 2.3462(7) Å) are similar to what has been found for the neutral complex **45** [146].

In order to investigate the influence of the NaOTf salt during the synthesis of complex **88**, we have performed the reduction of $[Cp^{\star}RuCl_2]_2$ (**74**) with zinc in acetonitrile in the absence of this salt. The formation of a trisacetonitrile complex $[Cp^{\star}Ru(CH_3CN)_3]^+$ (**89**) was observed but as the counterion, the tetrachlorozincate anion was formed, as revealed by single crystal X-ray analysis (Scheme 2.8, Figure 2.10).

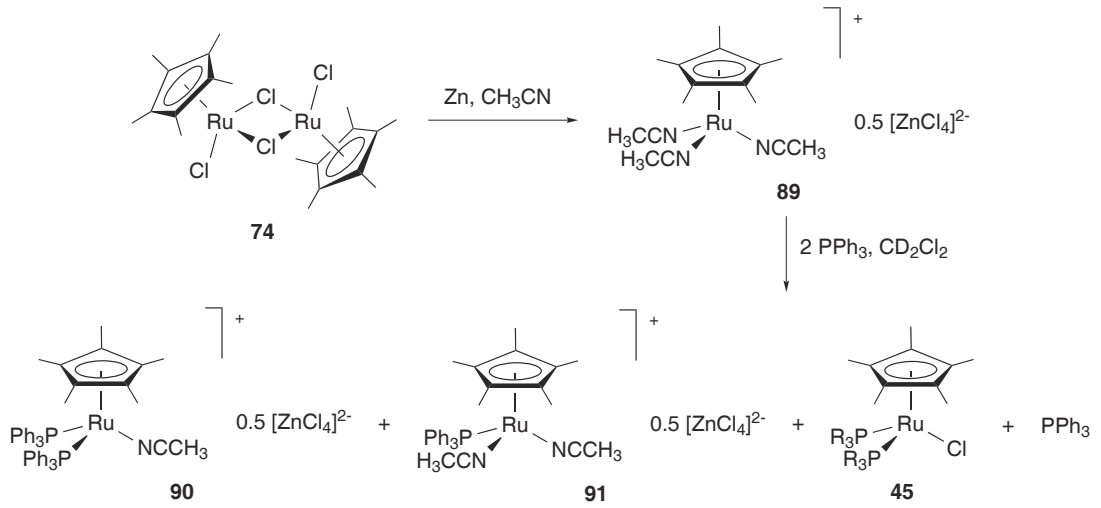


**Scheme 2.8:** Synthesis of the tetrachlorozincate complex **89** and its reaction with $PPh_3$.

Complex **89** proved to be not suited for a clean synthesis of a bis(triphenylphosphine) adduct: When two equivalents of $PPh_3$ were added to a solution of **89** in $CD_2Cl_2$, the desired cationic bisadduct **90** was formed but along with the neutral complex **45**, the

monoadduct **91**[11] [147], and free $PPh_3$, as evidenced by $^1H$ and $^{31}P$ NMR spectroscopy. From this mixture, it was possible to obtain single crystals of complex **90** by addition of pentane. A graphic representation of the structure of **90** is depicted in Figure 2.11.

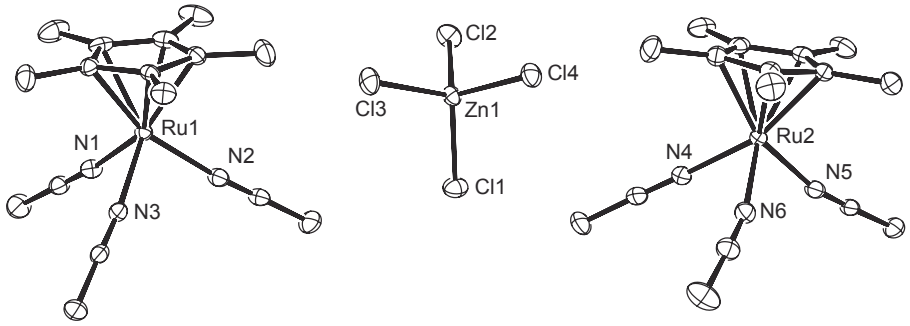


**Figure 2.10:** ORTEP drawing of the molecular structure of **89** in the crystal. The hydrogen atoms are omitted for clarity. Selected bond lengths (Å) and angles ( ° ): Ru1–N1 2.095(2), Ru1–N2 2.108(2), Ru1–N3 2.103(2), Ru2–N4 2.110(2), Ru2–N5 2.102(2), Ru2–N6 2.109(2); N1–Ru1–N2 88.19(8), N1–Ru1–N3 84.67(8), N3–Ru1–N2 90.60(7), N5–Ru2–N4 90.84(8), N5–Ru2–N6 91.66(8), N6–Ru2–N4 81.76(8).

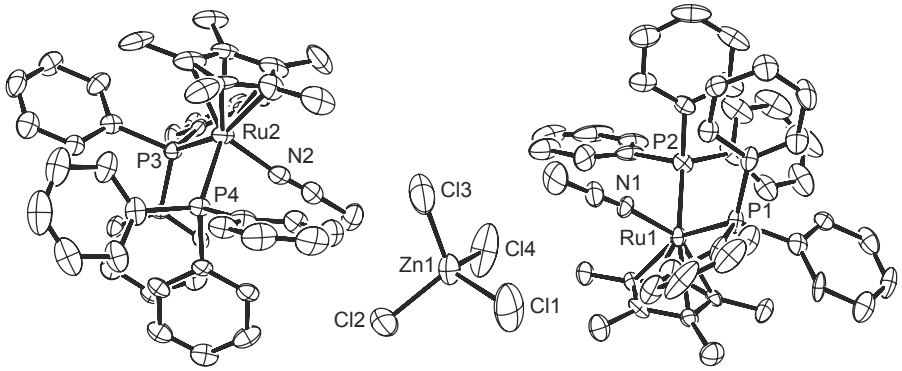


**Figure 2.11:** ORTEP drawing of the molecular structure of **90** in the crystal. The hydrogen atoms and the solvent molecules ($CH_2Cl_2$) are omitted for clarity. Selected bond lengths (Å) and angles ( ° ):Ru1–N1 2.037(6), Ru1–P1 2.3868(19), Ru1–P2 2.343(2), Ru2–N2 2.061(7), Ru2–P3 2.3556(19), Ru2–P4 2.346(2); N1–Ru1–P1 87.44(16), N1–Ru1–P2 88.12(18), P2–Ru1–P1 99.00(7), N2–Ru2–P4 89.28(18), N2–Ru2–P3 90.17(17), P4–Ru2–P3 97.19(7).

The bond lengths and angles found for the two crystallographically independent cations of complex **89** are very similar to those observed for other $[Cp^\star Ru(CH_3CN)_3]^+$ com-

11. When complex **88** is dissolved in $CD_3CN$, the formation of the monophosphine adduct $[Cp^\star Ru(PPh_3)(CH_3CN)_2]^+$ can be observed by NMR spectroscopy.

plexes [148, 149]. The N–Ru–N angles are close to 90 °. The geometry of the cations can thus be described as pseudo-octahedral with the Cp* ligand occupying three facial coordination sites. As it was observed for complex **88**, the P–Ru–P angles of **90** (99.00(7) and 97.19(7) °) are larger than the P–Ru–N angles (P–Ru–N = 87.44 – 90.17 °).

Complex **89** could be used as an alternative starting material for the synthesis of complex **88**. The addition of AgOTf to a solution of complex **89** in $CH_3CN$ allowed the exchange of the $ZnCl_4^{2-}$ counteranion for two $TfO^-$ anions. Subsequent reaction with 2 equivalents of $PPh_3$ led to the formation of the desired complex **88**.

### 2.4.2 ATRA activity of the cationic complex [Cp*Ru(PPh$_3$)$_2$(CH$_3$CN)]OTf

To evaluate the ability of the cationic complex **88** to catalyze ATRA reactions, we first investigated the addition of $CCl_4$ to styrene at 60 °C using a molar ratio of **88**/styrene/-$CCl_4$ = 1:300:432. The complete conversion of the olefin was observed within 2 h. For the neutral complex **45**, a conversion of 97 % was reported after 5 h [110, 112]. In order to obtain more information about differences in activity and stability of the catalysts **45** and **88**, we have investigated the time course of the reaction between styrene and $CCl_4$ at room temperature in chloroform with a molar ratio of Ru/styrene/$CCl_4$ = 1:300:600 (Figure 2.12). For reactions with the cationic catalyst **88**, a quantitative reaction was observed after 4 h. For reactions catalyzed by the neutral complex **45**, on the other hand, a very fast product formation was found for the first 20 min but then the rates dropped dramatically and the conversion reached a plateau at around 40 % yield. When the solvent was changed to toluene and the $CCl_4$ concentration was reduced, an increased lifetime of the catalyst was observed but still the final conversion (60 %) was lower than what was found for **88**. This data suggested that the neutral catalyst **45** shows a higher intrinsic activity than the cationic complex **88** but a significantly lower stability. This is in agreement with the observation of Simal *et al.* that complex **45** rapidly decomposed in presence of $CCl_4$: When 10 equivalents of $CCl_4$ were added to a solution of **45** in toluene at 20 °C, the complete conversion into a paramagnetic Ru(III) compound occurred within 2 h [112]. When a similar experiment was performed with the cationic complex **88**, only 40 % decomposition was observed after 2 h. For complex **45** it was suggested that $PPh_3$ dissociation is required to activate the catalyst [112]. This step is likely to be faster for the neutral complex **45** as compared to the cationic complex **88**, which may explain the higher initial activity of the former. The higher stability of the cationic complex **88**, on

the other hand, may be due to a different activity of the Ru(III) species formed by atom transfer but further investigations are needed to clarify this point.

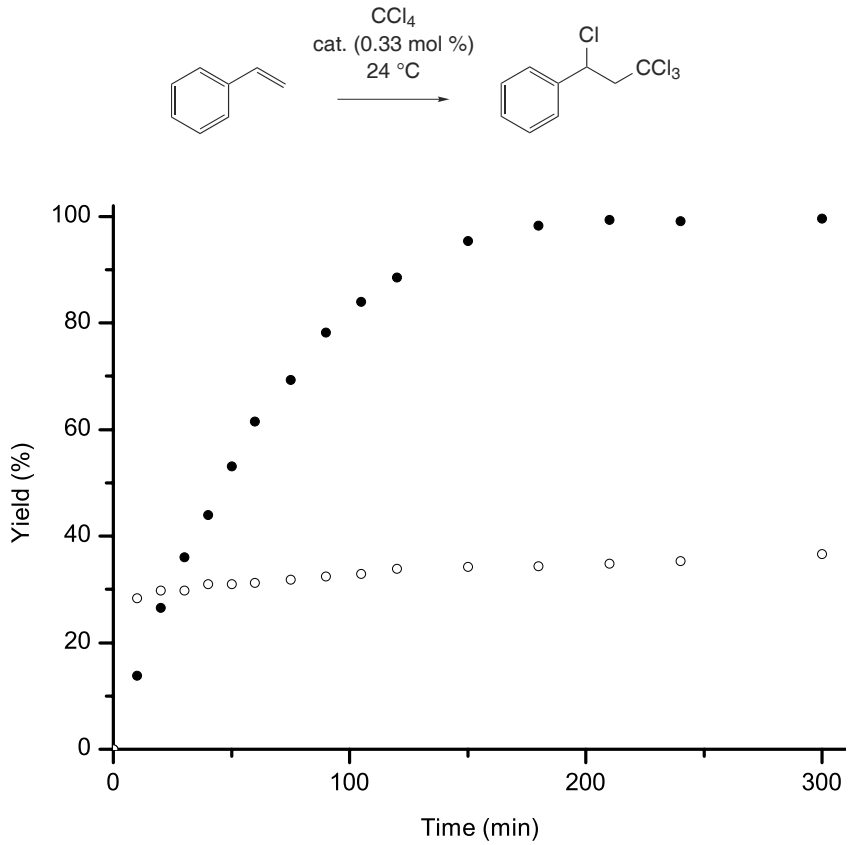


**Figure 2.12:** Time course of the reaction between styrene and $CCl_4$ catalyzed by complexes **45** (○) or **88** (●). Reaction conditions: cat./styrene/$CCl_4$ = 1:300:600, [**45** or **88**] = 4.6 mM, solvent = $CDCl_3$, reaction volume = 1 mL, $T = 24\,^{\circ}$C. The yield is based on the formation of the product as determined by $^1$H NMR.

The good performance of the cationic catalyst **88** was confirmed in other ATRA reactions (Table 2.6). As mentioned above, the reaction between styrene and $CCl_4$ could be completed within 5 h using 0.33 mol % of complex **88** at room temperature (Entry 1). Using only 0.02 mol % catalyst, a total TON of 3050 was measured after 5 weeks[12]. A remarkably fast and clean reaction was observed with methyl methacrylate and $CCl_4$ as the substrates (Entry 2). After 2 h at room temperature, a yield of 93 % was obtained. For the neutral catalyst **45**, for comparison, a yield of only 36 % was found after 24 h [112]. The olefins *n*-buthyl acrylate (Entry 3) and 1-decene (Entry 4) gave lower yields of 67 and

12. Reaction conditions: **88**/styrene/$CCl_4$ = 1:5000:7500, [**88**] = 0.28 mM, solvent = toluene-$d^8$, reaction volume = 2 mL, $T = 24\,^{\circ}$C.

77 %, respectively. For the former substrate, this was due to competing oligomerization reactions.

**Table 2.6:** ATRA reactions, catalyzed by the complex [Cp*Ru($PPh_3$)$_2$($CH_3CN$)]OTf (**88**).[a]

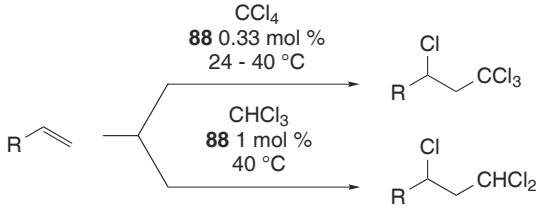


| Entry | Olefin | $CXCl_3$ | $T$ ($^\circ$C) | $t$ (h) | Conv. / Yield (%) |
|---|---|---|---|---|---|
| 1 | styrene | $CCl_4$ | 24 | 5 | 100 / 97 |
| 2 | methyl methacrylate | $CCl_4$ | 24 | 2 | 100 / 93 |
| 3 | *n*-butyl acrylate | $CCl_4$ | 24 | 10 | 98 / 67 |
| 4 | 1-decene | $CCl_4$ | 40 | 24 | 80 / 77 |
| 5 | styrene | $CHCl_3$ | 40 | 24 | 96 / 88 |
| 6 | *p*-chlorostyrene | $CHCl_3$ | 40 | 48 | 95 / 92 |
| 7 | *p*-methoxystyrene | $CHCl_3$ | 40 | 48 | 96 / 90 |
| 8 | methyl methacrylate | $CHCl_3$ | 40 | 24 | 96 / 33 |
| 9 | *n*-butyl acrylate | $CHCl_3$ | 40 | 24 | 99 / 15 |

[a] Reaction conditions: **88**/olefin/$CCl_4$ = 1:300:600, [**88**] = 4.6 mM, solvent = $CDCl_3$, reaction volume = 1 mL or **88**/olefin = 1:100, [**88**] = 13.8 mM, solvent-reactant = $CDCl_3$, reaction volume = 0.5 mL. The conversion is based on the consumption of the olefin and the yield is based on the formation of the product as determined by GC or $^1$H NMR spectroscopy after the time given.

In order to perform ATRA reactions with the significantly less active substrate $CHCl_3$, the reaction temperature was increased to 40 $^\circ$C and a catalyst concentration of 1 mol % was employed (Entries 5 – 9). Under these conditions, catalyst **88** provided the chloroform adducts of the aromatic olefins styrene, *p*-chlorostyrene, and *p*-methoxystyrene with good yields (Entries 5 – 7). A TON of 890 was obtained for the addition of $CHCl_3$ to styrene using 0.1 mol % of complex **88**[13]. This is, to the best of our knowledge, the highest value ever reported for a ruthenium-based catalyst[14]. For acrylate substrates, almost complete

13. A yield of 89 % was measured after 3 weeks using the following reaction conditions: **88**/styrene/$CHCl_3$ = 1/1000/9900, [**88**] = 1.38 mM, solvent-substrate = $CDCl_3$, reaction volume = 2 mL, $T$ = 40 $^\circ$C.

14. To the best of our knowledge, the highest turnover number for a Ru-catalyzed addition of $CHCl_3$ to

conversions were determined after 24 h. The yields of the desired addition products, however, were very modest due to competing polymerization reactions (Entries 8 and 9).

### 2.4.3 Attempts to improve the new catalyst [Cp*Ru(PPh$_3$)$_2$(CH$_3$CN)]OTf

The results, which are described in the previous subsection, demonstrate that a simple modification such as the conversion of the chloro complex **45** into the cationic acetonitrile complex **88** can result in a significantly increased catalyst stability. But still, other catalyst modifications could be considered: The use of different phosphine ligands, for example, could strongly affect the performance.

Complexes of the general formula [Cp*Ru(PP)(CH$_3$CN)]OTf (PP = 2 PPh$_3$, PCy$_3$[15], dppb, or dcypb) were synthesized using the cationic complex [Cp*Ru(CH$_3$CN)$_3$]OTf (**92**) and stoichimetric amount of the phosphine (Scheme 2.9). In dichloromethane, these reactions are fast and quantitative. Therefore, the solutions of the resulting products were assayed for catalytic activity without purification. The results are displayed in Table 2.7.

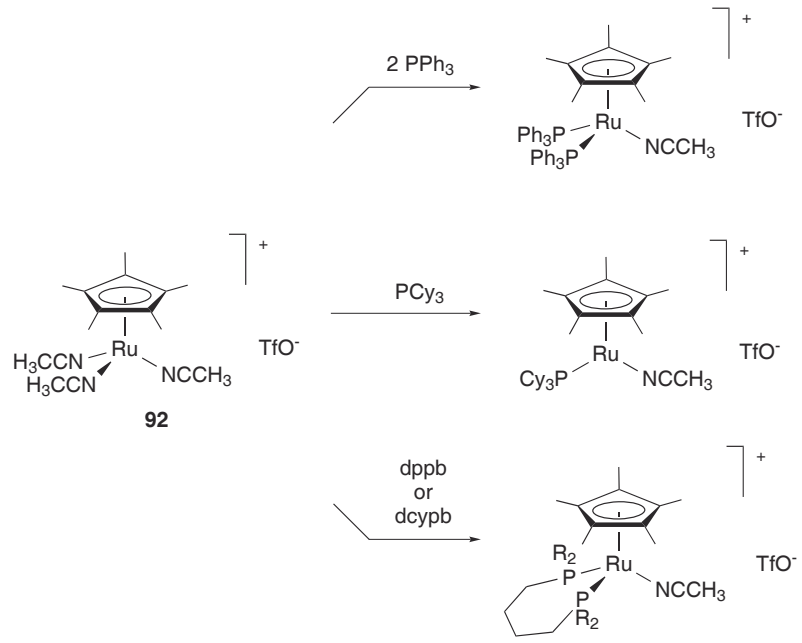


**Scheme 2.9:** Method for the synthesis of cationic complexes of the general formula [Cp*Ru(PP)(CH$_3$CN)]OTf (PP = 2 PPh$_3$, PCy$_3$, dppb, or dcypb).

As expected, the complex **92** alone was not able to catalyze the reaction (Entry 1). The

styrene was reported for the complex [Cp*RuCl(PPh$_3$)$_2$] (**45**) (TON = 207, 85 °C, 24 h) [112].

15. The steric demand of the PCy$_3$ ligand may prevent the formation of a bisadduct, as observed for the corresponding neutral chloro complex [150, 151].

**Table 2.7:** Addition of $CCl_4$ to styrene, catalyzed by combinations of the complex [Cp*Ru-($CH_3CN)_3$]OTf (**92**) with different phosphines.[a]

| Entry | Catalyst | Conv. (%) |
|---|---|---|
| 1 | **92** | 0 |
| 2 | **92** + 2 $PPh_3$ | 50 |
| 3 | **92** + 1 $PPh_3$ | 37 |
| 4 | **92** + dppb | 13 |
| 5 | **92** + 2 $PCy_3$ | 5 |
| 6 | **92** + 1 $PCy_3$ | 3 |
| 7 | **92** + dcypb | 20 |
| 8 | **88** | 57 |

[a] Reaction conditions: Ru/styrene/$CCl_4$ = 1:300:432, [Ru] = 4.6 mM, solvent = $CH_2Cl_2$, reaction volume = 1 mL, $T = 30\,^{\circ}$C. The conversion is based on the consumption of the olefin as determined by GC after 1 h reaction.

mixture of complex **92** and two equivalents of $PPh_3$ displayed a conversion very similar to that observed with the isolated complex **88** (Entries 2 and 8). This confirms that a clean formation of the bisphosphine complex occurs in solution. When only one equivalent of the phosphine was added (Entry 3), a consistently lower conversion was observed. This highlights the superior performance of the bisphosphine complex when compared to the corresponding monophosphine complex. The catalyst system with the chelating phosphine dppb showed a very low activity. It is interesting to note that this intrinsic advantage of two monodentate phosphines $PPh_3$ over a bidentate phosphine dppb was already observed in the frame of the combinatorial catalysis project (Section 2.2). The use of mono- and bidentate cyclohexylphosphines could not rival the bis(triphenylphosphine) catalyst **88** (Entries 5 – 7).

## 2.5 [(Arene)$RuCl_2$]$_2$ and $PCy_3$ as Catalyst Precursors for ATRA Reactions[16]

### 2.5.1 Atom-transfer radical addition reactions under mild conditions with [($C_6H_3{}^iPr_3$)$RuCl_2$]$_2$ and $PCy_3$ as the catalyst precursors

The complex [(cymene)$RuCl_2(PCy_3)$] (**14**) has emerged as a versatile catalyst precursor for synthetically important transformations such as ring closing- [153, 154] and ring opening- [155–160] olefin metathesis reactions and atom-transfer radical polymerizations [97–100]. An attractive feature of this catalyst is the fact that it can be prepared in-situ from commercially available [(cymene)$RuCl_2$]$_2$ (**13**) and $PCy_3$. Somewhat surprising was the observation of A. Demonceau and co-workers that complex **14**—despite its good activity in ATRP reactions—fails to catalyze atom-transfer radical additions of $CCl_4$ to olefins [108], although ATRP and ATRA are mechanistically very similar [95, 96].

The activation of **14** is thought to proceed by a thermally or photochemically induced replacement of the arene ligand [97–100, 153–160][17]. We reasoned that a sterically more demanding $\pi$-ligand might facilitate this replacement due to steric congestion with the $PCy_3$ ligand. The commonly used hexamethylbenzene complex [($C_6Me_6$)$RuCl_2$]$_2$ (**73**) was not considered because of its low solubility and because it had been reported that the reaction with $PCy_3$ does not give the monomeric complex [($C_6Me_6$)$RuCl_2(PCy_3)$] [162]. Instead, we focused on the trisisopropylbenzene complex [($C_6H_3{}^iPr_3$)$RuCl_2$]$_2$ (**72**), which can be obtained easily from **13** by arene exchange [163].

First, a coworker[18] investigated the ATRP of methyl methacrylate (MMA) by using ethyl 2-bromo-2-methylpropionate as the initiator and a mixture of **72** and $PCy_3$, as the catalyst precursors (**72**/$PCy_3$/initiator/MMA = 1:2:4:1600). The reaction was carried out at a temperature of only 50 °C, which is significantly below the 80 – 85 °C commonly employed for ruthenium catalyzed MMA polymerizations[19]. After 24 h, PMMA could be isolated in 90 % yield. A comparison of the initial turnover frequencies revealed that under these mild conditions, the new catalyst **72**/$PCy_3$ (TOF = 59 $h^{-1}$) is one order of magnitude more active than the previously reported system **13**/$PCy_3$ (TOF =

16. Part of the work described in this section have been published, see ref. [101, 152].

17. For an early report on arene replacement reactions of [(cymene)$RuCl_2(PR_3)$] complexes see ref. [161].

18. The ATRP experiments were performed by Dr. Michel Haas, a postdoctoral researcher in the group of K. Severin.

19. See references cited in ref. [101].

5 $h^{-1}$), which was considered to be one of the most active Ru-based catalyst system described so far. Other olefinic monomers, such as ethyl methacrylate, were successfully polymerized [101].

Encouraged by the success of the new catalyst system in ATRP reactions, we have investigated the ATRA of $CCl_4$ and of $CHCl_3$ to styrene. Again, the catalyst was prepared in-situ by mixing **72** with two equivalents of $PCy_3$ (**72**/styrene/$CHCl_3$ = 1:300:450). Two reactions were carried out in toluene at 40 °C: one in the presence of a light source of moderate intensity, the other in the dark. Reactions with $CCl_4$ gave nearly zero conversion, whereas a conversion of 65 % (yield: 63 %) was observed after 24 h for reactions with $CHCl_3$ that had no influence of the light source. These results were surprising in view of the higher intrinsic reactivity of $CCl_4$ but in accordance with the observation that complex **14** is not able to promote the addition of $CCl_4$ to styrene [108].

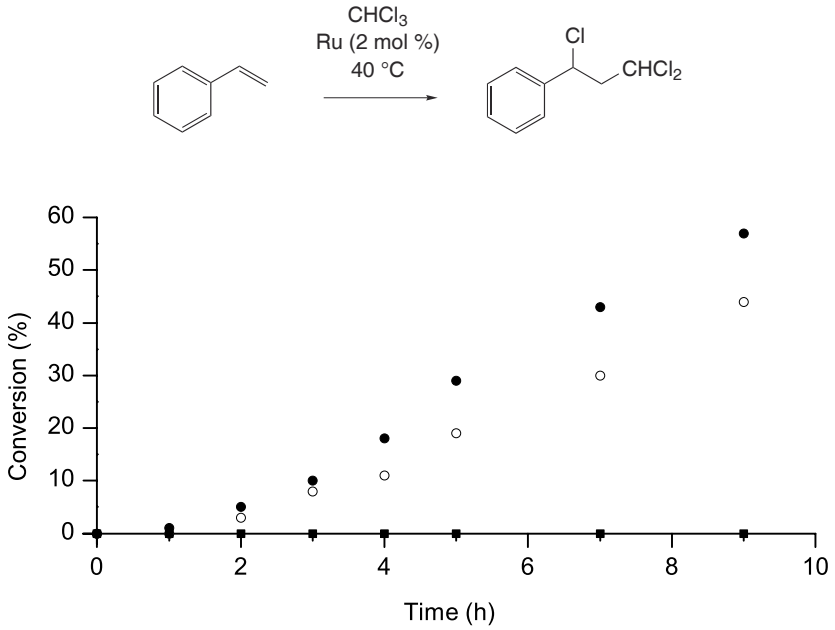


**Figure 2.13:** Time course of reactions between styrene and $CHCl_3$, catalyzed by [($C_6H_3{}^iPr_3$)-$RuCl_2$]$_2$ (**72**) + 2 $PCy_3$ (•), **72** + 1 $PCy_3$ (○), and [(cymene)$RuCl_2$]$_2$ (**13**) + 2 $PCy_3$ (■). Reaction conditions: **13** or **72**/styrene/$CHCl_3$ = 1:100:150, [**13** or **72**] = 13.8 mM, solvent = toluene, reaction volume = 1 mL, $T$ = 60 °C, no light. The conversion is based on the consumption of styrene as determined by GC.

The time course of reactions between styrene and $CHCl_3$ catalyzed by complex **72** in the presence of one and two equivalents of $PCy_3$ is depicted in Figure 2.13 ([**72**] = 1 mol %). An induction period is clearly visible, which indicates that catalyst activation must

take place. A Ru/$PCy_3$ ratio of 1:1 is advantageous, although the rates at a later stage of this reaction (4 – 9 h) are similar to the reaction rates observed when substoichiometric amounts of $PCy_3$ are present. As in the case of the polymerization reactions, the nature of the $\pi$-ligand was found to be crucial: Reactions performed with the cymene complex **13** instead of the trisisopropylbenzene complex **72** gave zero conversion[20].

**Table 2.8:** ATRA reactions catalyzed by $[(C_6H_3{}^iPr_3)RuCl_2]_2$ (**72**)/$PCy_3$ or $[\{(C_6H_3{}^iPr_3)Ru(\mu\text{-}Cl)_3RuCl(PCy_3)\}_2(\mu\text{-}N_2)]$ (**94**).

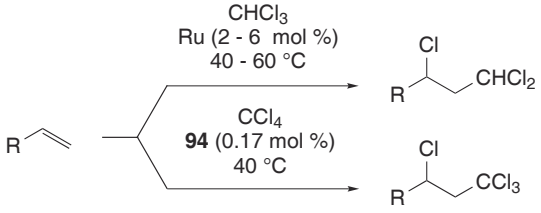


| Entry | Catalyst | Olefin | $CXCl_3$ | $T$ ($^\circ$C) | $t$ (h) | Conv./Yield (%) |
|---|---|---|---|---|---|---|
| 1 | **72**/$PCy_3$ | styrene | $CHCl_3$ | 40 | 48 | 95/91[a] |
| 2 | **72**/$PCy_3$ | *p*-chlorostyrene | $CHCl_3$ | 40 | 48 | 93/84[a] |
| 3 | **72**/$PCy_3$ | *p*-methoxystyrene | $CHCl_3$ | 40 | 48 | 98/95[b] |
| 4 | **72**/$PCy_3$ | 1-vinylnaphtalene | $CHCl_3$ | 60 | 48 | 73/69[b] |
| 5 | **72**/$PCy_3$ | MMA | $CHCl_3$ | 40 | 48 | 92/15[a] |
| 6 | **72**/$PCy_3$ | 1-decene | $CHCl_3$ | 40 | 48 | 14/14[a] |
| 7 | **94** | styrene | $CHCl_3$ | 40 | 1 | 25/19[c] |
| 8 | **94** | styrene | $CHCl_3$ | 40 | 48 | 93/88[c] |
| 9 | **94** | styrene | $CCl_4$ | 40 | 2 | 99/98[d] |
| 10 | **94** | MMA | $CCl_4$ | 40 | 5 | 89/65[d] |
| 11 | **94** | 1-decene | $CCl_4$ | 40 | 5 | 67/66[d] |

[a] **72**/$PCy_3$/olefin/$CHCl_3$ = 1:2:100:150, [**72**] = 13.8 mM, reaction volume = 0.5 mL; [b] **72**/$PCy_3$/olefin/$CHCl_3$ = 3:6:100:150, [**72**] = 41.4 mM, reaction volume = 0.5 mL; [c] **94**/olefin/$CHCl_3$ = 1:200:300, [**94**] = 6.9 mM, reaction volume = 0.5 mL; [d] **94**/olefin/$CCl_4$ = 1:600:900, [**94**] = 2.3 mM, reaction volume = 1 mL. All reactions were performed in toluene in absence of light. The conversion is based on the consumption of the olefin and the yield is based on the formation of the product as determined by GC or $^1$H NMR spectroscopy after the time given.

20. At higher temperatures or upon photochemical activation, the ATRA of $CHCl_3$ to styrene was also observed for reactions with **13** and $PCy_3$.

To test the scope and the limitations of the new catalyst system, **72**/$PCy_3$, we investigated ATRA reactions with different olefins (Table 2.8). The $CHCl_3$ adducts of the aromatic olefins *p*-chlorostyrene, *p*-methoxystyrene, 1-vinylnaphthalene and styrene (Entries 1 – 4) were obtained in yields between 69 and 95 % with a ruthenium catalysts concentration of 2 – 6 mol % at 40 °C (Entries 1 – 3) or 60 °C (Entry 4). It should be noted that for a Ru-based catalyst, synthetically useful yields above 80 % have been described only for the carbene complex $[RuCl_2(CHPh)(PCy_3)_2]$ (**12**) (2.5 – 7.5 mol %, 65 – 80 °C) [107,164]. Using a substrate/**72** ratio of 1000:1, we were able to obtain the $CHCl_3$ adduct of styrene in 57 % yield after two weeks[21]. This corresponds to 285 turnovers per ruthenium, which is, to the best of our knowledge, one of the highest value ever reported[22]. MMA is a less suited substrate because polymerization becomes a significant side reaction, in accordance with the results described above (Entry 5). The substrate 1-decene was found to be difficult to convert (Entry 6).

To obtain more information about the mode of activation for reactions with the new catalyst system, we examined solutions of **72** and $PCy_3$ in toluene-$d^8$ by $^1$H and $^{31}$P NMR spectroscopy. At room temperature, an equilibrium between **72**, $PCy_3$ and the monomeric complex $[(C_6H_3{}^{i}Pr_3)RuCl_2(PCy_3)]$ (**93**) was rapidly established, with 25 % of the ruthenium being present in the form of **72** and 75 % in the form of the monomer **93** (Scheme 2.10). This reaction was followed by slow liberation of the arene ligand. At 40 °C, this displacement proceeded with a half-life of $t_{1/2} = 5$ h. When the reaction mixture was allowed to cool to room temperature, an orange, crystalline complex precipitated. This compound was identified by a co-worker[23] as the tetranuclear complex $[\{(C_6H_3{}^{i}Pr_3)Ru(\mu\text{-}Cl)_3RuCl(PCy_3)\}_2(\mu\text{-}N_2)]$ (**94**) based on elemental and crystallographic analysis [101]. For comparison, the reaction between the cymene complex **13** and $PCy_3$ was investigated. In this case, the equilibrium was found to be completely on the side of the monomeric complex **14**, and arene displacement required significantly harsher reaction conditions ($t_{1/2}$ = 13 h, 60 °C). When the heating was stopped after 12 h, an orange complex precipitated. Again, the result of the elemental analysis suggested that a tetranuclear

21. Reaction conditions: **72**/$PCy_3$/styrene/$CHCl_3$ = 1/2/1000/1500, [**72**] = 1.38 mM, solvent = toluene-$d^8$, reaction volume = 2 mL, $T$ = 40 °C.

22. Besides complex $[Cp^{\star}Ru(PPh_3)_2(CH_3CN)]OTf$ (**88**), which gave TONs up to 890 under similar reaction conditions (Section 2.4), see Footnote 14, p. 56.

23. The synthesis and characterization of complex **94** was carried out by Dr. Euro Solari, a scientific co-worker in the group of K. Severin.

dinitrogen complex (**95**) of low solubility had formed.

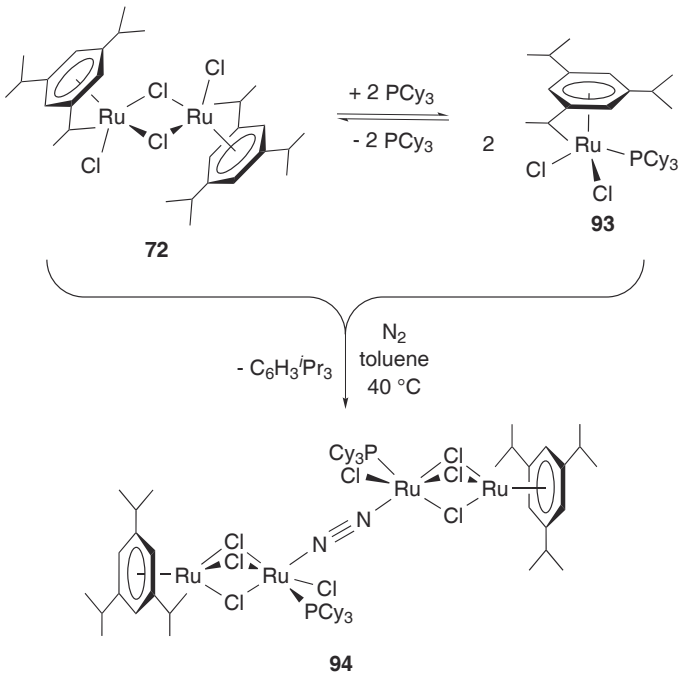


**Scheme 2.10:** In the presence of $PCy_3$, the dimeric complex **72** is in equilibrium with the monomeric complex **93**. Partial loss of the arene ligand leads to the formation of the tetranuclear complex **94**.

The tetranuclear complex **94** is a very active ATRA catalyst. For the addition of $CHCl_3$ to styrene, for example, a yield of 19 % was observed after only one hour at 40 °C (Table 2.8, Entry 7). The final yield after 48 h was similar to what was found for **72**/$PCy_3$ (Entry 8). Interestingly, complex **94** can also effect the addition of $CCl_4$ to olefins (Entries 9 – 11). The observed TOFs are comparable to the best ATRA catalysts described so far, despite the low reaction temperature[24]. In this context it is interesting to note that two other complexes containing a {Ru–N=N–Ru} structural motif were reported to catalyze atom-transfer radical reactions: the tetranuclear complex [{(tpc)Rh($\mu$-Cl)$_3$Ru(dcypb)}$_2$-($\mu$-$N_2$)] (**82**), introduced in Subsection 2.2.2, and a binuclear complex, developed by G. van Koten *et al.* [165]. For both complexes it was suggested that catalyst activation proceeds via a $CCl_4$-induced loss of the $N_2$ ligand, and a similar mode of activation appears likely for reactions with **94**.

Since the mixture of **72** and $PCy_3$ was inactive for $CCl_4$ additions, $CCl_4$ seemed to

24. A yield of 70 % was measured after 30 min with the reaction conditions: **94**/styrene/$CCl_4$ = 0.5:300:450, [**94**] = 2.3 mM, solvent = toluene-$d^8$, reaction volume = 1 mL, $T$ = 40 °C. This corresponds to a TOF of 420 $h^{-1}$.

interfere with catalyst activation. Control experiments showed that this is indeed the case. $CCl_4$ was found to react immediately with $PCy_3$ to give a trichloromethylphosphonium salt[25]. The phosphine is thus removed form the equilibrium between **72** and **93**, which prevents the formation of the catalytically active ruthenium complex[26].

### 2.5.2 ATRA reactions catalyzed by [(cymene)$RuCl_2$]$_2$/$PCy_3$

The mixture of the complex [($C_6H_3{}^iPr_3$)$RuCl_2$]$_2$ (**72**) and $PCy_3$ can be used to efficiently catalyze atom-transfer radical reactions at exceptionally low temperatures. There is strong evidence that catalyst activation proceeds by a $PCy_3$-induced substitution of the arene ligand. The rate of this reaction was found to be slower for the cymene complex **13** than for the more sterically demanding $C_6H_3{}^iPr_3$ complex **72**. As a consequence, **72**/$PCy_3$ could be used to catalyze the ATRA of $CHCl_3$ to styrene at a temperature of 40 °C, whereas [(cymene)$RuCl_2$]$_2$ (**13**)/$PCy_3$ required either a higher temperature or an activation by light.

**Table 2.9:** Addition of $CHCl_3$ to styrene, catalyzed by mixtures of [(arene)$RuCl_2$]$_2$ and $PCy_3$.[a]

| Entry | Arene | Phosphine | Conv. (%) |
|---|---|---|---|
| 1 | benzene | $PCy_3$ | 69 |
| 2 | cymene | $PCy_3$ | 84 |
| 3 | $C_6H_3Et_3$ | $PCy_3$ | 85 |
| 4 | $C_6H_3{}^iPr_3$ | $PCy_3$ | 79 |
| 5 | $C_6Me_6$ | $PCy_3$ | 0 |
| 6 | $C_6H_5CO_2Et$ | $PCy_3$ | 84 |
| 7 | $C_6H_3Me_3$ | $PCy_3$ | 27 |
| 8 | toluene | $PCy_3$ | 60 |
| 9 | cymene | $PCy_2$(naph) | 5 |
| 10 | cymene | PBu(adam)$_2$ | 47 |

[a] Reaction conditions: Ru/$PCy_3$/styrene/$CHCl_3$ = 2:2:100:150, [Ru] = 27.6 mM, solvent = toluene, reaction volume = 0.5 ml, $T$ = 40 °C, with light. The conversion is based on the consumption of styrene as determined by GC after 10 h.

25. $PPh_3$ shows a similar reactivity [166].

26. When **72** and $PCy_3$ are heated in toluene prior to the addition of the two substrates styrene and $CCl_4$, conversions are observed.

We investigated whether other $[(\text{arene})RuCl_2]_2$ complexes could generate catalytically active species in the presence of $PCy_3$. Atom-transfer radical additions of $CHCl_3$ to styrene were performed with 2 mol % of ruthenium at a temperature of 40 °C under the light of a conventional 40 W globe (Table 2.9).

Most of the combinations displayed substantial activity (27 – 85 %, Entries 1 – 7). As expected, the $\{(C_6Me_6)Ru\}$ complex gave zero conversion (Entry 5). Under these conditions, the {(cymene)Ru} complex (84 %, Entry 2) was found to be as effective as the $\{(C_6H_3{}^{i}Pr_3)Ru\}$ complex (79 %, Entry 4). This is of special interest, since the complex $[(\text{cymene})RuCl_2]_2$ (**13**) has the advantage to be commercially available. The utilization of the sterically demanding ligands dicyclohexyl-1-naphtalenylphosphine ($PCy_2$(naph); Entry 9) and diadamantyl-*n*-butylphosphine ($PBu(adam)_2$; Entry 10) resulted in lower conversions.

**Table 2.10:** Addition of $CHCl_3$ to different olefins, catalyzed by $[(\text{cymene})RuCl_2]_2$ (**13**)/$PCy_3$.[a]

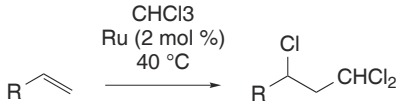


| Entry | Olefin | Conv./Yield (%)[a] |
|---|---|---|
| 1 | styrene | 96/88 |
| 2 | *p*-chlorostyrene | 97/86 |
| 3 | *p*-methoxystyrene | 94/88 |
| 4 | 1-vinylnaphtalene | 41/37 |
| 5 | MMA | 90/15 |
| 6 | 1-decene | 25/24 |

[a] Reaction conditions: **13**/$PCy_3$/olefin/$CHCl_3$ = 1:2:100:200, [**13**] = 13.8 mM, solvent = toluene-$d^8$, reaction volume = 500 $\mu$l, $T$ = 40 °C, with light. The conversion is based on the consumption of the olefin and the yield is based on the formation of the product as determined by GC or $^1$H NMR spectroscopy after 24 h.

Further investigations demonstrated that **13**/$PCy_3$ is a remarkably efficient catalyst system for the addition of $CHCl_3$ (Table 2.10). Almost complete conversions with 86 – 88 % yield were observed for styrene and derivatives after only 24 hours (Entries 1 – 3). This catalytic performance is superior to what was observed for **72**/$PCy_3$, for which 48 hours

were needed to reach similar conversions (Table 2.8, p. 60). As observed with **72**/$PCy_3$, the reactions with MMA produce significant amounts of oligomers (Entry 5) and the substrates 1-vinylnaphtalene and 1-decene were found to be more difficult to convert.

### 2.5.3 A bimetallic ruthenium ethylene complex as a catalyst precursor for the Kharasch reaction

As outlined in the two previous subsections, mixtures of the chloro-bridged dimers **72** or **13** and $PCy_3$ proved to be efficient catalysts for addition reactions of $CHCl_3$ to aromatic olefins under mild conditions. As a product of the reaction between **72** and $PCy_3$, the tetranuclear complex [{($C_6H_3{}^iPr_3$)Ru($\mu$-Cl)$_3$RuCl($PCy_3$)}$_2$($\mu$-$N_2$)] (**94**) has been identified, which itself proved to be a very efficient catalyst. The general utility of complex **94** in atom transfer radical reactions, however, is limited by its low solubility. Therefore, we have investigated whether it was possible to replace the bridging nitrogen ligand by other labile two-electron-donor ligands. Furthermore, we wanted to focus on the {(cymene)Ru} system, which would allow the use of the commercially available complex **13** as the starting material.

As a potential substitute for the $\mu$-$N_2$ ligand of the catalyst precursor **94**, olefins appeared to be of special interest since olefin $\pi$-complexes have been discussed as intermediates in the catalytic cycle of ruthenium-catalyzed Kharasch reactions [106]. The reaction of complex **13** with 1 equivalent of $PCy_3$ in the presence of various olefins has been investigated by a co-worker[23, p.61]. When the reaction was performed under an atmosphere of ethylene, complex [(cymene)Ru($\mu$-Cl)$_3$RuCl($PCy_3$)($\eta^2$-$C_2H_4$)] (**96**) could be obtained in the form of red crystals in 80 % yield (Scheme 2.11) [152].

Complex **96** is well soluble in methylene chloride and moderately soluble in aromatic solvents such as benzene and toluene. In solution, the ethylene ligand was found to be rather labile.

**Scheme 2.11**

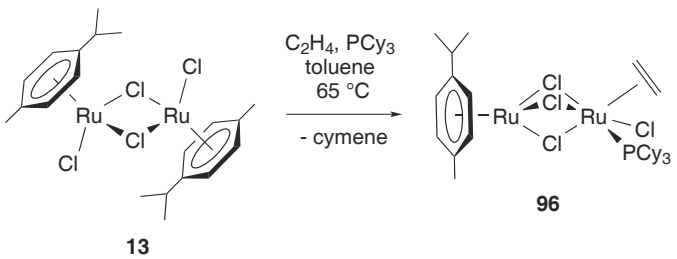


**13** **96**

The ability of complex **96** to catalyze the addition of $CCl_4$ and $CHCl_3$ to olefins has been investigated. With $CCl_4$ and styrene as the substrates and 0.33 mol % of complex **96**, a very fast and clean reaction was observed at room temperature. After only 30 min, a yield of 88 % was obtained, and after 2 h, the reaction was complete (Table 2.11, Entry 1). The initial turnover frequency was determined to be 1100 $h^{-1}$ at 24 °C, 1550 $h^{-1}$ at 40 °C, and 1650 at 60 °C[27]. These values are comparable to those found for the most active ruthenium catalyst described so far, a half-sandwich dicarbollide complexes of the formula [RuH(9-$SR_2$-7,8-$C_2B_9H_{11}$)($PPh_3$)$_2$] [117, 118]. The activity of the new catalyst **96** was so high that the addition of $CCl_4$ to styrene could be performed at 0 °C. After 10 h, a quantitative conversion was observed (Entry 2). When the substrate to catalyst concentration ratio was increased to 2000:1 (0.05 mol % of **96**), it was still possible to obtain a yield of 90 % (TON = 1800)[28]. Due to partial catalyst deactivation, however, significantly longer reaction times were required (21 d).

Other olefins such as *p*-methoxystyrene (Entry 3) and acrylates (Entries 4 – 7) were also converted to the corresponding $CCl_4$ adducts in good yields at 0 or 24 °C using 0.33 mol % of complex **96**. As expected, a reaction temperature of 0 °C resulted in slower rates (Entries 5 and 7). For methyl methacrylate as the substrate, however, the low reaction temperature was found to be beneficial, because the reaction proceeded with slightly fewer side products and gave a higher TON.

With 1-decene, a difficult substrate for Kharasch additions, a conversion of 92 % and a yield of 81 % was determined after 24 h (Entry 8). Here, it was advantageous to use a relatively low $CCl_4$ to olefin ratio of 1.5:1. For higher ratios, faster rates and fewer side products were observed but the lifetime of the catalyst was reduced and the final yield was therefore lower.

For addition reactions with the significantly less active substrate $CHCl_3$, the reaction temperature was increased to 40 °C and a catalyst concentration of 1.0 mol % was employed. Under these conditions, the chloroform adducts of the aromatic substrates styrene and *p*-chlorostyrene were obtained in very good yields (Entries 9 and 10). It should be noted that, so far, there have been only very few catalysts for which synthetically useful

27. To measure the initial rates, the reactions were performed with 0.1 – 0.2 mol % of complex **96**. The initial TOF was calculated from the yield determined after 5 min.

28. Reaction conditions: **96**/styrene/$CCl_4$ = 1:2000:4000, solvent = toluene-$d^8$ saturated with $D_2O$, reaction volume = 2 mL, $T$ = 24 °C.

**Table 2.11:** Kharasch additions of $CXCL_3$ (X = H, Cl) to olefins, catalyzed by the complex [(cymene)Ru($\mu$-Cl)$_3$RuCl(PCy$_3$)($\eta^2$-$C_2H_4$)] (**96**).[a]

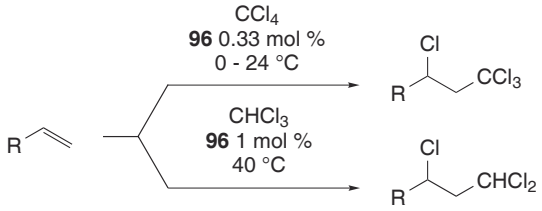


| Entry | Olefin | $CXCl_3$ | $CXCl_3$:olefin | $t$ (h) | $T$ ($^\circ$C) | Conv./Yield (%) |
|---|---|---|---|---|---|---|
| 1[c] | styrene | $CCl_4$ | 4 | 2 | 24 | 98/98 |
| 2[c] | styrene | $CCl_4$ | 4 | 10 | 0 | $\geq$99/$\geq$99 |
| 3[b,c] | *p*-methoxystyrene | $CCl_4$ | 4 | 1 | 24 | 96/96 |
| 4 | MMA | $CCl_4$ | 4 | 5 | 24 | 78/62 |
| 5 | MMA | $CCl_4$ | 4 | 12 | 0 | $\geq$99/86 |
| 6 | *n*-butylacrylate | $CCl_4$ | 4 | 5 | 24 | 80/60 |
| 7 | *n*-butylacrylate | $CCl_4$ | 4 | 48 | 0 | 79/55 |
| 8[b,c] | 1-decene | $CCl_4$ | 1.5 | 24 | 24 | 92/81 |
| 9[c] | styrene | $CHCl_3$ | 4 | 48 | 40 | 94/94 |
| 10[c] | *p*-chlorostyrene | $CHCl_3$ | 4 | 48 | 40 | 93/89 |
| 11 | MMA | $CHCl_3$ | 4 | 48 | 40 | 92/25 |

[a] Reaction conditions: **96**/olefin = 1:300 ($CCl_4$) or 1:100 ($CHCl_3$), [**96**] = 4.6 mM ($CCl_4$) or 13.8 mM ($CHCl_3$), solvent = toluene-$d^8$, reaction volume = 1 mL ($CCl_4$) or 0.5 mL ($CHCl_3$), all reaction were performed under an atmosphere of dry dinitrogen. The conversion is based on the consumption of the olefin and the yield on the formation of the product, as determined by GC or $^1$H NMR spectroscopy after the time given. [b] Solvent = $CD_2Cl_2$. [c] Solvent saturated with $D_2O$.

yields of over 80 % for this type of reaction have been reported [101,107,164]. For MMA, a conversion of 92 % was determined after 48 h (Entry 11). The yield of the desired addition product, however, was very modest, due to competing polymerization reactions.

Interestingly, for the aromatic olefins styrene, *p*-methoxystyrene, and *p*-chlorostyrene, catalyst **96** gave slightly better results when the solvents ($CH_2Cl_2$ and toluene) contained small amounts of water. For 1-decene and *n*-butyl acrylate, traces of water did not effect the reaction, whereas for MMA, water was detrimental to the addition reaction. Currently, we have no explanation for this "water-effect", but it is interesting to note

that an increased activity in the presence of small amounts of water was also observed for the bimetallic catalyst [Cp*Rh($\mu$-Cl)$_3$RuCl(PPh$_3$)$_2$] (**26**), described in Section 2.2. For the data summarized in Table 2.11, the "optimal" solvents ($\pm$ H$_2$O) were employed.

With regard to the mechanism of the reaction, it seems likely that the ethylene ligand of complex **96** is initially cleaved off to provide a free coordination site at which subsequent catalytic transformations can occur. This hypothesis was substantiated by the isolation and structural characterization of the mixed-valence Ru(II)-Ru(III) complex [(cymene)Ru($\mu$-Cl)$_3$RuCl$_2$(PCy$_3$)] (**97**) (Figure 2.14), which was obtained by reaction of complex **96** with CCl$_4$ (Scheme 2.12). The formation of this complex is in accord with the general assumption that a reversible oxidation of the metal complex is a key step in ATRA reactions. Furthermore, a GC-MS analysis of the reaction mixture revealed the presence of hexachloroethane and of the Kharasch adduct of the ethylene ligand, 1,1,1,3-tetrachloropropane, which demonstrates that the initial ethylene ligand of catalyst **96** also undergo a Kharasch addition.

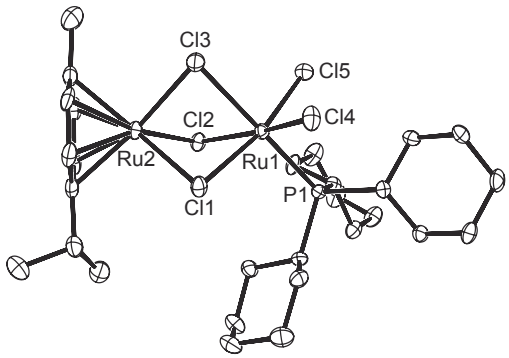


**Figure 2.14:** ORTEP drawing of the molecular structure of **97** in the crystal, the hydrogen atoms and solvent molecules are omitted for clarity. Selected bound lengths (Å) and angles ($^\circ$): Ru–Cl$^{b[a]}$ 2.45, Ru1–Cl$^{t[a]}$ 2.31, Ru1–P1 2.3304(13); Cl4–Ru1–Cl5 94.79(6), Cl–Ru1–P1$^{[a]}$ 90.34; [a] Average values; $b$ = bridging, $t$ = terminal.

From a structural point of view, complex **97** is very similar to complex [(cymene)Ru($\mu$-Cl)$_3$RuCl$_2$(PPh$_3$)] (**65**) (Figure 2.2, p. 32). The more basic and sterically demanding PCy$_3$ ligand resulted in a slightly longer Ru–P bond length for **97** (2.330 Å) as compared to **65** (2.228 Å). The angles between the terminal chloro ligands, the Ru, and the phosphine ligand, however, are very similar for the two complexes (92.12 and 88.55 $^\circ$ for **97** and 89.20 and 91.18 $^\circ$ for **65**).

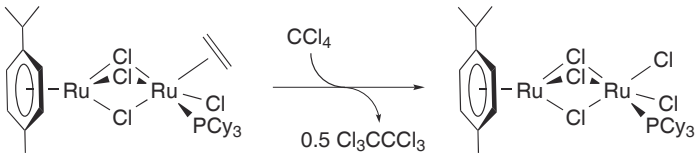


**Scheme 2.12:** Oxidation of complex **96** in presence of $CCl_4$.

## 2.6 Synthesis, Structure, and Reactivity of Homo- and Heterobimetallic Complexes of the General Formula [LM($\mu$-Cl)$_3$RuCp$^\star$] (LM = (arene)Ru, Cp$^\star$Ir, or Cp$^\star$Rh)[29]

The synthesis of mixed complexes with three halogeno-bridges can most conveniently be accomplished by metathesis reactions starting with the corresponding homodimeric compounds (see Introduction, Scheme 1.7, p. 8, Methods E and F). This method allows to synthesize a structurally diverse set of homo- and heterobimetallic complexes in relatively short time. This was substantiated by our work about combinatorial synthesis and catalysis (Sections 2.1 – 2.3) [23, 123]. Alternative pathways such as ligand transfer [24, 26] or substitution [101, 152, 168, 169] reactions have also been explored. In the following section, we introduce a new procedure, which allows to synthesize complexes of the general formula [LM($\mu$-Cl)$_3$RuCp$^\star$] (LM = (arene)Ru, Cp$^\star$Ir, or Cp$^\star$Rh) in excellent yields.

### 2.6.1 Synthesis

For the synthesis of mixed complexes containing the {Cp$^\star$RuCl} fragment, the tetrameric complex [Cp$^\star$RuCl]$_4$ (**102**) seemed to be well suited. It was known that the chloro-bridges of **102** can be easily cleaved [144, 170–176]. The reaction of **102** with two equivalents of a dimeric half-sandwich complex [($\pi$-ligand)MCl$_2$]$_2$ was thus expected to give the mixed complex [($\pi$-ligand)M($\mu$-Cl)$_3$RuCp$^\star$] in an entropically favored reaction. Complex **102** can be obtained by reduction of [Cp$^\star$RuCl$_2$]$_2$ (**74**) with LiHBEt$_3$ [171] or with Zn [174, 175]. Alternatively, it can be obtained by reaction of the methoxy-bridged complex [Cp$^\star$Ru(OMe)]$_2$ (**103**) with Me$_3$SiCl [173,176]. The latter method was chosen for our reactions. For the synthesis of the homo- and heterobimetallic complexes **104** – **108**, the tetramer **102** was generated in situ by addition of Me$_3$SiCl to complex **103** in CH$_2$Cl$_2$. Subsequent addition of [($\pi$-ligand)MCl$_2$]$_2$ gave the mixed products **104** – **108** (Scheme 2.13). Complex **102** displays a high solubility in a variety of non-polar organic solvents and even in hydrocarbons such as pentane. It was thus possible to use a slight excess of **103** (1.2 ×) with respect to the dimer [($\pi$-ligand)MCl$_2$]$_2$ because additional **102** could easily be removed by washing with pentane. The homobimetallic product **108**, on the other hand, was itself soluble in pentane. We therefore used a slight excess of [(C$_6$H$_3$$^i$Pr$_3$)-

29. Part of the work described in this section has been published, see ref. [167].

$RuCl_2]_2$ (**72**) (1.2 ×) and purified the product **108** by extraction with pentane.

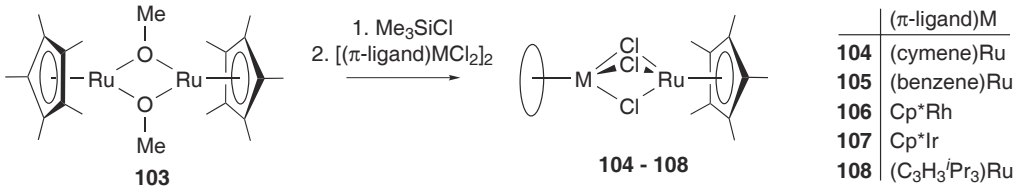


| | (π-ligand)M |
|---|---|
| **104** | (cymene)Ru |
| **105** | (benzene)Ru |
| **106** | Cp*Rh |
| **107** | Cp*Ir |
| **108** | ($C_3H_3{}^iPr_3$)Ru |

**Scheme 2.13:** Synthesis of the complexes **104** – **108**.

### 2.6.2 Structure

The new complexes **104** – **108** were characterized by $^1$H and $^{13}$C NMR spectroscopy and by elemental analysis. In addition, the complexes **104** and **107** were analyzed by single crystals X-ray analysis (Figures 2.15 and 2.16).

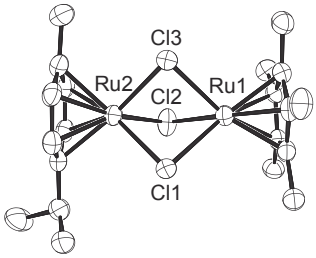


**Figure 2.15:** ORTEP drawing of the molecular structure of **104** in the crystal. The hydrogen atoms are omitted for clarity. Selected bond lengths (Å) and angles (°): Ru1–Cl1 2.5591(3), Ru1–Cl2 2.5024(14), Ru1–Cl3 2.5075(14), Ru2–Cl1 2.4521(13), Ru2–Cl2 2.4222(13), Ru2–Cl3 2.4205(13); Ru1–Cl1–Ru2 83.70(4), Ru1–Cl2–Ru2 85.53(4), Ru1–Cl3–Ru2 85.45(4), Cl1–Ru1–Cl2 76.70(4), Cl1–Ru2–Cl2 80.23(5).

The crystallographic analyses confirmed that the two metal fragments are connected by three chloro-bridges. The planes defined by the π-ligands and the plane defined by the three bridging chloro ligands are nearly parallel to each other. For complex **104**, the distances of the chloro atoms to the Ru atom attached to the cymene π-ligand (Ru–Cl = 2.42 – 2.45 Å) are shorter than those to the Ru atom attached to the Cp*ligand (Ru–Cl = 2.50 – 2.56 Å). A likely explanation for this difference is the increased Lewis acidity of the $\{(cymene)Ru\}^{2+}$ fragment compared to the $\{Cp^*Ru\}^+$ fragment. The two Ru atoms in **104** are 3.344 Å apart from each other. This is longer than what was found for the cationic dimer $[(cymene)Ru(\mu\text{-}Cl)_3Ru(cymene)]^+$ (Ru···Ru = 3.283(3) Å) [177].

In the highly symmetrical dimer **107**, a $\{Cp^*Ru\}^+$ fragment is connected via three

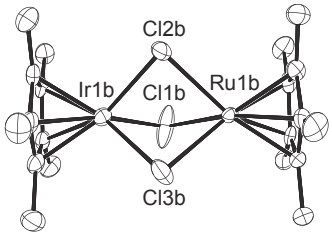


**Figure 2.16:** ORTEP drawing of the molecular structure of **107** in the crystal. Only one of the two crystallographically independent molecules is shown. The hydrogen atoms are omitted for clarity. Selected bond lengths (Å) and angles (°): Ru1b–Cl1b 2.516(3), Ru1b–Cl2b 2.509(3), Ru1b–Cl3b 2.523(3), Ir1b–Cl1b 2.413(3), Ir1b–Cl2b 2.410(3), Ir1b–Cl3b 2.428(3); Ru1b–Cl1b–Ir1b 85.32(8), Ru1b–Cl2b–Ir1b 85.54(8), Ru1b–Cl3b–Ir1b 84.86(8), Cl1b–Ru1b–Cl2b 77.90(10), Cl1b–Ir1b–Cl2b 81.85(119).

chloro-bridges to a $\{Cp^{\star}Ir\}^{2+}$ fragment. As it was observed for **104**, the M–Cl bond distances are shorter for the more Lewis acidic metal fragment: the Ir–Cl distances range from 2.41 to 2.45 Å, whereas the Ru–Cl distances range from 2.50 to 2.52 Å. Complex **107** is isoelectronic to the mixed valence Ru(II)-Ru(III) complex $[Cp^{\star}Ru(\mu\text{-}Cl)_3RuCp^{\star}]$ described by Koelle *et al.* [173, 178]. Due to the lack of structural data for the latter, a direct comparison was not possible.

### 2.6.3 Reactivity

The prevalence of polynuclear ruthenium complexes with the $M(\mu\text{-}Cl)_3Ru$ structural motif suggests that the connection via three chloro-bridges is thermodynamically very stable. In fact, it has been shown that some catalysts can be deactivated via the formation of face-bridged dimers [179]. In order to investigate the kinetic stability of the bimetallic complexes described above, crossover experiments were performed. Thus, a solution of complex $[Cp^{\star}Rh(\mu\text{-}Cl)_3RuCl(PPh_3)_2]$ (**26**) was mixed with a solution of complex **108** (both in $CD_2Cl_2$) and a $^1H$ NMR spectrum was recorded immediately after mixing. Apart from signals of the complexes **26** and **108**, the signals of two other complexes were observed (Figure 2.17). These were identified to be the mixed complexes **106** and $[(C_6H_3{}^{i}Pr_3)Ru(\mu\text{-}Cl)_3RuCl(PPh_3)_2]$ (**63**) by comparison with the $^1H$ NMR spectra of authentical samples (Scheme 2.14). The time-invariant integrals of the respective signals showed a nearly equimolar distribution of the four species. This suggests that a dynamic equilibrium between the four complexes was rapidly established after the mixing process.

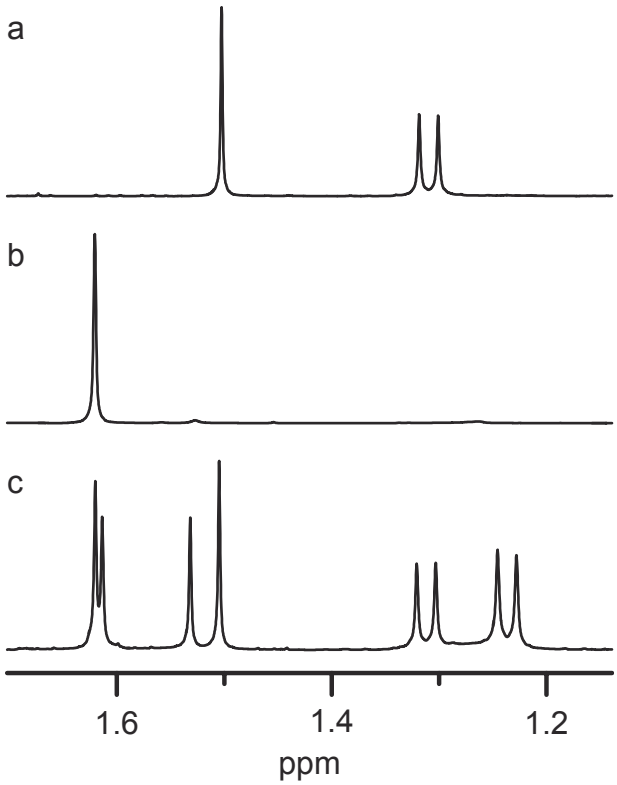


**Figure 2.17:** Part of the $^1$H NMR spectrum of a) complex **108**, b) complex **26**, and c) an equimolar mixture of complex **26** and **108**, for which the additional signals of the complexes **106** and **63** are visible.

The results described above are in agreement with a report from Stephenson *et al.* in which they show that upon mixing of $[(C_6H_6)Ru(\mu\text{-}Cl)_3Ru(C_6H_6)]^+$ and $[(C_6H_6)Os(\mu\text{-}Cl)_3Os(C_6H_6)]^+$, the heterobimetallic complex $[(C_6H_6)Ru(\mu\text{-}Cl)_3Os(C_6H_6)]^+$ is obtained in equilibrium with the two homobimetallic starting materials [180]. We have previously shown that the triply bridged complex [(dcypb)($N_2$)Ru($\mu$-Cl)$_3$RuCl(dcypb)] (**67**) reacts rapidly with doubly bridged complexes of the general formula $[LMCl_2]_2$ (LM = (cymene)Ru, Cp$^\star$Rh, Cp$^\star$Ir) to give the mixed complexes [LM($\mu$-Cl)$_3$RuCl(dcypb)] (Section 2.2). Taken together, these results point to the fact that [L'$_n$M($\mu$-Cl)$_3$RuL$_n$] complexes are generally very labile, despite their apparent thermodynamic stability. The complexes **104** – **108** are soluble in a variety of organic solvents such as acetone, THF, $CH_2Cl_2$ and $Et_2O$. The very lipophilic **108** can even be dissolved in pentane. Aromatic solvents, on the other hand, are not suited because of the very high tendency of the $\{Cp^\star Ru\}^+$ fragment to form sandwich complexes of the general formula [Cp$^\star$Ru(arene)]X [171, 173–176, 181–185]. When complex **106** was dissolved in benzene, crystals of the ionic complex [Cp$^\star$Ru(benzene)][Cp$^\star$RhCl$_3$] (**109**) formed after a few hours (Scheme 2.15).

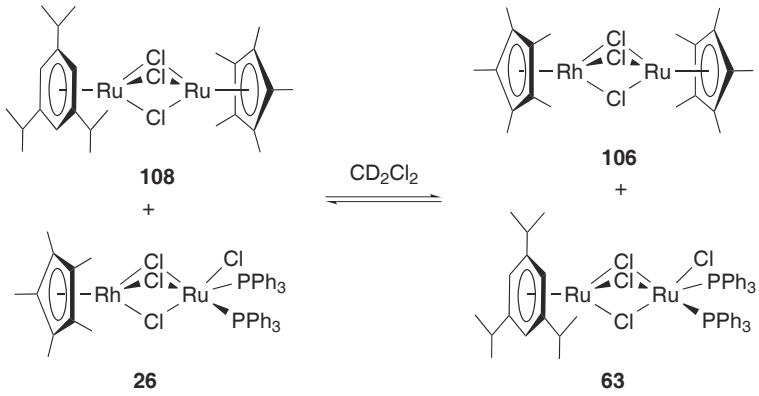


**Scheme 2.14:** In solution ($CD_2Cl_2$), the complexes **26** and **108** are in a dynamic equilibrium with the complexes **106** and **63**.

Larger amounts of **109** could be obtained by slow diffusion of hexane into a solution of **106** in benzene.

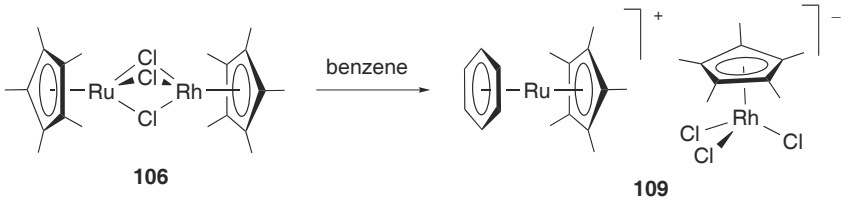


**Scheme 2.15:** The ionic complex **109** is obtained by reaction of complex **106** with benzene.

The structure of complex **109** was analyzed by single crystal X-ray analysis (Figure 2.18). The bond lengths found for the cation $[Cp^{\star}Ru(C_6H_6)]^+$ (Ru–$C_{benzene}$ = 2.21 – 2.22 Å; Ru–$C_{Cp^{\star}}$ = 2.18 – 2.19 Å) are very similar to those reported for related $[Cp^{\star}Ru(arene)]^+$ complexes [181, 184, 186]. The corresponding anion $[Cp^{\star}RhCl_3]^-$ displays a typical "piano stool" geometry with Rh–Cl bond lengths of 2.4114(14) – 2.420(2) Å. The formation of this anion is rather unusual[30] given the thermodynamic stability of the $[Cp^{\star}Rh(\mu\text{-}Cl)_3RhCp^{\star}]^+$ cation [24,188,189]. It underlines the fact that the generation of $[Cp^{\star}Ru(C_6H_6)]^+$ is the driving force for the reaction.

30. In solution, the complex $[(Cp^{\star}RhCl_2)_2(\mu\text{-}NH_2NMe_2)]$ was found to be in an equilibrium with ionic species $[Cp^{\star}RhCl(\mu\text{-}NH_2NMe_2)]_2^{2+}$ 2 $[Cp^{\star}RhCl_3]^-$ [187].

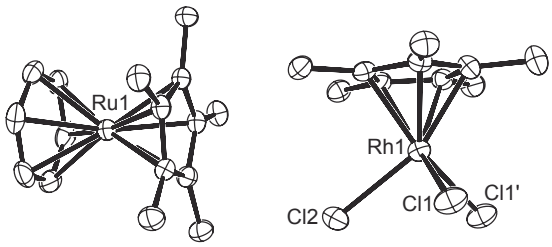


**Figure 2.18:** 4. ORTEP drawing of the molecular structure of **109** in the crystal. The hydrogen atoms are omitted for clarity. Selected bond lengths (Å) and angles ( $^\circ$ ): Rh1–Cl1 2.4114(14), Rh1–Cl2 2.420(2); Cl1–Rh1–Cl2 90.97(5), Cl1–Rh1–Cl1' 91.15(7).

## 2.7 A new trinuclear complex of ruthenium

The reactions of complex $[(PPh_3)_2ClRu(\mu\text{-}Cl)_3Ru(PPh_3)_2(acetone)]$ (**21**) with dimeric complexes $[L_nRuCl(\mu\text{-}Cl)]_2$ of octahedral transition metals give mixed complexes of the formula $[L_nM(\mu\text{-}Cl)_3RuCl(PPh_3)_2]$ (Scheme 2.16). For reactions with metal complexes adopting a square planar geometry, however, a triply bridged compound is unlikely to form. Alternative reaction products might be trinuclear complexes of the formula $[L_nM(\mu\text{-}Cl)_2Ru(PPh_3)_2(\mu\text{-}Cl)_2ML_n]$ (Scheme 2.16). With regard to the screening experiments described in Sections 2.2 and 2.3, the iridium complex **9**, the rhodium complexes **10** and **2**, the palladium complexes **78**, **79**, **17**, **80**, and **81**, and the platinum complex **15** could possibly form this kind of compounds.

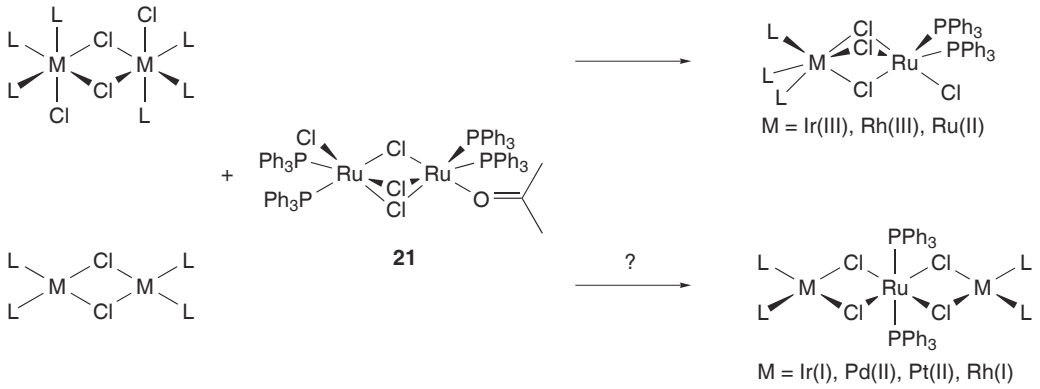


**Scheme 2.16:** Reactions of **21** with octahedral or square planar transition metal complexes.

We investigated the reactions of complex **21** with several of the above-mentioned square planar complexes. The resulting products were often mixtures of compounds, as revealed by $^1H$ and $^{31}P$ NMR spectroscopy. To our surprise, when pentane was allowed to diffuse slowly into a dichloromethane solution of **21** and $[PtCl(PEt_3)_2]_2(BF_4)_2$ (**15**) crystals of the complex $[Ru_3Cl_6(PPh_3)_5]$ (**110**) formed (Scheme 2.17), which was characterized by single crystal X-ray analysis (Figure 2.19).

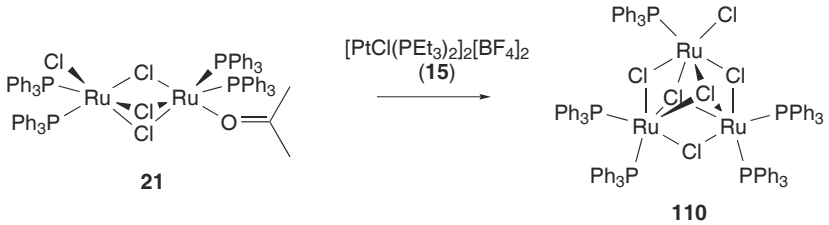


**Scheme 2.17:** Formation of complex **110**

The three ruthenium atoms of complex **110** are in a triangular arrangement and

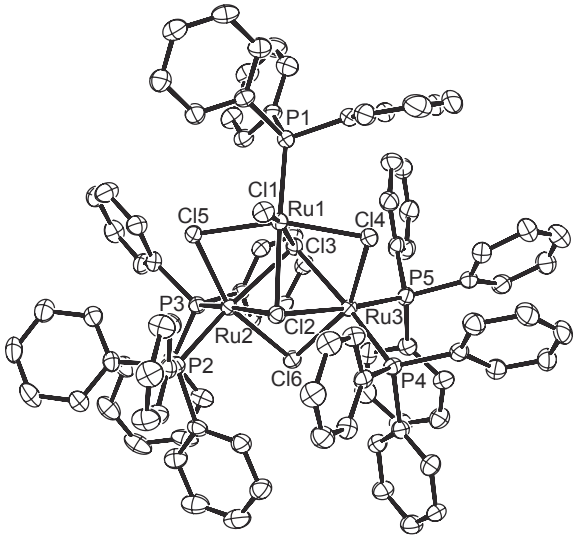


**Figure 2.19:** ORTEP drawing of the molecular structure of **110** in the crystal. The hydrogen atoms, and the solvent molecules are not shown for clarity.

are linked by three $\mu_2$-bridging chlorides and two $\mu_3$-face-capped chlorides. Two of the ruthenium atoms have, in addition, two triphenylphosphine ligands and the third one has one triphenylphosphine ligand and a terminal chloride ligand. The geometry around each ruthenium atom can thus be described as a distorted octahedron. As generally observed for chloro-bridged complexes, the Ru–Cl distance is shorter for the terminal chloro ligand than for the bridging chloro ligands. The Ru1–P1 bond length is shorter (2.2168(15) Å) than what observed for the other Ru–P bonds (2.289 – 2.306 Å), most likely due to the increased steric bulk around the ruthenium atoms bearing two triphenylphosphine ligands, which limits the approach of the ligands. For the same reason, the P1–Ru1–Cl1 angle (90.74(6) $^\circ$) is narrower than those described by the two other ruthenium atoms and their associated phosphorus atoms (97.19(6) and 96.80(6) $^\circ$).

Similar complexes having a $Ru_3Cl_5$ core have been reported [190–193]. However, the latter displayed a quasi $D_3$ symmetry, with all three ruthenium atoms being chemically identical, bearing either a chelating phosphine ligand (1,2-*bis*(diphenylphosphino)benzene [191] or binap [192, 193]) or two tripenylphosphine ligands [190]. These complexes are positively charged, with an outersphere counter anion. The distances between two ruthenium atoms (3.230 – 3.331 Å) and the distances between the ruthenium atoms and the bridging chloro ligands (2.396 – 2.501 Å) for the neutral complex **110** are consistent with those reported for the cationic complexes (Ru$\cdots$Ru 3.219 – 3.383 Å, Ru–Cl 2.370 – 2.557 Å) [190–192]. Compared with those found for the very similar complex

**Table 2.12:** Selected bond lengths (Å) and angles (°) of **110**.

| Interatomic distances (Å) | | | | | |
|---|---|---|---|---|---|
| Ru1···Ru2 | 3.230 | Ru3–P5 | 2.2900(18) | Ru2–Cl3 | 2.5014(15) |
| Ru1···Ru3 | 3.235 | Ru1–Cl1 | 2.3736(17) | Ru2–Cl5 | 2.4486(15) |
| Ru2···Ru3 | 3.331 | Ru1–Cl2 | 2.4903(14) | Ru2–Cl6 | 2.3967(15) |
| Ru1–P1 | 2.2168(15) | Ru1–Cl3 | 2.3956(16) | Ru3–Cl2 | 2.4688(17) |
| Ru2–P2 | 2.2888(17) | Ru1–Cl4 | 2.4258(14) | Ru3–Cl3 | 2.4786(13) |
| Ru2–P3 | 2.3056(16) | Ru1–Cl5 | 2.4370(14) | Ru3–Cl4 | 2.4117(15) |
| Ru3–P4 | 2.2901(14) | Ru2–Cl2 | 2.4387(14) | Ru3–Cl6 | 2.4751(15) |
| Interatomic angles (°) | | | | | |
| Ru1···Ru2···Ru3 | 59.06 | P4–Ru3–P5 | 96.80(6) | Ru1–Cl2–Ru3 | 81.42(5) |
| Ru1···Ru3···Ru2 | 58.92 | Ru1–Cl5–Ru2 | 82.77(5) | Ru2–Cl2–Ru3 | 85.48(5) |
| Ru2···Ru1···Ru3 | 62.02 | Ru1–Cl4–Ru3 | 83.92(5) | Ru1–Cl3–Ru2 | 82.51(5) |
| Cl2–Ru1–P1 | 90.74(6) | Ru2–Cl6–Ru3 | 86.24(5) | Ru1–Cl3–Ru3 | 83.13(5) |
| P2–Ru2–P3 | 97.19(6) | Ru1–Cl2–Ru2 | 81.88(4) | Ru2–Cl3–Ru3 | 83.95(5) |

$[Ru_3Cl_5(PPh_3)_6]^+$ (82.9 – 84.6 °) [190], the P–Ru–P angles are wider for complex **110** (97.19(6) and 96.80(6) °). The steric repulsion experienced by the five $PPh_3$ ligands for the neutral cluster is decreased as compared with that of the charged cluster, which itself bears six of these bulky ligands.

Regarding the formation of complex **110**, it is important to note that, due to its very low solubility, the dissolution of complex **21** is accompanied with a chemical transformation. The coordinated acetone ligand may dissociate with concomitant formation of $\{RuCl_2(PPh_3)_2\}_n$ oligomers. A recombination of the $\{RuCl_2(PPh_3)_2\}$ fragments may be the origin of the formation of the neutral cluster complex **110**. It remains to be seen, however, whether complex **21** alone can transform into **110**, or whether the participation of a reactant for the abstraction of a phosphine ligand is necessary. In the case under study, the Pt(II) complex **15** may have played this role, with concomitant formation of the mononuclear charged complex $[PtCl(PEt_3)_2(PPh_3)]^+$.

# Chapter 3

# Conclusion

BIMETALLIC complexes, in which two different metal fragments are connected by either two or three halogeno-bridges, have recently emerged as a promising new class of catalysts. The exchange of the metal fragments of two symmetrical, halogeno-bridged dimers in a metathesis reaction represents the most general and easiest way to obtain this type of compounds. When the appropriate starting materials are employed, this reaction can give rise to structurally defined products in quantitative yield. In Sections 2.1 and 2.6 of this thesis, we described the homo- and heterobimetallic complexes [($\pi$-ligand)M($\mu$-Cl)$_3$RuL$_m$] (($\pi$-ligand)M = (arene)Ru, Cp$^\star$Ir, or Cp$^\star$Rh; RuL$_m$ = RuCl(PPh$_3$)$_2$ or RuCp$^\star$). The complexes with the fragment {RuCl(PPh$_3$)$_2$} (Section 2.1) were prepared by reaction of [(PPh$_3$)$_2$ClRu($\mu$-Cl)$_3$Ru(PPh$_3$)$_2$(acetone)] (**21**) with [($\pi$-ligand)MCl$_2$]$_2$ and those with the fragment {RuCp$^\star$} (Section 2.6) by reaction of [Cp$^\star$Ru(OMe)]$_2$ (**103**) with Me$_3$SiCl and subsequent addition of [($\pi$-ligand)MCl$_2$]$_2$ (Scheme 3.1). Several representatives of the two families of compounds were structurally characterized. It is important to note that these reactions allowed to synthesize a structurally diverse set of mixed complexes in a relatively short time. This is of interest for the generation of libraries of compounds in a combinatorial fashion. Furthermore, crossover experiments have demonstrated that these complexes undergo scrambling reactions. The chloro-bridges are thus kinetically very labile, a fact which is of importance for possible applications in catalysis.

**Scheme 3.1**

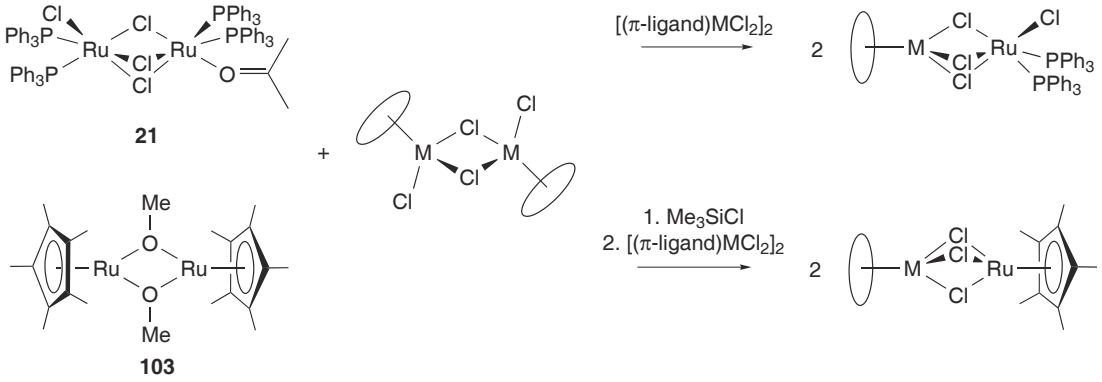


Complexes with the fragment {RuCl(PPh$_3$)$_2$} were found to be able to catalyze atom-transfer radical addition (ATRA) reactions. Our efforts to increase the number of candidates and applications in combinatorial catalysis were reported in Sections 2.2 and 2.3. As outlined in Section 2.2, structurally related complexes with chelating 1,4-*bis*(diphenylphosphino)butane (dppb) or 1,4-*bis*(dicyclohexylphosphino)butane (dcypb) ligands, instead of the two PPh$_3$ ligands, could be synthesized using the aqua complex [(dppb)Cl-

Ru($\mu$-Cl)$_2$($\mu$-OH$_2$)RuCl(dppb)] (**66**) or the dinitrogen complex [(dcypb)(N$_2$)Ru($\mu$-Cl)$_3$-RuCl(dcypb)] (**67**) instead of **21**. To investigate whether compounds of this type are useful catalyst precursors for ATRA reactions, 69 different complexes were prepared and tested in a combinatorial fashion by mixing chloro complexes of Ru(II), Ru(III), Ru(IV), Rh(I), Rh(III), Ir(I), Ir(III), Pd(II), and Pt(II) with **21**, **66**, and **67** (Figure 3.1). Using the Kharasch addition of $CCl_4$ to styrene as a benchmark reaction for ATRA, we identified two chloro-bridged Rh-Ru complexes, [Cp$^\star$Rh($\mu$-Cl)$_3$RuCl(PPh$_3$)$_2$] (**26**) and [{(tpc)Rh($\mu$-Cl)$_3$Ru(dcypb)}$_2$($\mu$-N$_2$)] (**82**), which show an exceptionally high activity.

**Figure 3.1**

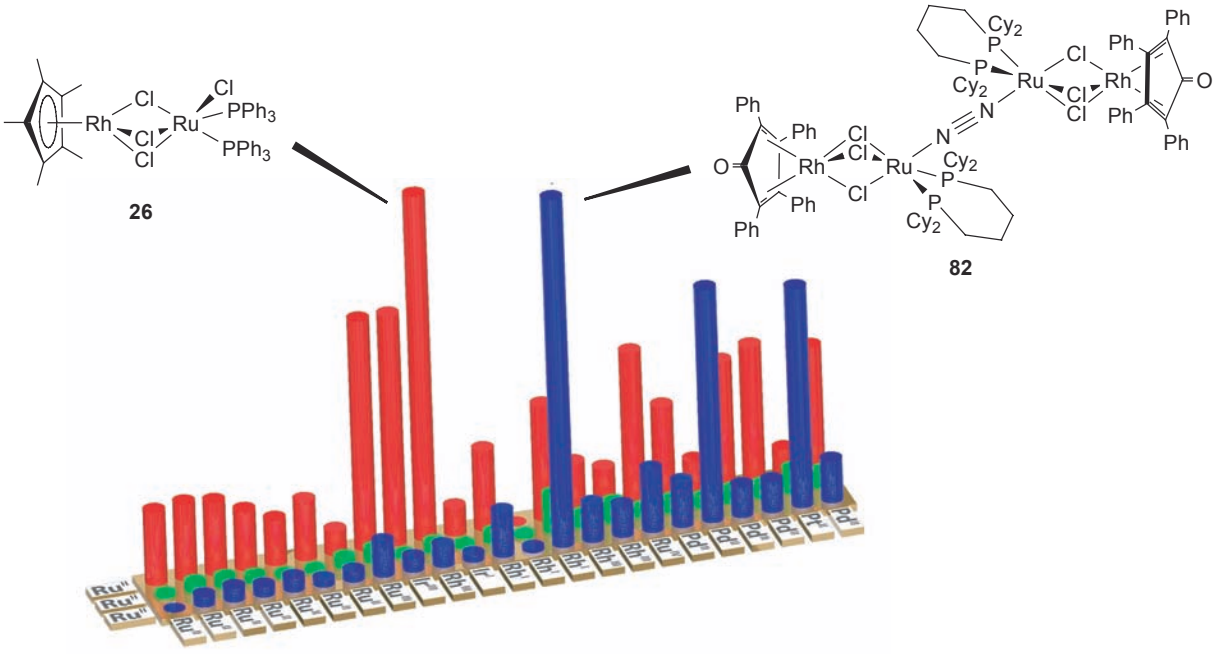


With an initial TOF of 1200 h$^{-1}$ and a maximum TON of 4500, they are among the best ATRA catalysts described so far. Aside from their high catalytic activity, the complexes **26** and **82** offer some important advantages. Since they are obtained in reactions that are fast and quantitative, they can be generated in-situ, prior to catalysis, without isolating the complex. The corresponding starting materials are easily accessible, in particular for **26**. Of special interest is the good performance of the catalysts in organic solvents of moderate purity (saturated with water). Extensive purification of the solvents, as is required for other catalysts for the Kharasch reaction, is therefore not necessary. This application clearly demonstrates the potential of halogeno-bridged heterobimetallic complexes in homogeneous catalysis. This class of compounds, however, is less suited for catalytic reactions with substrates acting as strong donor ligands (e.g., CO),

because cleavage of the halogeno-bridges is expected. Despite this limitation, we believe that libraries of homo- and heterobimetallic halogeno-bridged complexes will increasingly be used for the discovery of new transition metal catalysts.

Our research on ATRA catalysis has led us to develop and improve catalysts, which are not necessarily composed of heterobimetallic complexes. In Section 2.4, for instance, we reported that the catalytic performance of the half-sandwich complex [Cp*RuCl($PPh_3$)$_2$] (**45**) could be increased when positively charged species were generated by abstraction of a chloro ligand. As a consequence, we synthesized and assayed the cationic complex [Cp*Ru($PPh_3$)$_2$($CH_3CN$)]OTf (**88**), which displayed an increased catalyst stability compared to the neutral analogue **45** (Figure 3.2).

**Figure 3.2**

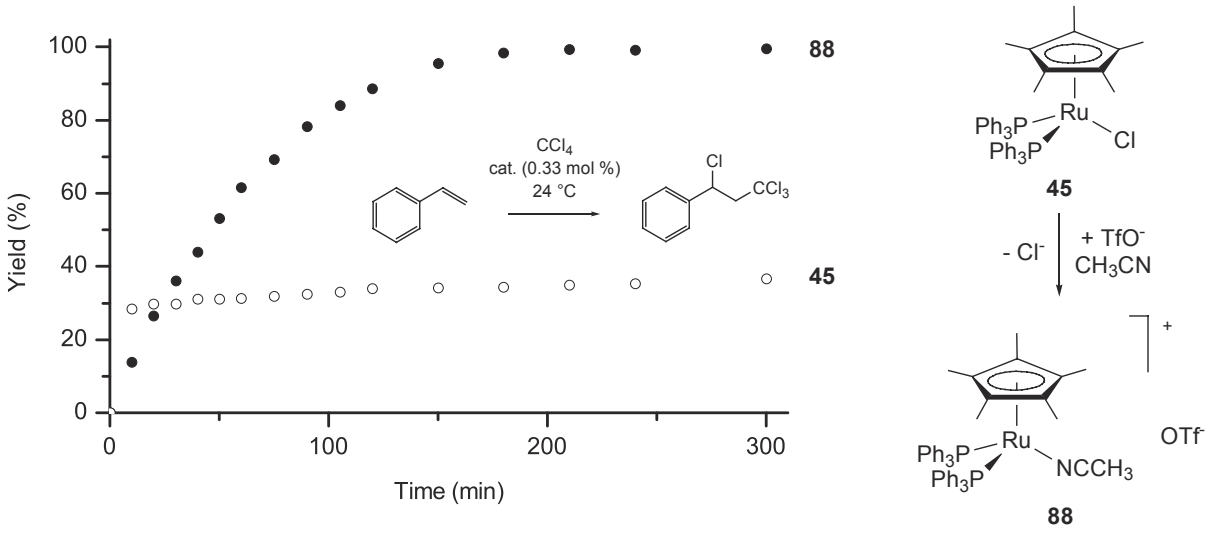


A total TON of 890 was measured for the addition of $CHCl_3$ to styrene, which represents, to the best of our knowledge, the highest value ever reported for a Ru-based catalyst. These results demonstrate that a simple modification such as the conversion of a chloro complex into a cationic acetonitrile complex may result in a significantly increased catalyst stability. Since catalyst stability is a problem for several of the newly developed complexes and, apart from optimizing the reaction conditions (temperature, concentration, etc.), solutions to this dilemma are not evident, it seems worthwhile to consider modifications of this type in further investigations.

In Section 2.5 of this thesis we discussed our efforts to develop new catalysts based on [(arene)$RuCl_2$]$_2$ and $PCy_3$. The complex [(cymene)$RuCl_2$($PCy_3$)] (**14**), which proved to be an efficient catalyst for atom-transfer radical polymerizations, was reported to be

unable to catalyze ATRA reactions with $CCl_4$. We were able to explain this rather surprizing phenomenon and we demonstrated that very good conversions and yields could be observed with $CHCl_3$. We showed that when the complex $[(C_6H_3{}^iPr_3)RuCl_2]_2$ (**72**) was employed instead of the complex $[(cymene)RuCl_2]_2$ (**13**), the formation of the catalytically active species was faster and ATRA reactions could be carried out under exceptionally mild conditions. As a product of the reaction between **72** and $PCy_3$, the tetranuclear complex $[\{(C_6H_3{}^iPr_3)Ru(\mu\text{-}Cl)_3RuCl(PCy_3)\}_2(\mu\text{-}N_2)]$ (**94**) was identified (Figure 3.3), which itself proved to be a very efficient catalyst.

**Figure 3.3**

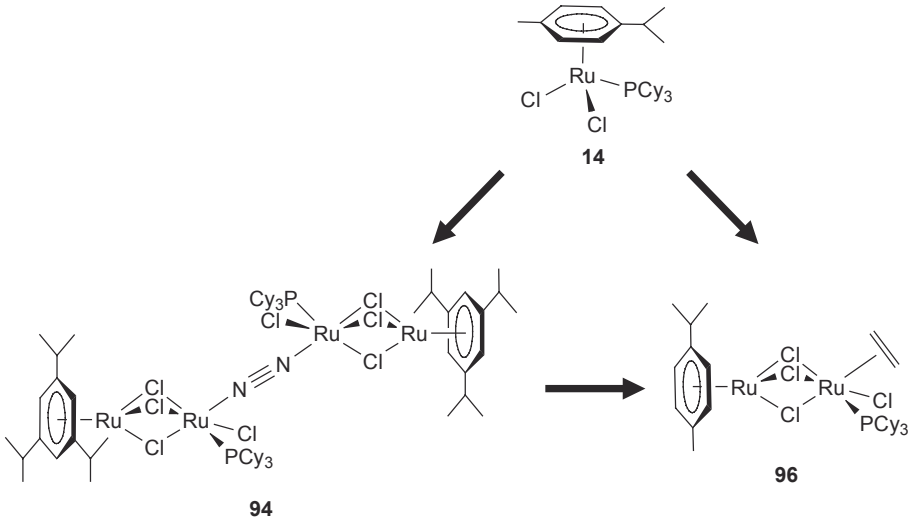


The general utility of complex **94** in ATRA reactions, however, was limited due to its low solubility. When the $C_6H_3{}^iPr_3$ and the $N_2$ ligands of **94** were exchanged for a cymene and an ethylene ligands, respectively, the mixed complex $[(cymene)Ru(\mu\text{-}Cl)_3RuCl(PCy_3)(\eta^2\text{-}C_2H_4)]$ (**96**) was obtained (Figure 3.3). The activity of **96** was so high that Kharasch additions of $CCl_4$ to 1-olefins could be carried out at a temperature as low as 0 °C. The observed TOFs at higher temperatures (1100 $h^{-1}$ at 24 °C and 1550 $h^{-1}$ at 40 °C) were comparable to those reported for the most active catalysts. From a practical perspective, complex **96** offers the advantage of being available in a one step procedure from commercially available starting materials.

Over the last 6 years, we and other laboratories have described several new ruthenium catalysts for ATRA reactions. Most of these can be used at temperatures between 60 and 85 °C. Selected catalysts are also able to provide excellent results at ambient temperature

and for the most active catalysts, the initial TOFs exceed 1000 $h^{-1}$. This is clearly superior to what is found for $[RuCl_2(PPh_3)_3]$ (**38**), which has been used as the ruthenium catalyst of choice for more than two decades. Complex **38**, however, is very robust and allows to perform "difficult" reactions at elevated temperatures. Many of the highly active catalysts suffer from a limited long-term stability. As a result, rather low TONs are observed for more challenging substrates such as 1-octene or 1-decene. Furthermore, it should be noticed that most of the new catalysts have only been used to catalyze standard reactions such as the addition of $CCl_4$ or $CHCl_3$ to terminal olefins. Since it has been shown that the catalyst performance strongly depends on the substrate employed, it needs to be demonstrated that the new complexes are also advantageous for other applications in organic synthesis. Additional motivation will come from the fact that Kharasch catalysts can often be employed for ATRP reactions and vice versa. Since these types of controlled radical processes are increasingly being used in organic synthesis and polymer science, a bright future for novel ruthenium catalysts is expected.

# Chapter 4

# Experimental Part

**General:** All reactions were performed under an atmosphere of dry dinitrogen, using standard Schlenk and vacuum-line techniques or a glovebox. The solvents, the liquid substrates and the internal standards for the ATRA reactions, and $Me_3SiCl$ were dried and distilled according to standard procedures [194] and stored under dinitrogen. The olefinic substrates were stored at a temperature of -18 °C. The solvents and the other reactives were kept at room temperature.

Triphenylphosphine (99 %), 2-vinylnaphtalene (98 %), and Zn dust (<10 microns, 98+ %) were obtained from Aldrich; NaOTf (97+ %), and tricyclohexylphosphine (≥90 %) and the complexes $[RuCl_2(CHPh)(PCy_3)_2]$ (**12**) (≥97 %) and $[(allyl)PdCl]_2$ (**17**) (≥98 %) were obtained from Fluka. Before use, the commercial chemicals were put under an atmosphere of dry dinitrogen. The complexes $[RhCl(CO)_2]_2$ (**2**) [195], $[IrCl(cod)]_2$ (**9**) [196], $[RhCl(cod)]_2$ (**10**) [197], $[(cymene)RuCl_2]_2$ (**13**) [198], $[PtCl(PEt_3)_2]_2(BF_4)_2$ (**15**) [199], $[(PPh_3)_2ClRu(\mu\text{-}Cl)_3Ru(PPh_3)_2(acetone)]$ (**21**) [26], $[Cp^\star IrCl_2]_2$ (**22**) [200], $[Cp^\star RhCl_2]_2$ (**23**) [200], $[(C_{10}H_{16})RuCl_2]_2$ (**33**) [201], $[RuCl_2(PPh_3)_3]$ (**38**) [202], $[Cp^\star RuCl(PPh_3)_2]$ (**45**) [145], $[(dppb)ClRu(\mu\text{-}Cl)_2(\mu\text{-}OH_2)RuCl(dppb)]$ (**66**) [124], $[(dcypb)(N_2)Ru(\mu\text{-}Cl)_3RuCl(dcypb)]$ (**67**) [125], $[(benzene)RuCl_2]_2$ (**68**) [161], $[(C_6H_5CO_2Et)RuCl_2]_2$ (**69**) [203], $[(C_6H_3Me_3)RuCl_2]_2$ (**70**) [163], $[(C_6H_3Et_3)RuCl_2]_2$ (**71**) [163], $[(C_6Me_6)RuCl_2]_2$ (**73**) [198], $[Cp^\star RuCl_2]_2$ (**74**) [204], $[RhCl(tpc)]_2$ (**75**) [205], $[(allyl)_2RhCl]_2$ (**76**) [206], $[(ppy)_2RhCl]_2$ (**77**) [207], $[PdCl_2(PEt_3)]_2$ (**78**) [208], $[(C_9H_{12}N)PdCl]_2$ (**80**) [209] and $[Cp^\star Ru(OMe)]_2$ (**103**) [204] were prepared according to literature procedures. The complex $[PdCl(PEt_3)_2]_2(BF_4)_2$ (**79**) was prepared in an analogous fashion as complex **15** [199]. The complex $[(C_{11}H_{14}NO_2)PdCl]_2$ (**81**) was prepared in an analogous fashion as the Pt complex **80** [209].

The $^1H$, $^{13}C$, and $^{31}P$ NMR spectra were recorded on a Bruker Avance DPX 400 or a Bruker Avance 200 spectrometer with the residual protonated solvents[1] ($^1H$) or the solvents[2] ($^{13}C$) as internal standards or a solution of $H_3PO_4$ in $D_2O$ as external standard ($^{31}P$). All spectra were recorded at room temperature unless other temperatures are mentioned.

The GC analyses were performed with a WCOT Fused Silica column (30m), coupled

1. acetone-$d^6$ 2.04, acetonitrile-$d^3$ 1.93, benzene-$d^6$ 7.15, chloroform-$d^1$ 7.24, methyl alcohol-$d^4$ 3.30, 4.78, methylene chloride-$d^2$ 5.32, toluene-$d^8$ 2.09, 6.98, 7.00, 7.09.

2. acetone-$d^6$ 29.8, 206.0, acetonitrile-$d^3$ 1.3, 118.2, benzene-$d^6$ 128.0, chloroform-$d^1$ 77.0, methyl alcohol-$d^4$ 49.0, methylene chloride-$d^2$ 53.8, toluene-$d^8$ 20.4, 125.2, 128.0, 128.9, 137.5.

to a Varian Saturn 2200 mass spectrometer for the GC-MS analyses.

The IR spectra were recorded at room temperature on a Spectrum One FT-IR Perkin-Elmer spectrometer.

**General method for the synthesis of the complexes 24, 26, and 61 – 64:** A mixture of $[(PPh_3)_2ClRu(\mu\text{-}Cl)_3Ru(PPh_3)_2(acetone)]$ (**21**) (20 – 200 mg, 13.2 – 132 $\mu$mol) and the appropriate chloro-bridged complex (1 eq.) in $CH_2Cl_2$ (5 – 10 mL) was stirred until a homogeneous solution was obtained. The solvent volume was then reduced to one half and the concentrated solution was poured into pentane (20 – 50 mL), which resulted in the precipitation of the complex. The latter was isolated by filtration, washed with $Et_2O$ (2 × 5 mL) and dried under vacuum (yield: 87 – 96 %).

**Complex 24:** Red powded. Crystals suitable for X-ray analysis were obtained by slow diffusion of pentane into a two layers system, in which a solution of **24** in $CH_2Cl_2$ was covered by a 1:1 mixture of $Et_2O$ and $CH_2Cl_2$. – $^1$H NMR (400 MHz, $CDCl_3$): $\delta$ = 1.17 (d, $^3J$ = 6.8 Hz, 6 H, $CH(CH_3)_2$), 2.09 (s, 3 H, $CH_3$), 2.76 (sept, $^3J$ = 6.8 Hz, 1 H, $CH(CH_3)_2$), 5.12, 5.31 (2 × d, $^3J$ = 5.0 Hz, 4 H, CH, cymene), 6.98 – 7.32 (m, 30 H, Ph) ppm. – $^{13}$C NMR (101 MHz, $CD_2Cl_2$): $\delta$ = 18.7, 22.3 ($CH_3$, cymene), 31.2, 78.7 (CH, cymene), 95.6, 101.7 (C, cymene), 126.1 – 136.3 (Ph) ppm. – $^{31}$P NMR (162 MHz, $CD_2Cl_2$): $\delta$ = 50.2 ppm.

**Complex 26:** Dark red powder. Crystals suitable for X-ray analysis were obtained by slow diffusion of pentane into a solution of **26** in THF. – $^1$H NMR (400 MHz, $CD_2Cl_2$): $\delta$ = 1.62 (s, 15 H, Cp$^\star$), 6.98 – 7.41 (m, 30 H, Ph) ppm. – $^{13}$C NMR (101 MHz, $CD_2Cl_2$): $\delta$ = 9.4 ($CH_3$, Cp$^\star$), 94.1 (C, Cp$^\star$), 126.2 – 136.6 (Ph) ppm. – $^{31}$P NMR (162 MHz, $CD_2Cl_2$): $\delta$ = 50.0 ppm.

**Complex 61:** Red powder. – $^1$H NMR (400 MHz, $CD_2Cl_2$): $\delta$ = 2.10 (s, 9 H, $C_6H_3(CH_3)_3$), 5.01 (s, 3 H, $C_6H_3(CH_3)_3$), 7.00 – 7.34 (m, 30 H, Ph) ppm. – $^{13}$C NMR (101 MHz, $CD_2Cl_2$): $\delta$ = 18.8 ($CH_3$), 77.3 (CH), 96.5 (C), 127.1 – 136.5 (Ph) ppm. – $^{31}$P NMR (196 MHz, $CD_2Cl_2$): $\delta$ = 50.4 ppm.

**Complex 62:** Red powder. Crystals suitable for X-ray analysis were obtained by slow diffusion of pentane into a solution of **62** in $CH_2Cl_2$. – $^1$H NMR (400 MHz, $CD_2Cl_2$): $\delta$ = 1.22 (t, $^3J$ = 7.7 Hz, 9 H, $CH_3$), 2.48 (q, $^3J$ = 7.7 Hz, 6 H, $CH_2$), 5.10 (s, 3 H, CH, $C_6H_3Et_3$), 7.00 – 7.37 (m, 30 H, Ph) ppm. – $^{13}$C NMR (101 MHz, $CD_2Cl_2$): $\delta$ = 18.8 ($CH_3$), 26.4 ($CH_2$), 75.7 (CH, $C_6H_3Et_3$), 100.8 (C, $C_6H_3Et_3$), 127.0 – 136.5 (Ph) ppm. – $^{31}$P NMR (162 MHz, $CD_2Cl_2$): $\delta$ = 50.3 ppm. – Elemental analysis: calcd (%) for $C_{48}H_{48}Cl_4P_2Ru_2 \times H_2O$ (1032.8): C 54.96, H 4.81; found: C 55.11, H 4.70.

**Complex 63:** Red powder. Crystals suitable for X-ray analysis were obtained by slow diffusion of pentane into a solution of **63** in a 1:1 mixture of $C_6H_6$ and $CH_2Cl_2$. – $^1$H NMR (400 MHz,

$CD_2Cl_2$): $\delta = 1.25$ (d, $^3J = 6.9$ Hz, 18 H, $CH(CH_3)_2$), 2.80 (hept, $^3J = 6.9$ Hz, 3 H, $CH(CH_3)_2$), 5.27 (s, 3 H, CH, $C_6H_3{}^i\mathrm{Pr}_3$), 7.00 – 7.32 (m, 30 H, Ph) ppm. – $^{13}$C NMR (101 MHz, $CD_2Cl_2$): $\delta$ = 22.5 ($CH(CH_3)_2$), 31.4 ($CH(CH_3)_2$), 75.1 (CH, $C_6H_3{}^i\mathrm{Pr}_3$), 102.5 (C, $C_6H_3{}^i\mathrm{Pr}_3$), 136.8 – 166.7 (Ph) ppm. – $^{31}$P NMR (162 MHz, $CD_2Cl_2$): $\delta$ = 49.8 ppm. – Elemental analysis: calcd (%) for $C_{51}H_{54}Cl_4P_2Ru_2$ (1072,9): C 57.09, H 5.07; found: C 57.26, H 5.06.

**Complex 64:** Orange powder. Crystals suitable for X-ray analysis were obtained by slow diffusion of pentane into a solution of **64** in $CH_2Cl_2$. – $^1$H NMR (200 MHz, $CD_2Cl_2$): $\delta$ = 2.01 (s, 18 H, $C_6Me_6$), 6.98-7.33 (m, 30 H, Ph) ppm. – $^{13}$C NMR (51 MHz, $CD_2Cl_2$): $\delta = 15.9$ ($CH_3$), 89.2 (C, $C_6Me_6$), 126.6-136.7 (m, Ph) ppm. – $^{31}$P NMR (81 MHz, $CD_2Cl_2$): $\delta$ = 50.3 ppm.

**Reaction of complex 24 with $CHCl_3$, crystal structure of complex 65:** When pentane was allowed to slowly diffuse into a solution of [(cymene)Ru($\mu$-Cl)$_3$RuCl($PPh_3$)$_2$] in $CHCl_3$, dark red crystals formed, which could be used for the structural characterization of **65**.

**Crystal structure of complex 67:** Crystals of **67**, suitable for X-ray analysis, were obtained by slow diffusion of pentane into a solution of **67** in benzene.

**Synthesis of complex 72:** Complex **72** was synthesized according to ref. [163] with a slightly modified procedure. [(cymene)$RuCl_2$]$_2$ (3.00 g, 4.90 mmol) was heated to 190 °C in $C_6H_3{}^i\mathrm{Pr}_3$ (250 mL) for 5 hours. The reaction mixture was then allowed to cool down to room temperature. Complex **72** was crystallized overnight in the fridge, isolated by filtration and washed with hexane (3 × 20 mL). The filtrate was dissolved in a 1:1 mixture of dichloromethane and hexane (100 mL) and the resulting solution was filtered. The dichloromethane was the evaporated under vacuum. This resulted in the precipitation of complex **72**, which was isolated by filtration, washed with pentane (2 × 20 mL) and dried under vacuum. Additional **72** could possibly be obtained by crystallizing the hexane solution (after the evaporation of the dichloromethane) overnight in the freezer and treating the crystalline **72** as previously mentioned. Yield: 65 – 85 %.

**Synthesis of complex 82:** A mixture of [(dcypb)($N_2$)Ru($\mu$-Cl)$_3$RuCl(dcypb)] (109.8 mg, 86.2 $\mu$mol) and [RhCl(tpc)]$_2$ (90.2 mg, 86.2 $\mu$mol) in $CH_2Cl_2$ (10 mL) was stirred until a homogeneous solution was obtained. The solution was then poured in hexane (100 mL) to precipitate a red powder, which was filtered off, washed with pentane (2 × 20 mL) and dried under a flow of dinitrogen for at least 5 hours. Yield: 87.0 mg (87 %).
Crystals suitable for X-ray analysis were obtained by slow diffusion of pentane into a solution

of **82** in $CH_2Cl_2$. – IR: $\nu_{co}$ at 1650 $cm^{-1}$. – $^1$H NMR (400 MHz, $CD_2Cl_2$): $\delta$ = 1.10 – 2.25 (m, 104 H, dcypb), 7.05 – 7.85 (m, 40 H, tpc) ppm. – $^{13}$C NMR (101 MHz, $CD_2Cl_2$): $\delta$ = 21 – 41 (dcypb), 127 – 134 (tpc) ppm. – $^{31}$P NMR (162 MHz, $CD_2Cl_2$); $\delta$ = 43.0 ppm. – Elemental analysis: calcd (%) for $C_{114}H_{144}N_2O_2Cl_6P_4Rh_2Ru_2 \times 0.5\ C_6H_{14}$ (2362.0): C 59.49, H 6.44, N 1.19; found: C 59.76, H 6.50, N 1.09.

**Synthesis of complex 83:** $[RhCl(tpc)]_2$ (43.4 mg, 41.5 $\mu$mol) and $[(dcypb)(N_2)Ru(\mu\text{-}Cl)_3RuCl(dcypb)]$ (52.9 mg, 41.5 $\mu$mol) were dissolved in a 1:1 mixture of acetone and $CH_2Cl_2$ (6 mL) and stirred for 20 min at room temperature. The solution was then concentrated to 2 mL and poured into hexane (5 mL). The precipitate red powder was isolated by filtration, washed with additional solvent (2 × 3 mL) and dried under vacuum. Yield: 74.0 mg (74 %).

– $^1$H NMR ($CD_2Cl_2$, 400 MHz): $\delta$ = 0.84 – 2.28 (m, dcypb and acetone), 7.04 – 7.88 (m, tcp) ppm. – $^{31}$P MNR ($CD_2Cl_2$, 162 MHz): $\delta$ = 43.0 ($N_2$ complex **82**), 49.7 (acetone complex **83**) ppm.

**Synthesis of complex 84:** $[RhCl(tpc)]_2$ (35.6 mg, 34 $\mu$mol) and $[(PPh_3)_2ClRu(\mu\text{-}Cl)_3\text{-}Ru(PPh_3)_2(acetone)]$ (51.4 mg, 34 $\mu$mol) were dissolved in a 1:1 mixture of acetone and $CH_2Cl_2$ (6 mL) and stirred for 20 min at room temperature. The solution was then concentrated to 2 mL and poured into hexane (5 mL). The precipitate red powder was isolated by filtration, washed with additional solvent (2 × 3 mL) and dried under vacuum. Yield: 86.9 mg (70 %).

– $^1$H NMR ($CD_2Cl_2$, 400 MHz): $\delta$ = 2.12 (s, acetone), 6.71 – 7.82 (m, Ph) ppm. – $^{31}$P MNR ($CD_2Cl_2$, 162 MHz): $\delta$ = 41.1 ppm.

**Synthesis of complex 88: a) From $[Cp^\star RuCl_2]_2$:** Zn (0.2 g, 3.1 mmol) and NaOTf (84 mg, 488 $\mu$mol) were added to a solution of $[Cp^\star RuCl_2]_2$ (100 mg, 162 $\mu$mol) in $CH_3CN$ (5 mL) and the mixture was stirred for 2 h at room temperature. The yellow solution was filtered and the remaining Zn was washed with additional solvent (2 × 3 mL). After evaporation of the solvent, the resulting powder was dissolved in $CH_2Cl_2$ (5 mL), filtered, and the filtrate was washed with additional $CH_2Cl_2$ (2 × 3 mL). $PPh_3$ (256 mg, 976 $\mu$mol) was added to the combined solutions. After 20 min stirring, the mixture was concentrated to 2 mL and poured into a flask containing hexane (15 mL) in order to precipitate the product as a yellow powder, which was then isolated by filtration, washed with hexane (2 × 3 mL), and dried under vacuum. Yield: 294 mg (95 %). **b) From**

**[Cp*Ru(CH$_3$CN)$_3$]OTf:** [Cp*Ru(CH$_3$CN)$_3$]OTf (150 mg, 295 $\mu$mol) and PPh$_3$ (232 mg, 885 $\mu$mol) were stirred for 1 h in $CH_2Cl_2$ (20 mL) at room temperature. The solvent was then removed under vacuum. The resulting powder was suspended in $Et_2O$ (20 mL), isolated by filtration, washed with pentane (2 × 10 mL) and finally dried under vacuum. Yield: 261 mg (93 %).

Single crystals were obtained by slow diffusion of pentane into a solution of **88** in $CH_2Cl_2$. – $^1$H NMR (400 MHz, $CD_2Cl_2$): $\delta$ = 1.13 (t, $^4J_{H,P}$ = 1.6 Hz, 15 H, Cp*), 2.65 (t, $^5J_{H,P}$ = 0.6 Hz, 3H, $CH_3CN$), 7.13 – 7.46 (m, 30 H, Ph) ppm. – $^{13}$C NMR (101 MHz, $CD_2Cl_2$):$\delta$ = 5.9 ($CH_3CN$), 9.7 ($CH_3$, Cp*), 93.1 (C, Cp*), 128.2 – 134.2 (Ph), 129.3 ($CH_3CN$) ppm. – $^{31}$P NMR (162 MHz, $CD_2Cl_2$): $\delta$ = 42.20 ppm. – Elemental analysis: calcd. (%) for $C_{49}H_{48}F_3NO_3P_2SRu$ × $H_2O$ (969.0): C 60.73, H 5.20, N 1.45; found C 60.84, H 5.17, N 1.56.

**Decomposition experiment of complex 88 in presence of $CCl_4$:** Complex **88** (2.8 mg, 2.9 $\mu$mol) and $CCl_4$ (2.9 $\mu$L, 30.1 $\mu$mol) were dissolved in $CD_2Cl_2$ (500 $\mu$L). The reaction was followed by $^1$H and $^{31}$P NMR (400 and 162 MHz, respectively) for 10 h at ambient temperature.

**Synthesis of complex 89:** A solution of [Cp*RuCl$_2$]$_2$ (736 mg, 1196 $\mu$mol) in $CH_3CN$ (35 mL) was added Zn (5.0 g, 76.5 mmol) and stirred for 5 h at room temperature. The initial dark brown colour changed to bright yellow. The solution was then filtered and the remaining Zn washed with additional solvent (15 mL). After evaporation of the solvent under vacuum, the resulting powder was suspended in $Et_2O$ (15 mL), isolated by filtration, washed with additional $Et_2O$ (15 mL) and dried under vacuum. Yield: 1030 mg (93 %).

Single crystals were obtained by slow diffusion of $Et_2O$ into a solution of **89** in $CH_3CN$. – $^1$H NMR (400 MHz, $CD_3CN$): $\delta$ = 1.59 (s, 15 H, Cp*) ppm. – $^{13}$C NMR (101 MHz, $CD_3CN$): $\delta$ = 9.7 ($CH_3$, Cp*), 80.6 (C, Cp*) ppm. – Elemental analysis: calcd. (%) for $C_{32}H_{48}C_{14}N_6Ru_2Zn$ × $CH_2Cl_2$ (967.2): C 42.22, H 5.32, N 10.14; found: C 42.36, H 5.36, N 9.67.

**Reaction of complex 89 with PPh$_3$, crystal structure of complex 90:** PPh$_3$ (5.7 mg, 21.7 $\mu$mol) was added to a solution of complex [Cp*Ru(CH$_3$CN)$_3$]0.5 $ZnCl_4$ (5.0 mg, 5.4 $\mu$mol) in $CD_2Cl_2$ (500 $\mu$L). The resulting bright orange solution was analyzed by $^1$H and $^{31}$P NMR spectroscopy. The reaction was found to form a mixture of compounds. The expected cationic bis(triphenylphosphine) complex **90** formed along with the neutral complex [Cp*RuCl(PPh$_3$)$_2$], the mono(triphenylphosphine) com-

plex [Cp*Ru($PPh_3$)($CH_3CN$)$_2$]0.5 $ZnCl_4$ and free triphenylphosphine.

Single crystals of **90** were obtained by slow diffusion of pentane into the reaction mixture. NMR (400 ($^1$H), 162 ($^{31}$P) MHz), aromatic protons, free $CH_3CN$ and $PPh_3$ are omitted): **90:** – $^1$H: $\delta$ = 1.13 (t, $^4J_{H,P}$ = 1.6 Hz, 15 H, Cp*), 2.87 (t, $^5J_{H,P}$ = 1.4 Hz, 3 H, $CH_3CN$) ppm. – $^{31}$P: $\delta$ = 43.0 ppm. **45:** – $^1$H: $\delta$ = 1.01 (t, $^4J_{H,P}$ = 1.4 Hz, 15 H, Cp*) ppm. – $^{31}$P: $\delta$ = 41.0 ppm. **91:** – $^1$H: $\delta$ = 1.42 (d, $^4J_{H,P}$ = 1.6 Hz, 15 H, Cp*), 2.22 (d, $^5J_{H,P}$ = 1.2 Hz, 6 H, $CH_3CN$) ppm. – $^{31}$P: $\delta$ = 48.9 ppm.

**Synthesis of complex 92: a) From [Cp*RuCl$_2$]$_2$:** A solution of [Cp*$RuCl_2$]$_2$ (100 mg, 162 $\mu$mol) in $CH_3CN$ (5 ml) was added NaOTf (84 mg, 488 $\mu$mol) and Zn dust (0.2 g, 3.1 mmol) and stirred at room temperature for 2 hours. The reaction solution was then filtered, the remaining solid washed with $CH_3CN$ (2 × 1.5 ml), and evaporated under vacuum. The solid was then dissolved in $CH_2Cl_2$ (5 ml) and the resulting solution filtered and evaporated under vacuum. Finally, the yellow powder was suspended in hexane (5 mL), filtered, washed with hexane (2 × 1.5 mL) and dried under vacuum. Yield: 122.7 mg (74 %). **b) From [Cp*Ru(CH$_3$CN)$_3$]0.5 ZnCl$_4$:** A solution of [Cp*Ru($CH_3CN$)$_3$]0.5 $ZnCl_4$ (752 mg, 812 $\mu$mol) in $CH_3CN$ (25 ml) was added AgOTf (626 mg, 2436 $\mu$mol) and stirred for 2 h at room temperature. The solution was then filtered and the precipitate washed with additional solvent (2 × 10 ml). After evaporation of the solvent under vacuum, the resulting yellow powder was suspended in $Et_2O$ (50 mL), then isolated by filtration, washed with additional $Et_2O$ (2 × 10 mL) and dried under vacuum. Yield: 721 mg (87 %).

– $^1$H NMR (400 MHz, $CD_2Cl_2$ 2): $\delta$ = 1.59 (s, 15 H, Cp*), 2.33 (br, 9 H, $CH_3CN$) ppm. – Elemental analysis: calcd. (%) for $C_{17}H_{24}F_3N_3O_3SRu$ (508.5): C 40.15, H 4.76, N 8.26; found: C 40.27, H 4.95, N 8.61.

**Reaction of PCy$_3$ with CCl$_4$:** $CCl_4$ (45 $\mu$L, 466 $\mu$mol) was added to a solution of $PCy_3$ (2.6 mg, 2.2 $\mu$mol) in toluene-$d^8$. The resulting mixture was analysed by $^{31}$P NMR and MS spectroscopy.

– $^{31}$P NMR (toluene-$d^8$, 162 MHz): $\delta$ = 41.9 ppm. – MS M/Z = 154.2 ($CCl_4$), 295.4 ($Cy_3P$=C), 329.3 ($Cy_3P$=CCl), 363.2 ($Cy_3P$=$CCl_2$), 447.3 ($Cy_3P$=CCl($CCl_3$)), 481.2 ($Cy_3P$–$CCl_2$($CCl_3$)).

**Synthesis of complex 97:** Red crystals of **97** were obtained upon heating a solution of complex [(cymene)Ru($\mu$-Cl)$_3$RuCl($PCy_3$)($\eta^2$-$C_2H_4$)] (20.1 mg, 25.6 $\mu$mol) in a mixture of toluene (0.5 mL) and $CCl_4$ (1.0 mL) to 40 °C for 2 h under an inert atmosphere. After

cooling to room temperature, the product was isolated, washed with hexane (2 × 1 mL) and pentane (1 mL), and dried under vacuum (yield 83 %).

– Elemental analysis: calcd. (%) for $C_{28}H_{47}Cl_5PRu_2$ × 3/4 $CCl_4$ (909.4): C 37.97, H 5.21; found: C 37.64, H 5.11.

**General method for the synthesis of the complexes 104 – 107:** $Me_3SiCl$ (71 $\mu$L, 561 $\mu$mol) was added to a solution of $[Cp^\star Ru(OMe)]_2$ (100 mg, 187 $\mu$mol) in $CH_2Cl_2$ (10 mL). After addition of the respective dimer $[(\pi\text{-ligand})MCl_2]_2$ (156 $\mu$mol), the solution was stirred for 20 min. The solvent was then removed in vacuum and the resulting powder was suspended in pentane (10 mL) in order to dissolve the excess of complex $[Cp^\star RuCl]_4$. The product was isolated by filtration, washed with additional pentane (3 × 2 mL) and dried under vacuum (yield: 88 – 96 %).

**Complex 104:** Red powder. Crystals suitable for X-ray analysis were obtained by slow diffusion of pentane in a solution of **104** in dichloromethane. – $^1$H NMR (400 MHz, $CD_2Cl_2$): $\delta$ = 1.29 (d, $^3J$ = 7.1 Hz, 6 H, $CH(CH_3)_2$), 1.51 (s, 15 H, $CH_3$, $Cp^\star$), 2.18 (s, 3 H, $CH_3$, cymene), 2.82 (sept, $^3J$ = 7.1 Hz, 1 H, $CH(CH_3)_2$), 5.21, 5.43 (2 × d, $^3J$ = 6.0 Hz, 3 H, CH) ppm. – $^{13}$C NMR (101 MHz, $CD_2Cl_2$): $\delta$ = 10.4 ($CH_3$, $Cp^\star$), 19.0, 22.4 ($CH_3$, cymene), 31.6 ($CH(CH_3)_2$), 70.6 (C, $Cp^\star$), 77.8, 78.9 (CH, cymene), 95.3, 100.3 (C, cymene) ppm. – Elemental analysis: calcd. (%) for $C_{20}H_{29}Cl_3Ru_2$ (577.9): C 41.56, H 5.06; found: C 41.56, H 5.23.

**Complex 105:** Red powder. – $^1$H NMR (400 MHz, $CD_2Cl_2$): $\delta$ = 1.50 ($Cp^\star$), 5.60 (benzene) ppm. – $^{13}$C NMR (101 MHz, $CD_2Cl_2$): $\delta$ = 10.4 ($CH_3$, $Cp^\star$), 70.9 (C, $Cp^\star$), 80.5 (benzene) ppm. – Elemental analysis: calcd. (%) for $C_{16}H_{21}Cl_3Ru_2$ (521.8) C 36.83, H 4.06; found: C , H.

**Complex 106:** Red powder. – $^1$H NMR (400 MHz, $CD_2Cl_2$): $\delta$ = 1.52 ($Cp^\star$Ru), 1.61 ($Cp^\star$Rh) ppm. – $^{13}$C NMR (101 MHz, $CD_2Cl_2$): $\delta$ = 9.5, 10.5 ($CH_3$, $Cp^\star$), 70.0 (C, $Cp^\star$Ru), 93.6 (d, $^1J_{C,Rh}$ = 10 Hz, C, $Cp^\star$Rh) ppm. – Elemental analysis: calcd. (%) for $C_{20}H_{30}Cl_3RhRu$ (580.0): C 41.36, H 5.21; found: C 41.51, H 5.26.

**Complex 107:** Orange powder. Crystals suitable for X-ray analysis were obtained by slow diffusion of pentane into a solution of **107** in a mixture of dichloromethane/hexane 1:9. – $^1$H NMR (400 MHz, $CD_2Cl_2$): $\delta$ = 1.57, 1.58 ($Cp^\star$) ppm. – $^{13}$C NMR (101 MHz, $CD_2Cl_2$): $\delta$ = 9.5, 10.5 ($CH_3$, $Cp^\star$), 70.3, 85.2 (C, $Cp^\star$) ppm. – Elemental analysis: calcd. (%) for $C_{20}H_{30}Cl_3IrRu$ (670.1): C 35.85, H 4.51; found: C 35.99, H 4.57.

**Synthesis of Complexes 108:** $Me_3SiCl$ (30 $\mu$L, 240 $\mu$mol) was added to a solution of $[Cp^\star Ru(OMe)]_2$ (43 mg, 80 $\mu$mol) in $CH_2Cl_2$ (5 mL). After addition of $[(C_6H_3{}^iPr_3)RuCl_2]_2$ (72 mg, 96 $\mu$mol), the solution was stirred for 20 min. The solvent was then removed in vacuum and the product was extracted with pentane (2 × 5 mL). The product was

isolated by evaporation of the pentane and drying under vacuum. Yield: 94 mg (92 %). – $^1$H MNR (400 MHz, $CD_2Cl_2$): $\delta = 1.31$ (d, $^3J = 7.1$ Hz, 18 H, CH(C$H_3$)$_2$), 1.50 ($CH_3$, Cp$^\star$), 2.90 (sept, $^3J = 7.1$ Hz, 3 H, C$H$(C$H_3$($_2$), 5.09 (s, 3 H, CH) ppm. – $^{13}$C NMR (101 Mhz, $CD_2Cl_2$): $\delta = 10.5$ ($CH_3$, Cp$^\star$), 22.5 (CH($CH_3$)$_2$), 32.0 ($C$H(C$H_3$)$_2$), 70.3 (CH, $C_6H_3{}^{i}Pr_3$), 70.4 (C, Cp$^\star$), 106 (C, $C_6H_3{}^{i}Pr_3$) ppm. – Elemental analysis: calcd. (%) for $C_{25}H_{39}Cl_3Ru_2$ (648.1): C 46.33, H 6.07; found: C 46.30, H 6.13.

**Exchange reactions between complex 108 and complex 26:** Complex **108** (5.5 mg, 8.6 $\mu$mol) was dissolved in $CD_2Cl_2$ (500 $\mu$L) and a $^1$H NMR spectrum of the solution was recorded (400 MHz). A sample of complex **26** (8.7 mg, 8.6 $\mu$mol) was analyzed in the same fashion. The two solutions were subsequently mixed and immediately analyzed by $^1$H NMR spectroscopy (400 MHz).

**Synthesis of complex 109:** Complex **106** (15.0 mg, 25.8 $\mu$mol) was dissolved in benzene (2 mL). The resulting mixture was allowed to react for 2 hours, after which small crystals of complex 12 could already be observed. Slow addition of hexane (5 mL) by diffusion over 12 h resulted in the formation of crystalline 12, which was isolated by filtration. Yield: 12.5 mg (73 %). The reaction was quantitative as evidenced by $^1$H NMR analysis of the remaining solution.

– $^1$H NMR (400 MHz, $CD_2Cl_2$): $\delta = 1.57$, 2.07 (Cp$^\star$), 6.05 (benzene) ppm. – $^{13}$C NMR (101 MHz, $CD_2Cl_2$): $\delta = 9.4$, 11.3 ($CH_3$, Cp$^\star$), 87.7 (benzene), 94.4 (d, $^1J_{C-Rh} = 14$ Hz, C, Cp$^\star$Rh),97.1 (C, Cp$^\star$Ru) ppm. – Elemental analysis: calcd. (%) for $C_{26}H_{36}Cl_3RhRu$ (658.9): C 47.39, H 5.51; found: C 47.55, H 5.12.

**Typical procedure for the ATRA of $CCl_4$ to olefins:** (cat./olefin/$CCl_4$ = 1:300:432) 1000 $\mu$L of a stock solution of $CCl_4$, the olefin and the internal standard mesitylene in the reaction solvent were added to a 1.5 mL vial containing the solid catalyst (final conc.: [cat.] = 4.6 mM, [olefin] = 1.38 M, [$CCl_4$ ] = 1.99 M, [mesitylene] = 0.36 M). The resulting solution was placed in an oil bath tempered at the desired temperature. After the given time, a sample (20 $\mu$L) was removed from the reaction mixture, diluted with either toluene (1000 $\mu$L, GC or GC-MS) or $CDCl_3$ (550 $\mu$L, $^1$H NMR) and analyzed by gas chromatography and/or by $^1$H NMR. The kinetic experiments were performed in an analogous fashion by removing several samples at regular time intervals.

**Typical procedure for the ATRA of $CHCl_3$ to olefins:** (cat./olefin = 1:100, the chloroform was often itself employed as the solvent) 500 $\mu$L of a stock solution of the olefin

and the internal standard mesitylene in chloroform were added to a 1.5 mL vial containing the solid catalyst (final conc.: [cat.] = 13.8 mM, [olefin] = 1.38 M, [chloroform] = $\sim$ 10 M, [mesitylene] = 0.36 M). The resulting solution was placed in an oil bath tempered at the desired temperature. After the given time, a sample (20 $\mu$L) was removed from the reaction mixture, diluted with either toluene (1000 $\mu$L, GC or GC-MS) or $CDCl_3$ (550 $\mu$L, $^1$H NMR) and analyzed by gas chromatography and/or by $^1$H NMR. The kinetic experiments were performed in an analogous fashion by removing several samples at regular time intervals.

**X-ray Crystallography:** Details of the crystals, data collection, and structure refinement are listed in Tables C1 – C16. Diffraction data were collected with $Mo_{K\alpha}$ radiation on a 4-circle gognometer having a kappa geometry and equipped with an Oxford Diffraction KM4 Sapphire CCD detector (**62**, **63**, **67**, **82**, **88**, **89**, **90**, **97**, **107**), or a marresearch mar345 IPDS detector (**24**, **26**, **64**, **65**, **104**, **109**, **110**). Data reduction was carried out with CrisAlis RED, release 1.6.9. [210] or 1.7.0. [211]. Structure solution and refinement were performed with the SHELXTL software package, released 5.1. [212, 213]. The structures were refined using the full-matrix least-squares on $F^2$ with all non-H atoms anisotropically defined. The hydrogen atoms were placed in calculated positions using the riding model with $U_{iso} = aU_{eq}$(C) (where $a$ is 1.5 for methyl hydrogen atoms and 1.2 for others, and C is the parent carbon atom). Graphical representation of the molecular structures in the crystal were generated with the program ORTEP (ORTEP 3 for Windows version 1.076) [214].

# Appendix A – Abbreviations

adam = adamantyl

allyl = $\eta^3$-2-propenyl

$C_{10}H_{14}$ = $\eta^3$,$\eta^3$-2,7-dimethyl-2,6-octadiene-1,8-diyl

$C_6H_3Et_3$ = $\eta^6$-1,3,5-triethylbenzene

$C_6H_3Me_3$ = $\eta^6$-1,3,5-trimethylbenzene

$C_9H_{12}N$ = 2-[(dimethylamino-$\kappa$N)methyl]phenyl-$\kappa$C

$C_{11}H_{15}NO_2$ = 2-[1-(dimethylamino-$\kappa$N)-2-methoxy-2-oxoethyl]phenyl-$\kappa$C

Cp = $\eta^5$-cyclopentadienyl

Cp$^\star$ = $\eta^5$-pentamethylcyclopentadienyl

$C_6H_3{}^{i}Pr_3$ = $\eta^6$-1,3,5-tris(1-methylethyl)benzene

cod = $\eta^2$,$\eta^2$-1,5-cyclooctadiene

cymene = $\eta^6$-1-methyl-4-(1-methylethyl)benzene

dcypb = 1,4-*bis*(dicyclohexylphosphino)butane

dppb = 1,4-*bis*(diphenylphosphino)butane

mma = methyl methacrylate

naph = naphtalenyl

ppy = 2-(2-pyridinyl-$\kappa$N)phenyl-$\kappa$C

TfO = trifluoromethylsulfonate

tpc = $\eta^2$,$\eta^2$-2,3,4,5-tetraphenyl-2,4-cyclopentadien-1-one

# Appendix B – List of the Complexes

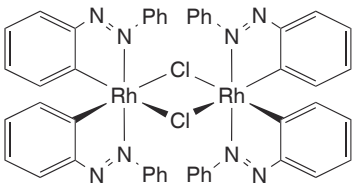

**1**

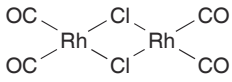

**2**

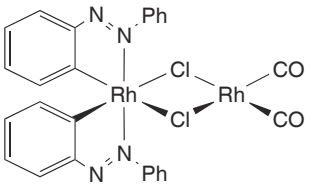

**3**

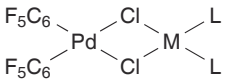

M = Ni, Pd, or Pt
LL = dpe or 2 $PEt_3$

**4**

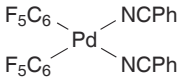

**5**

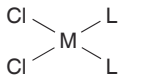

M = Ni, Pd, or Pt
L = dpe or 2 $PEt_3$

**6**

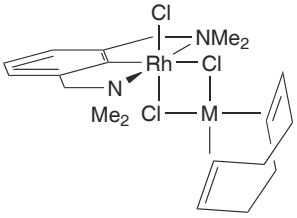

M = Ir or Rh

**7**

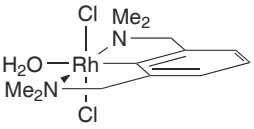

**8**

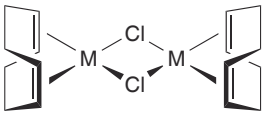

| | M |
|---|---|
| **9** | Ir |
| **10** | Rh |

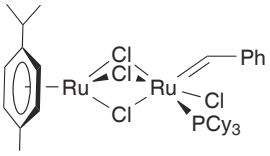

**11**

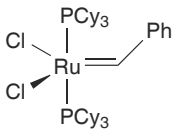

**12**

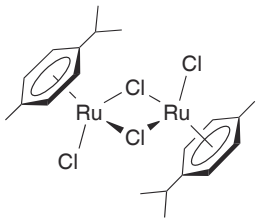

**13**

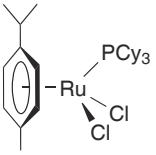

**14**

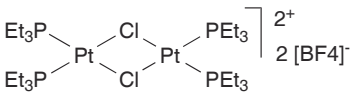

**15**

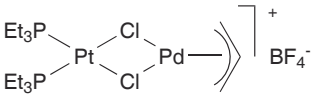

**16**

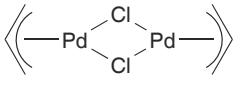

**17**

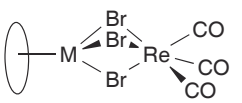

(π-ligand)M = (benzene)Ru
$(C_6H_3Et_3)$Ru
(cymene)Ru
Cp*Ir
Cp*Rh

**18**

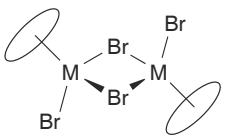

(π-ligand)M = (benzene)Ru
$(C_6H_3Et_3)$Ru
(cymene)Ru
Cp*Ir
Cp*Rh

**19**

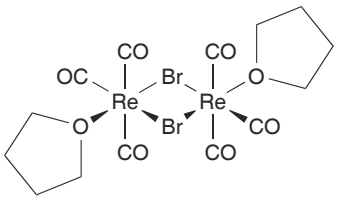

**20**

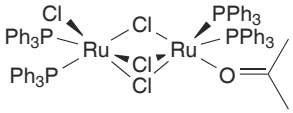

**21**

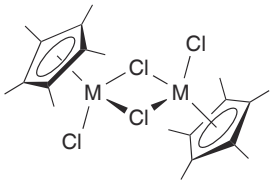

| | M |
|---|---|
| **22** | Ir |
| **23** | Rh |

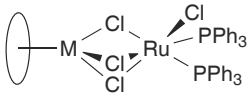

| | (π-ligand)M |
|---|---|
| **24** | (cymene)Ru |
| **25** | Cp*Ir |
| **26** | Cp*Rh |

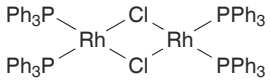

**27**

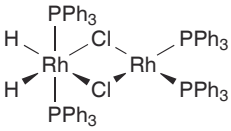

**28**

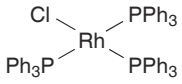

**29**

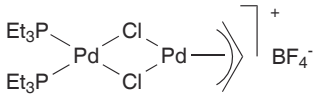

**30**

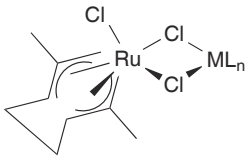

| | $L_nM$ |
|---|---|
| **31** | $(C_6H_9N)Pd$ |
| **32** | Cp*RhCl |

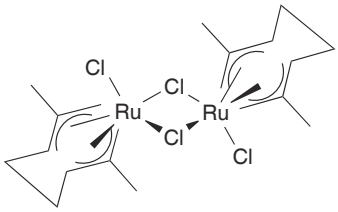

**33**

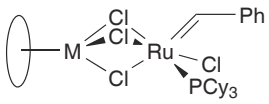

| | (π-ligand)M |
|---|---|
| **34** | (cymene)Os |
| **35** | ($^t$Bu$_2$Cp)Rh |

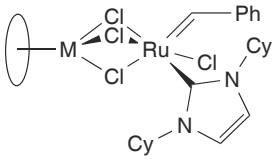

| | (π-ligand)M |
|---|---|
| **36** | (cymene)Ru |
| **37** | Cp*Rh |

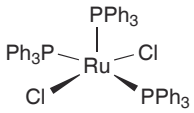

**38**

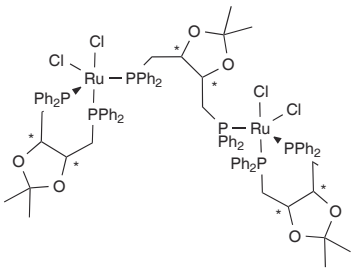

**39**

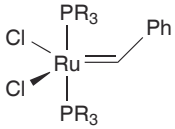

| | R |
|---|---|
| **40** | Ph |
| **41** | *o*-$C_5H_9$ |

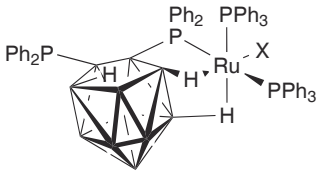

| | X |
|---|---|
| **42** | H |
| **43** | Cl |

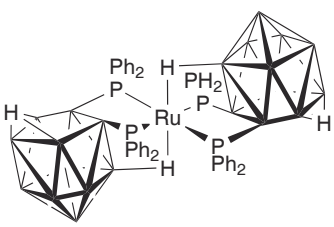

**44**

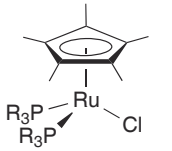

| | R |
|---|---|
| **45** | Ph |
| **46** | *p*-$CF_3C_6H_4$ |
| **47** | *p*-$CH_3OC_6H_4$ |

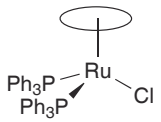

| | π-ligand |
|---|---|
| **48** | Cp |
| **49** | Ind |

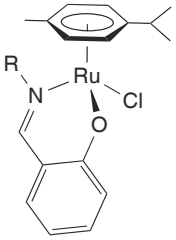

R = Me, $^t$Bu, or 2,6-Me-4-Br$C_6H_2$

**50**

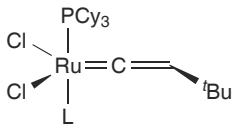

| | L |
|---|---|
| **51** | $PCy_3$ |
| **52** | *NN*-$Mes_2$Imi |

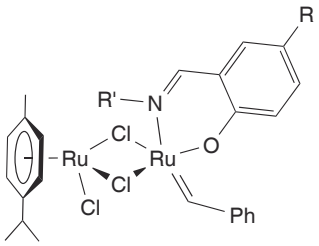

R = H or $NO_2$

R' = Me, 2,6-Me-4-Br$C_6H_2$, or 2,6-$^i$Pr$C_6H_3$

**53**

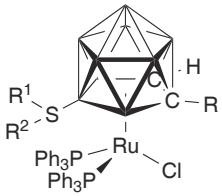

R = H or Me

$R^1$, $R^2$ = Me, Et, Ph, or $(CH_2)_2$

**54**

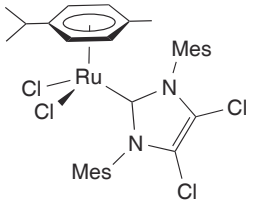

**55**

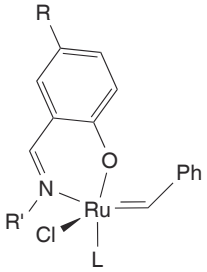

L = $PCy_3$ or (*NN*-*bis*-Mes)$H_2$Imi

R = H or $NO_2$

R' = Me, 2,6-Me-4-Br$C_6H_2$, or 2,6-$^i$Pr$C_6H_3$

**56**

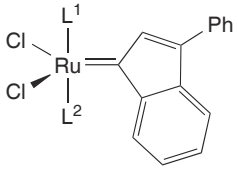

$L^1$ = $PPh_3$ or $PCy_3$

$L^2$ = $PCy_3$, $PCy_3$, or (*NN*-*bis*-Mes)$H_2$Imi

**57**

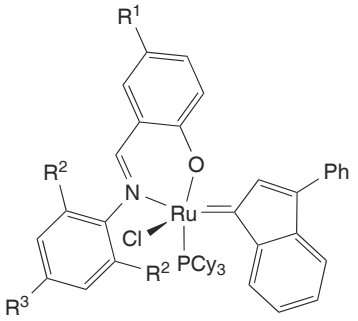

$R^1$ = H or $NO_2$

$R^2$ = $^i$Pr or Me

$R^3$ = H or Br

**58**

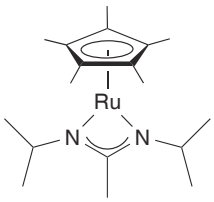

**59**

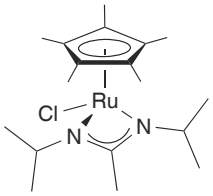

**60**

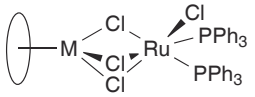

| | (π-ligand)M |
|---|---|
| **61** | $(C_6H_3Me_3)Ru$ |
| **62** | $(C_6H_3Et_3)Ru$ |
| **63** | $(C_6H_3{}^iPr_3)Ru$ |
| **64** | $(C_6Me_6)Ru$ |

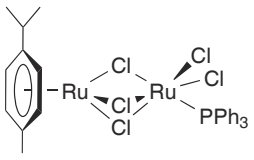

**65**

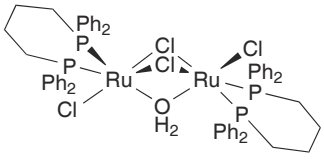

**66**

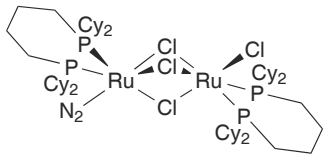

**67**

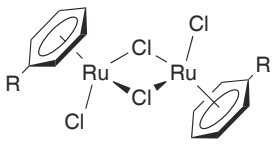

| | R |
|---|---|
| **68** | H |
| **69** | $CO_2Et$ |

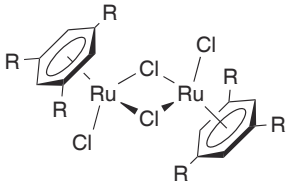

| | R |
|---|---|
| **70** | Me |
| **71** | Et |
| **72** | *i*Pr |

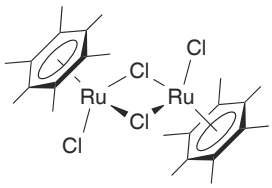

**73**

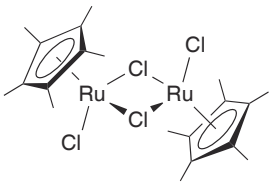

**74**

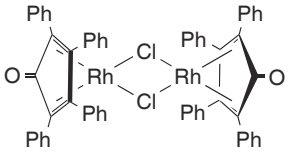

**75**

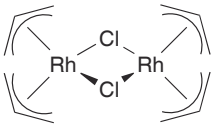

**76**

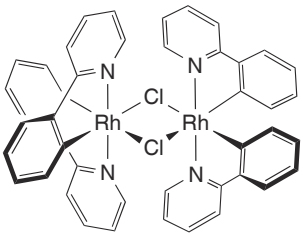

**77**

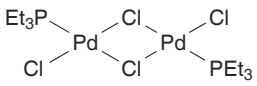

**78**

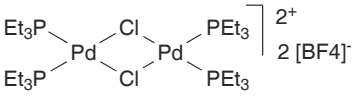

**79**

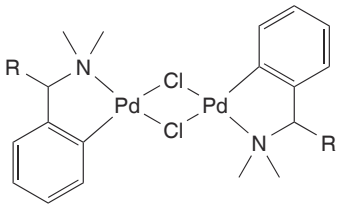

| | R |
|---|---|
| **80** | H |
| **81** | $CO_2Et$ |

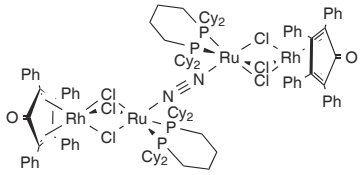

**82**

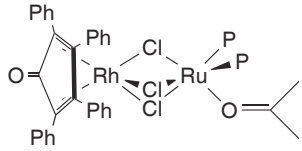

| | PP |
|---|---|
| **83** | dcypb |
| **84** | 2 $PPh_3$ |

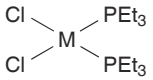

| | M |
|---|---|
| **85** | Pd |
| **86** | Pt |

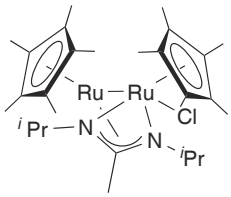

**87**

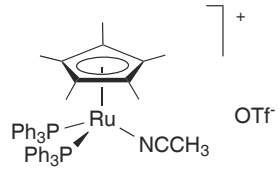

**88**

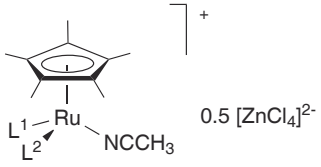

| | $L^1$, $L^2$ |
|---|---|
| **89** | $CH_3CN$, $CH_3CN$ |
| **90** | $PPh_3$, $PPh_3$ |
| **91** | CH3CN, PPh3 |

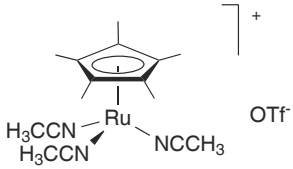

**92**

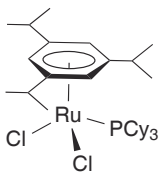

**93**

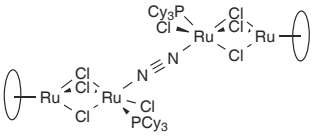

| | π-ligand |
|---|---|
| **94** | $C_6H_3{}^iPr_3$ |
| **95** | cymene |

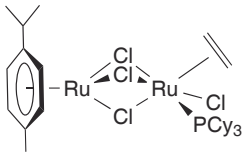

**96**

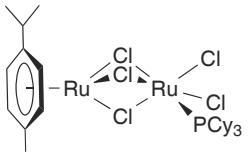

**97**

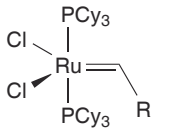

R = alkyl, aryl, vinyl

**98**

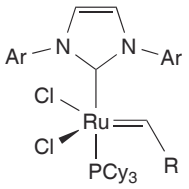

R = alkyl, aryl

**99**

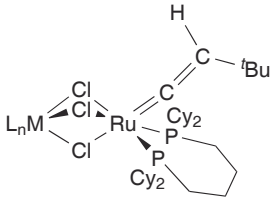

| | $L_nM$ |
|---|---|
| **100** | (dcypb)ClRu |
| **101** | (tcp)Rh |

$[Cp^*RuCl]_4$

**102**

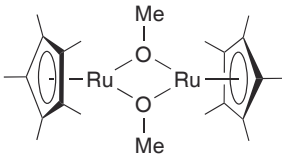

**103**

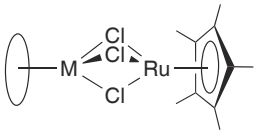

| | (π-ligand)M |
|---|---|
| **104** | (cymene)Ru |
| **105** | (benzene)Ru |
| **106** | Cp*Rh |
| **107** | Cp*Ir |
| **108** | $(C_3H_3{}^iPr_3)Ru$ |

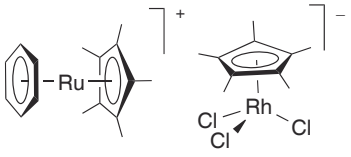

**109**

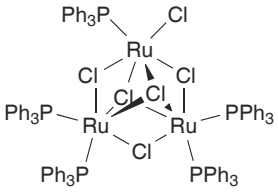

**110**

# Appendix C – Crystallographic Data

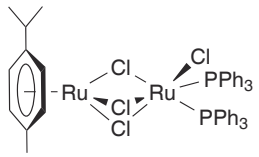


**Table C1:** Crystallographic data for complex **24**.

| | |
|---|---|
| Empirical formula | $C_{46}H_{44}Cl_4P_2Ru_2$ |
| Molecular weight (g mol$^{-1}$) | 1002.7 |
| Crystal size | 0.19 × 0.12 × 0.10 |
| Crystal system | triclinic |
| Space group | P-1 |
| a (Å) | 10.072(3) |
| b (Å) | 12.099(5) |
| c (Å) | 18.801(10) |
| $\alpha$ ($^\circ$) | 91.17(4) |
| $\beta$ ($^\circ$) | 100.77(4) |
| $\gamma$ ($^\circ$) | 109.93(4) |
| Volume (Å$^3$) | 2107.2(16) |
| Z | 2 |
| Density (g cm$^{-3}$) | 1.580 |
| Temperature (K) | 140(2) |
| Absorption coefficient (mm$^{-1}$) | 1.079 |
| $\Theta$ range ($^\circ$) | 3.29 to 25.02 |
| Index ranges | -11 → 11, -14 → 14, -22 → 21 |
| Reflections collected | 12838 |
| Independent reflections | 6981 ($R_{int}$ = 0.0654) |
| Absorption correction | empirical (DELABS) |
| Max. and min. transmission | 0.5100 and 0.0670 |
| Data / restraints / parameters | 6981 / 0 / 488 |
| Goodness-of-fit on F$^2$ | 0.966 |
| Final R indices (I>2$\sigma$(I)) | R1 = 0.0781, wR2 = 0.2036 |
| R indices (all data) | R1 = 0.1283, wR2 = 0.2486 |
| Largest diff. peak/hole (eÅ$^{-3}$) | 1.166 and -2.061 |

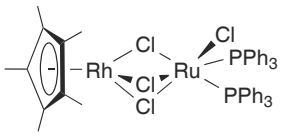


**Table C2:** Crystallographic data for complex **26**.

| | |
|---|---|
| Empirical formula | $C_{46}H_{45}Cl_4P_2RhRu$ |
| Molecular weight (g mol$^{-1}$) | 1005.6 |
| Crystal size | 0.30 × 0.25 × 0.21 |
| Crystal system | triclinic |
| Space group | P-1 |
| a (Å) | 11.937(2) |
| b (Å) | 13.200(2) |
| c (Å) | 14.3916(14) |
| $\alpha$ ($^\circ$) | 81.696(12) |
| $\beta$ ($^\circ$) | 77.383(14) |
| $\gamma$ ($^\circ$) | 71.811(17) |
| Volume (Å$^3$) | 2095.2(6) |
| Z | 2 |
| Density (g cm$^{-3}$) | 1.594 |
| Temperature (K) | 140(2) |
| Absorption coefficient (mm$^{-1}$) | 1.119 |
| $\Theta$ range ($^\circ$) | 3.54 to 25.02 |
| Index ranges | -14 → 14, -15 → 15, -77 → 16 |
| Reflections collected | 12667 |
| Independent reflections | 6930 ($R_{int}$ = 0.0619) |
| Absorption correction | empirical (DELABS) |
| Max. and min. transmission | 0.5630 and 0.1010 |
| Data / restraints / parameters | 6930 / 0 / 488 |
| Goodness-of-fit on $F^2$ | 1.135 |
| Final R indices (I>2$\sigma$(I)) | R1 = 0.0637, wR2 = 0.1766 |
| R indices (all data) | R1 = 0.0736, wR2 = 0.1948 |
| Largest diff. peak/hole (eÅ$^{-3}$) | 1.059 and -1.173 |

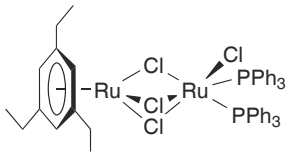


**Table C3:** Crystallographic data for complex **62** × 2 $C_6H_6$.

| | |
|---|---|
| Empirical formula | $C_{60}H_{60}Cl_4P_2Ru_2$ |
| Molecular weight (g $mol^{-1}$) | 1187.0 |
| Crystal size | 0.24 × 0.20 × 0.19 |
| Crystal system | triclinic |
| Space group | P-1 |
| a (Å) | 14.542(2) |
| b (Å) | 14.6755(18) |
| c (Å) | 14.740(2) |
| $\alpha$ ( $^\circ$ ) | 98.740(11) |
| $\beta$ ( $^\circ$ ) | 115.695(14) |
| $\gamma$ ( $^\circ$ ) | 100.165(11) |
| Volume ($Å^3$) | 2696.1(6) |
| Z | 2 |
| Density (g $cm^{-3}$) | 1.462 |
| Temperature (K) | 143(2) |
| Absorption coefficient ($mm^{-1}$) | 0.856 |
| $\Theta$ range ( $^\circ$ ) | 3.57 to 25.03 |
| ranges | -17 → 17, -17 → 15, -17 → 17 |
| Reflections collected | 16226 |
| Independent reflections | 8394 ($R_{int}$ = 0.0842) |
| Absorption correction | empirical (DELABS) |
| Max. and min. transmission | 0.8050 and 0.4200 |
| Data / restraints / parameters | 8394 / 231 / 613 |
| Goodness-of-fit on $F^2$ | 0.919 |
| Final R indices (I>2$\sigma$(I)) | R1 = 0.0644, wR2 = 0.1177 |
| R indices (all data) | R1 = 0.1413, wR2 = 0.1427 |
| Largest diff. peak/hole ($eÅ^{-3}$) | 0.896 and -0.835 |

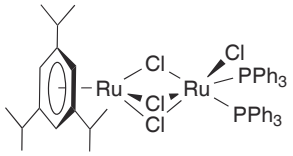


**Table C4:** Crystallographic data for complex **63** × $CH_2Cl_2$.

| | |
|---|---|
| Empirical formula | $C_{52}H_{56}Cl_6P_2Ru_2$ |
| Molecular weight (g $mol^{-1}$) | 1157.8 |
| Crystal size | 0.23 × 0.17 × 0.13 |
| Crystal system | monoclinic |
| Space group | Cc |
| a (Å) | 13.0300(12) |
| b (Å) | 17.2480(10) |
| c (Å) | 22.9595(16) |
| $\alpha$ ( $^\circ$ ) | 90 |
| $\beta$ ( $^\circ$ ) | 101.182(7) |
| $\gamma$ ( $^\circ$ ) | 90 |
| Volume ($Å^3$) | 5062.0(7) |
| Z | 4 |
| Density (g $cm^{-3}$) | 1.519 |
| Temperature (K) | 140(2) |
| Absorption coefficient ($mm^{-1}$) | 1.012 |
| $\Theta$ range ( $^\circ$ ) | 2.98 to 25.02 |
| Index ranges | -15 → 15, -20 → 20, -27 → 27 |
| Reflections collected | 14799 |
| Independent reflections | 7693 ($R_{int}$ = 0.0420) |
| Absorption correction | empirical (DELABS) |
| Max. and min. transmission | 0.8770 and 0.5930 |
| Data / restraints / parameters | 7693 / 2 / 559 |
| Goodness-of-fit on $F^2$ | 0.948 |
| Final R indices (I>2$\sigma$(I)) | R1 = 0.0337, wR2 = 0.0677 |
| R indices (all data) | R1 = 0.0424, wR2 = 0.0706 |
| Largest diff. peak/hole ($eÅ^{-3}$) | 0.560 and -0.854 |

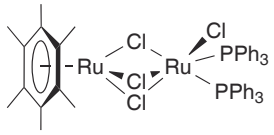


**Table C5:** Crystallographic data for complex **64** × 2 $CH_2Cl_2$.

| | |
|---|---|
| Empirical formula | $C_{50}H_{52}Cl_8P_2Ru_2$ |
| Molecular weight (g $mol^{-1}$) | 1200.6 |
| Crystal size | 0.28 × 0.21 × 0.16 |
| Crystal system | triclinic |
| Space group | P-1 |
| a (Å) | 10.885(5) |
| b (Å) | 11.254(3) |
| c (Å) | 22.354(7) |
| $\alpha$ ( $^\circ$ ) | 99.98(2) |
| $\beta$ ( $^\circ$ ) | 97.47(3) |
| $\gamma$ ( $^\circ$ ) | 109.14(3) |
| Volume ($Å^3$) | 2496.1(14) |
| Z | 2 |
| Density (g $cm^{-3}$) | 1.597 |
| Temperature (K) | 143(2) |
| Absorption coefficient ($mm^{-1}$) | 1.132 |
| $\Theta$ range ( $^\circ$ ) | 3.66 to 25.03 |
| Index ranges | -12 → 12, -12 → 12, -25 → 26 |
| Reflections collected | 15038 |
| Independent reflections | 8222 ($R_{int}$ = 0.1610) |
| Absorption correction | empirical (DELABS) |
| Max. and min. transmission | 0.7400 and 0.2990 |
| Data / restraints / parameters | 8222 / 0 / 569 |
| Goodness-of-fit on $F^2$ | 1.538 |
| Final R indices (I>2$\sigma$(I)) | R1 = 0.1162, wR2 = 0.3250 |
| R indices (all data) | R1 = 0.1461, wR2 = 0.4003 |
| Largest diff. peak/hole ($eÅ^{-3}$) | 2.916 and -1.976 |

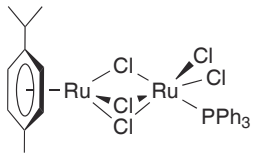


**Table C6:** Crystallographic data for complex **65** × $CHCl_3$.

| | |
|---|---|
| Empirical formula | $C_{29}H_{30}Cl_8PRu_2$ |
| Molecular weight (g $mol^{-1}$) | 895.2 |
| Crystal size | 0.28 × 0.25 × 0.19 |
| Crystal system | monoclinic |
| Space group | P2(1)/n |
| a (Å) | 19.773(4) |
| b (Å) | 9.6515(8) |
| c (Å) | 20.479(4) |
| $\alpha$ ( $^\circ$ ) | 90 |
| $\beta$ ( $^\circ$ ) | 118.49(2) |
| $\gamma$ ( $^\circ$ ) | 90 |
| Volume ($Å^3$) | 3434.8(10) |
| Z | 4 |
| Density (g $cm^{-3}$) | 1.731 |
| Temperature (K) | 143(2) |
| Absorption coefficient ($mm^{-1}$) | 1.568 |
| $\Theta$ range ( $^\circ$ ) | 3.54 to 25.02 |
| Index ranges | -22 → 23, -10 → 10, -24 → 24 |
| Reflections collected | 19093 |
| Independent reflections | 5745 ($R_{int}$ = 0.0341) |
| Absorption correction | empirical (DELABS) |
| Max. and min. transmission | 0.7130 and 0.2580 |
| Data / restraints / parameters | 5745 / 0 / 362 |
| Goodness-of-fit on $F^2$ | 1.105 |
| Final R indices (I>2$\sigma$(I)) | R1 = 0.0507, wR2 = 0.1355 |
| R indices (all data) | R1 = 0.0604, wR2 = 0.1511 |
| Largest diff. peak/hole ($eÅ^{-3}$) | 1.053 and -0.919 |

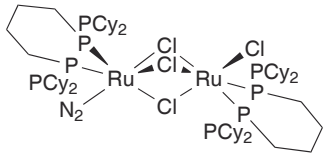


**Table C7:** Crystallographic data for complex **67** × $C_6H_6$.

| | |
|---|---|
| Empirical formula | $C_{62}H_{110}Cl_4N_2P_4Ru_2$ |
| Molecular weight (g $mol^{-1}$) | 1351.3 |
| Crystal size | 0.19 × 0.14 × 0.13 |
| Crystal system | triclinic |
| Space group | P-1 |
| a (Å) | 13.3866(10) |
| b (Å) | 13.7565(7) |
| c (Å) | 18.6809(15) |
| $\alpha$ ( $^\circ$ ) | 92.581(5) |
| $\beta$ ( $^\circ$ ) | 107.979(7) |
| $\gamma$ ( $^\circ$ ) | 93.809(5) |
| Volume ($Å^3$) | 3257.1(4) |
| Z | 2 |
| Density (g $cm^{-3}$) | 1.378 |
| Temperature (K) | 140(2) |
| Absorption coefficient ($mm^{-1}$) | 0.765 |
| $\Theta$ range ( $^\circ$ ) | 3.05 to 25.03 |
| Index ranges | -15 → 15, -15 → 15, -22 → 22 |
| Reflections collected | 19914 |
| Independent reflections | 10073 ($R_{int}$ = 0.0572) |
| Absorption correction | Semi-empirical from equivalents (MULABS) |
| Max. and min. transmission | 0.8595 and 0.8282 |
| Data / restraints / parameters | 10073 / 242 / 642 |
| Goodness-of-fit on $F^2$ | 0.987 |
| Final R indices (I>2$\sigma$(I)) | R1 = 0.0614, wR2 = 0.1199 |
| R indices (all data) | R1 = 0.1170, wR2 = 0.1339 |
| Largest diff. peak/hole (e$Å^{-3}$) | 1.125 and -0.773 |

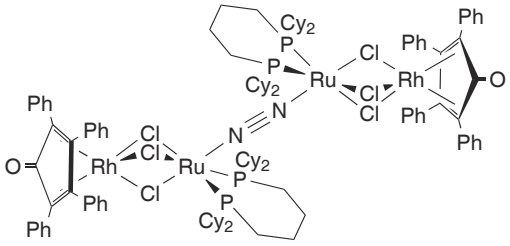


**Table C8:** Crystallographic data for complex **82** × $CH_2Cl_2$.

| | |
|---|---|
| Empirical formula | $C_{115}H_{146}Cl_8N_2O_2P_4Rh_2Ru_2$ |
| Molecular weight (g $mol^{-1}$) | 2403.8 |
| Crystal size | 0.36 × 0.25 × 0.13 |
| Crystal system | monoclinic |
| Space group | C2/c |
| a (Å) | 71.244(6) |
| b (Å) | 12.9605(11) |
| c (Å) | 24.9834(19) |
| $\alpha$ ( $^\circ$ ) | 90 |
| $\beta$ ( $^\circ$ ) | 94.136(11) |
| $\gamma$ ( $^\circ$ ) | 90 |
| Volume ($Å^3$) | 23009(3) |
| Z | 8 |
| Density (g $cm^{-3}$) | 1.388 |
| Temperature (K) | 140(2) |
| Absorption coefficient ($mm^{-1}$) | 0.829 |
| $\Theta$ range ( $^\circ$ ) | 2.63 to 25.03 |
| Index ranges | -84 → 84, -13 → 13, -29 → 29 |
| Reflections collected | 65671 |
| Independent reflections | 19222 ($R_{int}$ = 0.1233) |
| Absorption correction | None |
| Max. and min. transmission | |
| Data / restraints / parameters | 19222 / 455 / 1183 |
| Goodness-of-fit on $F^2$ | 1.055 |
| Final R indices (I>2$\sigma$(I)) | R1 = 0.0933, wR2 = 0.2296 |
| R indices (all data) | R1 = 0.1479, wR2 = 0.2712 |
| Largest diff. peak/hole (e$Å^{-3}$) | 1.821 and -1.636 |

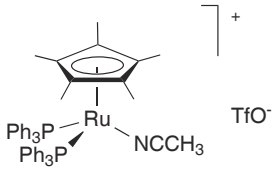


**Table C9:** Crystallographic data for complex **88**.

| | |
|---|---|
| Empirical formula | $C_{49}H_{48}N_2O_3P_2RuS$ |
| Molecular weight (g mol$^{-1}$) | 951.0 |
| Crystal size | 0.16 × 0.13 × 0.11 |
| Crystal system | triclinic |
| Space group | P-1 |
| a (Å) | 10.5409(4) |
| b (Å) | 13.3793(7) |
| c (Å) | 16.2230(9) |
| $\alpha$ ($^\circ$) | 88.977(4) |
| $\beta$ ($^\circ$) | 86.567(4) |
| $\gamma$ ($^\circ$) | 75.659(4) |
| Volume (Å$^3$) | 2212.64(18) |
| Z | 2 |
| Density (g cm$^{-3}$) | 1.427 |
| Temperature (K) | 140(2) |
| Absorption coefficient (mm$^{-1}$) | 0.529 |
| $\Theta$ range ($^\circ$) | 3.12 to 25.03 |
| Index ranges | -10 → 10, -15 → 15, -19 → 19 |
| Reflections collected | 13077 |
| Independent reflections | 6823 ($R_{int}$ = 0.0200) |
| Absorption correction | Semi-empirical from equivalents (MULABS) |
| Max. and min. transmission | 0.9638 and 0.8015 |
| Data / restraints / parameters | 6823 / 0 / 541 |
| Goodness-of-fit on F$^2$ | 1.044 |
| Final R indices (I>2$\sigma$(I)) | R1 = 0.0307, wR2 = 0.0799 |
| R indices (all data) | R1 = 0.0340, wR2 = 0.0822 |
| Largest diff. peak/hole (eÅ$^{-3}$) | 0.653 and -0.810 |

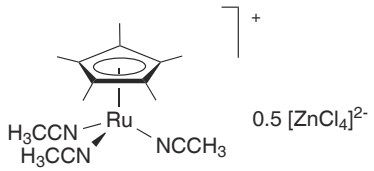


**Table C10:** Crystallographic data for complex **89**.

| | |
|---|---|
| Empirical formula | $C_{32}H_{48}Cl_4N_6Ru_2Zn$ |
| Molecular weight (g mol$^{-1}$) | 926.1 |
| Crystal size | 0.18 × 0.13 × 0.09 |
| Crystal system | triclinic |
| Space group | P-1 |
| a (Å) | 9.3648(4) |
| b (Å) | 12.9800(8) |
| c (Å) | 18.3753(10) |
| $\alpha$ ($^\circ$) | 72.891(5) |
| $\beta$ ($^\circ$) | 88.514(4) |
| $\gamma$ ($^\circ$) | 72.566(5) |
| Volume (Å$^3$) | 2031.94(18) |
| Z | 2 |
| Density (g cm$^{-3}$) | 1.514 |
| Temperature (K) | 140(2) |
| Absorption coefficient (mm$^{-1}$) | 1.611 |
| $\Theta$ range ($^\circ$) | 3.15 to 25.03 |
| Index ranges | -10 → 11, -15 → 15, -21 → 20 |
| Reflections collected | 12149 |
| Independent reflections | 6273 ($R_{int}$ = 0.0225) |
| Absorption correction | Empirical (DELABS) |
| Max. and min. transmission | 0.887 and 0.620 |
| Data / restraints / parameters | 6273 / 0 / 406 |
| Goodness-of-fit on $F^2$ | 0.985 |
| Final R indices (I>2$\sigma$(I)) | R1 = 0.0219, wR2 = 0.0567 |
| R indices (all data) | R1 = 0.0265, wR2 = 0.0581 |
| Largest diff. peak/hole (eÅ$^{-3}$) | 0.466 and -0.675 |

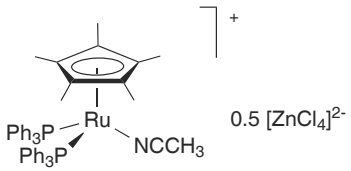


**Table C11:** Crystallographic data for complex **90** × 3 $CH_2Cl_2$.

| | |
|---|---|
| Empirical formula | $C_{99}H_{102}Cl_{10}N_2P_4Ru_2Zn$ |
| Molecular weight (g $mol^{-1}$) | 2065.7 |
| Crystal size | 0.22 × 0.20 × 0.11 |
| Crystal system | monoclinic |
| Space group | P2(1) |
| a (Å) | 10.6258(4) |
| b (Å) | 21.7283(11) |
| c (Å) | 20.4384(11) |
| $\alpha$ ( $^\circ$ ) | 90 |
| $\beta$ ( $^\circ$ ) | 90.815(4) |
| $\gamma$ ( $^\circ$ ) | 90 |
| Volume ($Å^3$) | 4718.3(4) |
| Z | 2 |
| Density (g $cm^{-3}$) | 1.454 |
| Temperature (K) | 140(2) |
| Absorption coefficient ($mm^{-1}$) | 0.966 |
| $\Theta$ range ( $^\circ$ ) | 2.99 to 25.03 |
| Index ranges | -11 → 10, -25 → 125, -24 → 24 |
| Reflections collected | 27665 |
| Independent reflections | 15206 ($R_{int}$ = 0.0498) |
| Absorption correction | Empirical (DELABS) |
| Max. and min. transmission | 0.823 and 0.458 |
| Data / restraints / parameters | 15206 / 1 / 1063 |
| Goodness-of-fit on $F^2$ | 0.923 |
| Final R indices (I>2$\sigma$(I)) | R1 = 0.0517, wR2 = 0.1063 |
| R indices (all data) | R1 = 0.0715, wR2 = 0.1135 |
| Largest diff. peak/hole (e$Å^{-3}$) | 1.158 and -0.707 |

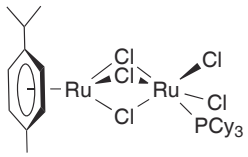


**Table C12:** Crystallographic data for complex **97** × $CCl_4$.

| | |
|---|---|
| Empirical formula | $C_{29}H_{47}Cl_9PRu_2$ |
| Molecular weight (g $mol^{-1}$) | 947.8 |
| Crystal size | 0.21 × 0.20 × 0.10 |
| Crystal system | monoclinic |
| Space group | P2(1)/c |
| a (Å) | 20.3160(16) |
| b (Å) | 10.0742(7) |
| c (Å) | 21.2411(16) |
| $\alpha$ ( $^\circ$ ) | 90 |
| $\beta$ ( $^\circ$ ) | 118.213(8) |
| $\gamma$ ( $^\circ$ ) | 90 |
| Volume ($Å^3$) | 3830.9(5) |
| Z | 4 |
| Density (g $cm^{-3}$) | 1.643 |
| Temperature (K) | 140(2) |
| Absorption coefficient ($mm^{-1}$) | 1.478 |
| $\Theta$ range ( $^\circ$ ) | 2.97 to 25.03 |
| Index ranges | -24 → 24, -11 → 11, -25 → 19 |
| Reflections collected | 21514 |
| Independent reflections | 6447 ($R_{int}$ = 0.0515) |
| Absorption correction | Semi-empirical from equivalents (MULABS) |
| Max. and min. transmission | 0.8438 and 0.7370 |
| Data / restraints / parameters | 6447 / 0 / 370 |
| Goodness-of-fit on $F^2$ | 0.913 |
| Final R indices (I>2$\sigma$(I)) | R1 = 0.0362, wR2 = 0.0683 |
| R indices (all data) | R1 = 0.0667, wR2 = 0.0758 |
| Largest diff. peak/hole ($eÅ^{-3}$) | 1.339 and -1.207 |

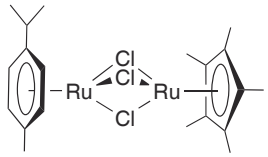


**Table C13:** Crystallographic data for complex **104**.

| | |
|---|---|
| Empirical formula | $C_{20}H_{29}Cl_3Ru_2$ |
| Molecular weight (g $mol^{-1}$) | 577.9 |
| Crystal size | 0.17 × 0.12 × 0.10 |
| Crystal system | monoclinic |
| Space group | P2(1)/c |
| a (Å) | 11.3160(6) |
| b (Å) | 17.108(3) |
| c (Å) | 11.617(2) |
| $\alpha$ ( $^\circ$ ) | 90 |
| $\beta$ ( $^\circ$ ) | 100.473(10) |
| $\gamma$ ( $^\circ$ ) | 90 |
| Volume ($Å^3$) | 2211.4(6) |
| Z | 4 |
| Density (g $cm^{-3}$) | 1.736 |
| Temperature (K) | 140(2) |
| Absorption coefficient ($mm^{-1}$) | 1.730 |
| $\Theta$ range ( $^\circ$ ) | 3.00 to 25.02 |
| Index ranges | -12 → 12, -20 → 20, -13 → 13 |
| Reflections collected | 13083 |
| Independent reflections | 3714 ($R_{int}$ = 0.0362) |
| Absorption correction | Semi-empirical from equivalents (MULABS) |
| Max. and min. transmission | 0.8179 and 0.6935 |
| Data / restraints / parameters | 3714 / 0 / 226 |
| Goodness-of-fit on $F^2$ | 1.114 |
| Final R indices (I>2$\sigma$(I)) | R1 = 0.0365, wR2 = 0.0880 |
| R indices (all data) | R1 = 0.0470, wR2 = 0.0955 |
| Largest diff. peak/hole ($eÅ^{-3}$) | 0.739 and -0.646 |

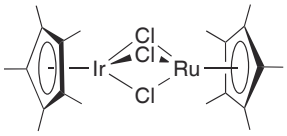


**Table C14:** Crystallographic data for complex **107**.

| | |
|---|---|
| Empirical formula | $C_{20}H_{30}Cl_3IrRu$ |
| Molecular weight (g mol$^{-1}$) | 670.1 |
| Crystal size | 0.30 × 0.28 × 0.11 |
| Crystal system | monoclinic |
| Space group | I2/a |
| a (Å) | 27.9257(14) |
| b (Å) | 10.6205(3) |
| c (Å) | 30.1330(14) |
| $\alpha$ ( $^\circ$ ) | 90 |
| $\beta$ ( $^\circ$ ) | 91.031(4) |
| $\gamma$ ( $^\circ$ ) | 90 |
| Volume (Å$^3$) | 8935.6(7) |
| Z | 16 |
| Density (g cm$^{-3}$) | 1.992 |
| Temperature (K) | 140(2) |
| Absorption coefficient (mm$^{-1}$) | 6.987 |
| $\Theta$ range ( $^\circ$ ) | 3.19 to 25.03 |
| Index ranges | -33 → 33, -11 → 11, -35 → 35 |
| Reflections collected | 24673 |
| Independent reflections | 7445 ($R_{int}$ = 0.0333) |
| Absorption correction | Semi-empirical from equivalents (MULABS) |
| Max. and min. transmission | 0.4376 and 0.2545 |
| Data / restraints / parameters | 7445 / 0 / 451 |
| Goodness-of-fit on F$^2$ | 1.061 |
| Final R indices (I>2$\sigma$(I)) | R1 = 0.0422, wR2 = 0.0965 |
| R indices (all data) | R1 = 0.0522, wR2 = 0.1001 |
| Largest diff. peak/hole (eÅ$^{-3}$) | 1.778 and -1.723 |

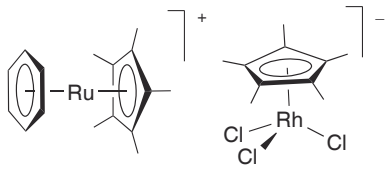


**Table C15:** Crystallographic data for complex **109**.

| | |
|---|---|
| Empirical formula | $C_{26}H_{36}Cl_3RhRu$ |
| Molecular weight (g $mol^{-1}$) | 658.9 |
| Crystal size | 0.19 × 0.12 × 0.11 |
| Crystal system | Orthorhombic |
| Space group | Pnma |
| a (Å) | 19.069(3) |
| b (Å) | 12.2265(7) |
| c (Å) | 11.346(3) |
| $\alpha$ ( $^\circ$ ) | 90 |
| $\beta$ ( $^\circ$ ) | 90 |
| $\gamma$ ( $^\circ$ ) | 90 |
| Volume ($Å^3$) | 2645.2(7) |
| Z | 4 |
| Density (g $cm^{-3}$) | 1.654 |
| Temperature (K) | 140(2) |
| Absorption coefficient ($mm^{-1}$) | 1.510 |
| $\Theta$ range ( $^\circ$ ) | 3.25 to 25.03 |
| Index ranges | -22 → 22, -13 → 13, -13 → 13 |
| Reflections collected | 16451 |
| Independent reflections | 2352 ($R_{int}$ = 0.0444) |
| Absorption correction | Semi-empirical from equivalents (MULABS) |
| Max. and min. transmission | 0.8633 and 0.7484 |
| Data / restraints / parameters | 2352 / 0 / 152 |
| Goodness-of-fit on $F^2$ | 1.151 |
| Final R indices (I>2$\sigma$(I)) | R1 = 0.0410, wR2 = 0.0853 |
| R indices (all data) | R1 = 0.0501, wR2 = 0.0896 |
| Largest diff. peak/hole (e$Å^{-3}$) | 0.941 and -0.745 |

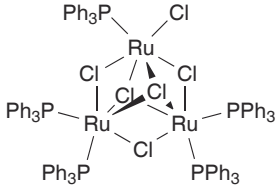


**Table C16:** Crystallographic data for complex **110** × 2 $CH_2Cl_2$.

| | |
|---|---|
| Empirical formula | $C_{92}H_{79}Cl_{10}P_5Ru_3$ |
| Molecular weight (g $mol^{-1}$) | 1997.1 |
| Crystal size | 0.21 × 0.16 × 0.15 |
| Crystal system | triclinic |
| Space group | P-1 |
| a (Å) | 15.244(4) |
| b (Å) | 15.603(6) |
| c (Å) | 20.804(4) |
| $\alpha$ ( $^\circ$ ) | 73.88(2) |
| $\beta$ ( $^\circ$ ) | 76.51(2) |
| $\gamma$ ( $^\circ$ ) | 65.97(3) |
| Volume ($Å^3$) | 4301(2) |
| Z | 2 |
| Density (g $cm^{-3}$) | 1.542 |
| Temperature (K) | 140(2) |
| Absorption coefficient ($mm^{-1}$) | 0.970 |
| $\Theta$ range ( $^\circ$ ) | 2.89 to 25.02 |
| Index ranges | -18 → 17, -18 → 18, -24 → 24 |
| Reflections collected | 28000 |
| Independent reflections | 14251 ($R_{int}$ = 0.0361) |
| Absorption correction | Semi-empirical from equivalents (MULABS) |
| Max. and min. transmission | 0.8922 and 0.7934 |
| Data / restraints / parameters | 14251 / 6 / 1012 |
| Goodness-of-fit on $F^2$ | 0.973 |
| Final R indices (I>2$\sigma$(I)) | R1 = 0.0440, wR2 = 0.1072 |
| R indices (all data) | R1 = 0.0688, wR2 = 0.1214 |
| Largest diff. peak/hole ($eÅ^{-3}$) | 1.407 and -0.828 |

# Bibliography

[1] G. Fauque, H. D. Peck Jr., J. J. G. Moura, B. H. Huynh, Y. Berlier, D. V. DerVartanian, M. Teixeira, A. E. Przybyla, P. A. Lespinat, I. Moura, J. LeGall, *FEMS Microbiol. Rev.* **1988**, *4*, 299–344.

[2] A. Volbeda, M.-H. Charon, C. Piras, E. C. Hatchikian, M. Frey, J. C. Fontecilla-Camps, *Nature* **1995**, *373*, 580–7.

[3] M. Pavlov, P. E. M. Siegbahn, M. R. A. Blomberg, R. H. Crabtree, *J. Am. Chem. Soc.* **1998**, *120*, 548–55.

[4] A. L. Gavrilova, B. Bosnich, *Chem. Rev.* **2004**, *104*, 349–83.

[5] G. J. Rowlands, *Tetrahedron* **2001**, *57*, 1865–82.

[6] B. Bosnich, *Inorg. Chem.* **1999**, *38*, 2554–62.

[7] D. E. Fenton, *Chem. Soc. Rev.* **1999**, *28*, 159–68.

[8] E. K. van den Beuken, B. L. Feringa, *Tetrahedron* **1998**, *54*, 12985–3011.

[9] D. G. McCollum, B. Bosnich, *Inorg. Chim. Acta* **1998**, *270*, 13–9.

[10] M. Shibasaki, H. Sasai, T. Arai, *Angew. Chem. Int. Ed.* **1997**, *36*, 1236–56.

[11] H. Steinhagen, G. Helmchen, *Angew. Chem. Int. Ed.* **1996**, *35*, 2339–42.

[12] M. A. Rida, A. K. Smith, *J. Mol. Catal. A: Chem.* **2003**, *202*, 87–95.

[13] G. P. Abramo, L. Li, T. J. Marks, *J. Am. Chem. Soc.* **2002**, *124*, 13966–7.

[14] N. D. Jones, B. R. James, *Adv. Synth. Catal.* **2002**, *344*, 1126–34.

[15] K.-i. Yamada, S. J. Harwood, H. Gröger, M. Shibasaky, *Angew. Chem. Int. Ed.* **1999**, *38*, 3504–6.

[16] G. Süss-Fink, *Angew. Chem. Int. Ed.* **1994**, *33*, 67–9.

[17] M. W. Göbel, *Angew. Chem. Int. Ed.* **1994**, *33*, 1141–3.

[18] M. I. Bruce, M. Z. Iqbal, F. G. A. Stone, *J. Organomet. Chem.* **1972**, *40*, 393–401.

[19] G. Lopez, G. Garcia, C. de Haro, G. Sanchez, J. Garcia, *J. Organomet. Chem.* **1986**, *317*, C23–4.

[20] A. A. H. van der Zeijden, G. van Koten, R. Luijk, K. Vrieze, C. Slob, H. Krabbendam, A. L. Spek, *Inorg. Chem.* **1988**, *27*, 1014–19.

[21] T. Weskamp, F. J. Kohl, W. Hieringer, D. Gleich, W. A. Herrmann, *Angew. Chem. Int. Ed.* **1999**, *38*, 2416–9.

[22] E. L. Dias, R. H. Grubbs, *Organometallics* **1998**, *17*, 2758–67.

[23] S. Gauthier, L. Quebatte, R. Scopelliti, K. Severin, *Chem. Eur. J.* **2004**, *10*, 2811–21.

[24] S. Gauthier, L. Quebatte, R. Scopelliti, K. Severin, *Inorg. Chem. Commun.* **2004**, *7*, 708–12.

[25] K. Severin, *Chem. Eur. J.* **2002**, *8*, 1514–8.

[26] A. C. da Silva, H. Piotrowski, P. Mayer, K. Polborn, K. Severin, *Eur. J. Inorg. Chem.* **2001**, *3*, 685–91.

[27] E. Kessenich, A. Schulz, K. Severin, *J. Raman Spectrosc.* **2001**, *32*, 241–50.

[28] A. C. da Silva, H. Piotrowski, P. Mayer, K. Polborn, K. Severin, *J. Chem. Soc., Dalton Trans.* **2000**, *17*, 2960–3.

[29] K. Polborn, K. Severin, *J. Chem. Soc., Dalton Trans.* **1999**, *5*, 759–64.

[30] K. Polborn, K. Severin, *Eur. J. Inorg. Chem.* **1998**, *8*, 1187–92.

[31] J. Halpern, *Inorg. Chim. Acta* **1982**, *62*, 31–7.

[32] K. Severin, K. Polborn, W. Beck, *Inorg. Chim. Acta* **1995**, *240*, 339–46.

[33] J. W. Szostak, *Chem. Rev.* **1997**, *97*, 347. (Special issue on combinatorial chemistry).

[34] R. B. Merrifield, *J. Am. Chem. Soc.* **1963**, *85*, 2149–54.

[35] B. A. Bunin, J. A. Ellman, *J. Am. Chem. Soc.* **1992**, *114*, 10997–8.

[36] K. Ding, H. Du, Y. Yuan, J. Long, *Chem. Eur. J.* **2004**, *10*, 2872–84.

[37] V. Percec, *Nature* **2003**, *424*, 135–6.

[38] P. Chen, *Angew. Chem. Int. Ed.* **2003**, *42*, 2832–47.

[39] C. Gennari, U. Piarulli, *Chem. Rev.* **2003**, *103*, 3071–100.

[40] P. Stambuli, James, F. Hartwig, John, *Curr. Opin. Chem. Biol.* **2003**, *7*, 420–6.

[41] V. Murphy, A. F. Volpe Jr., W. H. Weinberg, *Curr. Opin. Chem. Biol.* **2003**, *7*, 427–33.

[42] J. G. de Vries, A. H. M. de Vries, *Eur. J. Org. Chem.* **2003**, *5*, 799–811.

[43] A. Hagemeyer, B. Jandeleit, Y. Liu, D. M. Poojary, H. W. Turner, A. F. Volpe Jr., W. H. Weinberg, *Appl. Catal., A: General* **2001**, *221*, 23–43.

[44] S. R. Gilbertson, *Prog. Inorg. Chem.* **2001**, *50*, 433–71.

[45] M. T. Reetz, *Angew. Chem. Int. Ed.* **2001**, *40*, 284–310.

[46] R. H. Crabtree, *Chem. Commun.* **1999**, *17*, 1611–6.

[47] B. Jandeleit, D. J. Schaefer, T. S. Powers, H. W. Turner, W. H. Weinberg, *Angew. Chem. Int. Ed.* **1999**, *38*, 2494–532.

[48] K. D. Shimizu, M. L. Snapper, A. H. Hoveyda, *Chem. Eur. J.* **1998**, *4*, 1885–9.

[49] B. Jandeleit, W. H. Weinberg, *Chem. Ind.* **1998**, *19*, 795–8.

[50] W. H. Weinberg, B. Jandeleit, K. Self, H. Turner, *Curr. Opin. Solid State & Materials Science* **1998**, *3*, 104–10.

[51] S. Garbacia, R. Touzani, O. Lavastre, *J. Comb. Chem.* **2004**, *6*, 297–300.

[52] T. R. Boussie, G. M. Diamond, C. Goh, K. A. Hall, A. M. LaPointe, M. Leclerc, C. Lund, V. Murphy, J. A. W. Shoemaker, U. Tracht, H. Turner, J. Zhang, T. Uno, R. K. Rosen, J. C. Stevens, *J. Am. Chem. Soc.* **2003**, *125*, 4306–17.

[53] C. Markert, A. Pfaltz, *Angew. Chem. Int. Ed.* **2004**, *43*, 2498–500.

[54] J. W. Saalfrank, W. F. Maier, *Angew. Chem. Int. Ed.* **2004**, *43*, 2028–31.

[55] S. R. Stauffer, J. F. Hartwig, *J. Am. Chem. Soc.* **2003**, *125*, 6977–85.

[56] S. Yao, J.-C. Meng, G. Siuzdak, M. G. Finn, *J. Org. Chem.* **2003**, *68*, 2540–6.

[57] C.-C. Tai, T. Chang, B. Roller, P. G. Jessop, *Inorg. Chem.* **2003**, *42*, 7340–1.

[58] K. H. Shaughnessy, P. Kim, J. F. Hartwig, *J. Am. Chem. Soc.* **1999**, *121*, 2123–32.

[59] G. Liu, J. A. Ellman, *J. Org. Chem.* **1995**, *60*, 7712–13.

[60] S. R. Gilbertson, X. Wang, *Tetrahedron Lett.* **1996**, *37*, 6475–8.

[61] M. S. Kharasch, H. Engelmann, F. R. Mayo, *J. Org. Chem.* **1937**, *2*, 288–302.

[62] M. S. Kharasch, E. V. Jensen, W. H. Urry, *Science* **1945**, *102*, 128.

[63] M. DeMalde, F. Minisci, U. Pallini, E. Volterra, A. Quilico, *Chim. Ind.* **1956**, *38*, 371.

[64] D. Bellus, *Pure & Appl. Chem.* **1985**, *57*, 1827–38.

[65] C. K. Tseng, E. G. Teach, R. W. Simons, *Synth. Commun.* **1984**, *14*, 1027–31.

[66] H. Nagashima, H. Wakamatsu, K. Itoh, Y. Tomo, J. Tsuji, *Tetrahedron Lett.* **1983**, *24*, 2395–8.

[67] Y. Mori, J. Tsuji, *Tetrahedron* **1973**, *29*, 827–32.

[68] D. J. Burton, L. J. Kehoe, *Tetrahedron Lett.* **1966**, *42*, 5163–8.

[69] S. Murai, N. Sonoda, S. Tsutsumi, *J. Org. Chem.* **1964**, *29*, 2104–5.

[70] G. Sosnovsky, *Addition of Alkyl Polyhalides to Unsaturated Compounds*, Chapter 2, The Macmillian Compagny, New York, **1964**.

[71] G. M. Lee, S. M. Weinreb, *J. Org. Chem.* **1990**, *55*, 1281–5.

[72] T. K. Hayes, A. J. Freyer, M. Parvez, S. M. Weinreb, *J. Org. Chem.* **1986**, *51*, 5501–3.

[73] J. Elzinga, H. Hogeveen, *J. Org. Chem.* **1980**, *45*, 3957–69.

[74] C. Tanielian, R. Kieffer, A. Harfouch, *Tetrahedron Lett.* **1977**, *18*, 4589–92.

[75] Y. Mori, J. Tsuji, *Tetrahedron* **1972**, *28*, 29–35.

[76] T. Susuki, J. Tsuji, *J. Org. Chem.* **1970**, *35*, 2982–86.

[77] A. N. Nesmeyanov, R. K. Freidlina, E. C. Chukovskaya, R. G. Petrova, A. B. Belyavsky, *Tetrahedron* **1962**, *17*, 61–8.

[78] J. A. Osborn, F. H. Jardine, J. F. Young, G. Wilkinson, *J. Chem. Soc. A* **1966**, *12*, 1711–32.

[79] D. Evans, J. A. Osborn, F. H. Jardine, G. Wilkinson, *Nature* **1965**, *208*, 1203–4.

[80] H. Matsumoto, T. Nakano, Y. Nagai, *Tetrahedron Lett.* **1973**, *51*, 5147–50.

[81] W. J. Bland, R. Davis, J. L. A. Durrant, *J. Organomet. Chem.* **1985**, *280*, 397–406.

[82] W. J. Bland, R. Davis, J. L. A. Durrant, *J. Organomet. Chem.* **1984**, *267*, C45–8.

[83] H. Nagashima, H. Wakamatsu, N. Ozaki, T. Ishii, M. Watanabe, T. Tajima, K. Itoh, *J. Org. Chem.* **1992**, *57*, 1682–9.

[84] H. Nagashima, N. Ozaki, K. Seki, M. Ishii, K. Itoh, *J. Org. Chem.* **1989**, *54*, 4497–9.

[85] H. Nagashima, K.-i. Ara, H. Wakamatsu, K. Itoh, *J. Chem. Soc., Chem. Commun.* **1985**, *8*, 518–9.

[86] T. K. Hayes, R. Villani, S. M. Weinreb, *J. Am. Chem. Soc.* **1988**, *110*, 5533–43.

[87] H. Matsumoto, T. Nikaido, Y. Nagai, *J. Org. Chem.* **1976**, *41*, 396–8.

[88] H. Nagashima, H. Wakamatsu, K. Itoh, *J. Chem. Soc., Chem. Commun.* **1984**, *10*, 652–3.

[89] L. A. van de Kuil, Y. S. J. Veldhuizen, D. M. Grove, J. W. Zwikker, L. W. Jenneskens, W. Drenth, W. J. J. Smeets, A. L. Spek, G. van Koten, *Recl. Trav. Chim. Pays-Bas* **1994**, *113*, 267–77.

[90] M. Kameyama, N. Kamigata, *Bull. Chem. Soc. Jpn.* **1989**, *62*, 648–50.

[91] M. Kameyama, N. Kamigata, M. Kobayashi, *J. Org. Chem.* **1987**, *52*, 3312–16.

[92] S. Murai, R. Sugise, N. Sonoda, *Angew. Chem. Int. Ed.* **1981**, *20*, 475–6.

[93] M. Sawamoto, M. Kamigaito, *Chemtech* **1999**, *29*, 30–8.

[94] K. Matyjaszewski, *Chem. Eur. J.* **1999**, *5*, 3095–102.

[95] M. Kamigaito, T. Ando, M. Sawamoto, *Chem. Rev.* **2001**, *101*, 3689–745.

[96] K. Matyjaszewski, J. Xia, *Chem. Rev.* **2001**, *101*, 2921–90.

[97] F. Simal, D. Jan, L. Delaude, A. Demonceau, M.-R. Spirlet, A. F. Noels, *Can. J. Chem.* **2001**, *79*, 529–35.

[98] F. Simal, S. Sebille, L. Hallet, A. Demonceau, A. F. Noels, *Macromol. Symp.* **2000**, *161*, 73–85.

[99] F. Simal, D. Jan, A. Demonceau, A. F. Noels, *Controlled/Living Radical Polymerization*, (ED.: K. Matyjaszewsky), ACS Symposium Series 768, ACS, Washington (chap. 16), **2000**.

[100] F. Simal, A. Demonceau, A. F. Noels, *Angew. Chem. Int. Ed.* **1999**, *38*, 538–40.

[101] L. Quebatte, M. Haas, E. Solari, R. Scopelliti, Q. T. Nguyen, K. Severin, *Angew. Chem. Int. Ed.* **2005**, *44*, 1084–8.

[102] H. Matsumoto, T. Nakano, Y. Nagai, H. Kono, *Bull. Chem. Soc. Jpn.* **1978**, *51*, 2445–6.

[103] R. H. Grubbs, *Tetrahedron* **2004**, *60*, 7117–40.

[104] T. M. Trnka, R. H. Grubbs, *Acc. Chem. Res.* **2001**, *34*, 18–29.

[105] K. Severin, *Curr. Org. Chem.* **2005**, *in press*.

[106] L. Delaude, A. Demonceau, A. F. Noels, *Top. Organomet. Chem.* **2004**, *11*, 155–71.

[107] J. A. Tallarico, L. M. Malnick, M. L. Snapper, *J. Org. Chem.* **1999**, *64*, 344–5.

[108] F. Simal, A. Demonceau, A. F. Noels, *Tetrahedron Lett.* **1999**, *40*, 5689–93.

[109] F. Simal, S. Sebille, A. Demonceau, A. F. Noels, R. Nuñez, M. Abad, F. Teixidor, C. Viñas, *Tetrahedron Lett.* **2000**, *41*, 5347–51.

[110] F. Simal, L. Wlodarczak, A. Demonceau, A. F. Noels, *Tetrahedron Lett.* **2000**, *41*, 6071–4.

[111] T. Ando, M. Kamigaito, M. Sawamoto, *Macromolecules* **2000**, *33*, 5825–9.

[112] F. Simal, L. Wlodarczak, A. Demonceau, A. F. Noels, *Eur. J. Org. Chem.* **2001**, *14*, 2689–95.

[113] D. Motoda, H. Kinoshita, H. Shinokubo, K. Oshima, *Adv. Synth. Catal.* **2002**, *344*, 261–5.

[114] B. De Clercq, F. Verpoort, *Tetrahedron Lett.* **2001**, *42*, 8959–63.

[115] T. Opstal, F. Verpoort, *Tetrahedron Lett.* **2002**, *43*, 9259–63.

[116] B. De Clercq, F. Verpoort, *Tetrahedron Lett.* **2002**, *43*, 4687–90.

[117] O. Tutusaus, C. Viñas, R. Núñez, F. Teìxídor, A. Demonceau, S. Delfosse, A. F. Noels, I. Mata, E. Molins, *J. Am. Chem. Soc.* **2003**, *125*, 11830–1.

[118] O. Tutusaus, S. Delfosse, A. Demonceau, A. F. Noels, C. Viñas, F. Teixidor, *Tetrahedron Lett.* **2003**, *44*, 8421–5.

[119] A. Richel, S. Delfosse, C. Cremasco, L. Delaude, A. Demonceau, A. F. Noels, *Tetrahedron Lett.* **2003**, *44*, 6011–5.

[120] B. De Clercq, F. Verpoort, *J. Organomet. Chem.* **2003**, *672*, 11–6.

[121] T. Opstal, F. Verpoort, *New J. Chem.* **2003**, *27*, 257–62.

[122] H. Nagashima, M. Gondo, S. Masuda, H. Kondo, Y. Yamaguchi, K. Matsubara, *Chem. Commun.* **2003**, *3*, 442–3.

[123] L. Quebatte, R. Scopelliti, K. severin, *Angew. Chem. Int. Ed.* **2004**, *43*, 1520–4.

[124] K. S. MacFarlane, I. S. Thorburn, P. W. Cyr, D. E. K.-Y. Chau, S. J. Rettig, B. R. James, *Inorg. Chim. Acta* **1998**, *270*, 130–44.

[125] D. Amoroso, G. P. A. Yap, D. E. Fogg, *Can. J. Chem.* **2001**, *79*, 958–63.

[126] S. Gauthier, R. Scopelliti, K. Severin, *Helv. Chim. Acta* **2005**, *88*, 435–46.

[127] L. E. Harrington, J. F. Britten, D. W. Hughes, A. D. Bain, J.-Y. Thépot, M. J. McGlinchey, *J. Organomet. Chem.* **2002**, *656*, 243–57.

[128] H. K. Gupta, N. Rampersad, M. Stradiotto, M. J. McGlinchey, *Organometallics* **2000**, *19*, 184–91.

[129] L. Bonomo, C. Stern, E. Solari, R. Scopelliti, C. Floriani, *Angew. Chem. Int. Ed.* **2001**, *40*, 1449–52.

[130] V. Rodriguez, I. Atheaux, B. Donnadieu, S. Sabo-Etienne, B. Chaudret, *Organometallics* **2000**, *19*, 2916–26.

[131] D. G. Gusev, F. M. Dolgushin, M. Y. Antipin, *Organometallics* **2000**, *19*, 3429–34.

[132] K. Abdur-Rashid, D. G. Gusev, A. J. Lough, R. H. Morris, *Organometallics* **2000**, *19*, 1652–60.

[133] R. A. T. M. Abbenhuis, I. del Rio, M. M. Bergshoef, J. Boersma, N. Veldman, A. L. Spek, G. van Koten, *Inorg. Chem.* **1998**, *37*, 1749–58.

[134] J. R. Torres-Lubián, M. E. Sánchez-Castro, P. Juárez-Saavedra, J. Hernández-Martínez, B. Gordillo-Román, M. A. Paz-Sandoval, *J. Organomet. Chem.* **2002**, *663*, 127–33.

[135] S. Gauthier, R. Scopelliti, K. Severin, *Organometallics* **2004**, *23*, 3769–71.

[136] L. Quebatte, R. Scopelliti, K. Severin, *Eur. J. Inorg. Chem.* **2005**, *in press.*

[137] Y. Motoyama, M. Gondo, S. Masuda, Y. Iwashita, H. Nagashima, *Chem. Lett.* **2004**, *33*, 442–3.

[138] T. Opstal, F. Verpoort, *Angew. Chem. Int. Ed.* **2003**, *42*, 2876–9.

[139] B. De Clercq, F. Verpoort, *Macromolecules* **2002**, *35*, 8943–7.

[140] K. S. Singh, P. J. Carroll, M. R. Kollipara, *Polyhedron* **2005**, *24*, 391–6.

[141] K. M. Rao, E. K. Rymmai, *Polyhedron* **2003**, *22*, 307–12.

[142] R. Torres-Lubián, M. J. Rosales-Hoz, A. M. Arif, R. D. Ernst, M. A. Paz-Sandoval, *J. Organomet. Chem.* **1999**, *585*, 68–82.

[143] B. Steinmetz, W. A. Schenk, *Organometallics* **1999**, *18*, 943–6.

[144] P. J. Fagan, W. S. Mahoney, J. C. Calabrese, I. D. Williams, *Organometallics* **1990**, *9*, 1843–52.

[145] M. S. Chinn, D. M. Heinekey, *J. Am. Chem. Soc.* **1990**, *112*, 5166–75.

[146] I. A. Guzei, M. A. Paz-Sandoval, R. Torres-Lubián, P. Juárez-Saavedra, *Acta Cryst., Sec. C* **1999**, *55*, 1090–2.

[147] A. A. Zlota, M. Tilset, K. G. Caulton, *Inorg. Chem.* **1993**, *32*, 3816–21.

[148] C. Gemel, A. LaPensée, K. Mauthner, K. Mereiter, R. Schmid, K. Kirchner, *Monatsh. Chem.* **1997**, *128*, 1189–99.

[149] M. J. Burk, A. J. Arduengo III, J. C. Calabrese, R. L. Harlow, *J. Am. Chem. Soc.* **1989**, *111*, 8938–40.

[150] J. Huang, E. D. Stevens, S. P. Nolan, J. L. Petersen, *J. Am. Chem. Soc.* **1999**, *121*, 2674–8.

[151] T. Arliguie, C. Border, B. Chaudret, J. Devillers, R. Poilblanc, *Organometallics* **1989**, *8*, 1308–14.

[152] L. Quebatte, E. Solari, R. Scopelliti, K. Severin, *Organometallics* **2005**, *24*, 1404–6.

[153] A. Fürstner, T. Müller, *J. Am. Chem. Soc.* **1999**, *121*, 7814–21.

[154] A. Fürstner, L. Ackermann, *Chem. Commun.* **1999**, *1*, 95–6.

[155] J. Baran, I. Bogdanska, D. Jan, L. Delaude, A. Demonceau, A. F. Noels, *J. Mol. Catal. A: Chem.* **2002**, *190*, 109–16.

[156] D. Jan, L. Delaude, F. Simal, A. Demonceau, A. F. Noels, *J. Organomet. Chem.* **2000**, *606*, 55–64.

[157] A. Hafner, A. Mühlebach, P. A. van der Schaaf, *Angew. Chem. Int. Ed.* **1997**, *36*, 2121–4.

[158] A. Demonceau, A. W. Stumpf, E. Saive, A. F. Noels, *Macromolecules* **1997**, *30*, 3127–36.

[159] A. W. Stumpf, E. Saive, A. Demonceau, A. F. Noels, *J. Chem. Soc., Chem. Commun.* **1995**, *11*, 1127–8.

[160] A. Demonceau, A. F. Noels, E. Saive, A. J. Hubert, *J. Mol. Catal.* **1992**, *76*, 123–32.

[161] M. A. Bennett, A. K. Smith, *J. Chem. Soc., Dalton Trans.* **1974**, *2*, 233–41.

[162] M. A. Bennett, T.-N. Huang, J. L. Latten, *J. Organomet. Chem.* **1984**, *272*, 189–205.

[163] J. W. Hull, W. L. Gladfelter, *Organometallics* **1984**, *3*, 605–13.

[164] B. T. Lee, T. O. Schrader, B. Martín-Matute, C. R. Kauffman, P. Zhang, M. L. Snapper, *Tetrahedron* **2004**, *60*, 7391–6.

[165] I. del Río, G. van Koten, M. Lutz, A. L. Spek, *Organometallics* **2000**, *19*, 361–4.

[166] R. Appel, *Inorg. Synth.* **1986**, *24*, 107–9.

[167] L. Quebatte, R. Scopelliti, K. Severin, *Eur. J. Inorg. Chem.* **2005**, *submitted*.

[168] A.-R. Al-Ohaly, J. F. Nixon, *Inorg. Chim. Acta* **1985**, *103*, 83–93.

[169] R. A. Head, J. F. Nixon, *J. Chem. Soc., Dalton Trans.* **1978**, *8*, 901–9.

[170] U. Koelle, B.-S. Kang, U. Englert, *J. Organomet. Chem.* **1991**, *420*, 227–35.

[171] P. J. Fagan, M. D. Ward, J. C. Calabrese, *J. Am. Chem. Soc.* **1989**, *111*, 1698–719.

[172] B. K. Campion, R. H. Heyn, T. D. Tilley, *J. Chem. Soc., Chem. Commun.* **1988**, *4*, 278–80.

[173] U. Koelle, J. Kossakowski, *J. Organomet. Chem.* **1989**, *362*, 383–98.

[174] B. Chaudret, F. Jalón, M. Pérez-Manrique, F. Lahoz, F. J. Plou, R. Sánchez-Delgado, *New J. Chem.* **1990**, *14*, 331–8.

[175] B. Chaudret, F. A. Jalon, *J. Chem. Soc., Chem. Commun.* **1988**, *11*, 711–3.

[176] U. Koelle, J. Kossakowski, *J. Chem. Soc., Chem. Commun.* **1988**, *8*, 549–51.

[177] D. A. Tocher, M. D. Walkinshaw, *Acta Cryst., Sec. B* **1982**, *38*, 3083–5.

[178] U. Koelle, J. Kossakowski, *Inorg. Chim. Acta* **1989**, *164*, 23–32.

[179] D. Amoroso, G. P. A. Yap, D. E. Fogg, *Organometallics* **2002**, *21*, 3335–43.

[180] T. Arthur, T. A. Stephenson, *J. Organomet. Chem.* **1981**, *208*, 369–87.

[181] H. Aneetha, M. Jiménez-Tenorio, M. C. Puerta, P. Valerga, V. N. Sapunov, R. Schmid, K. Kirchner, K. Mereiter, *Organometallics* **2002**, *21*, 5334–46.

[182] J. W. Kriesel, S. König, M. A. Freitas, A. G. Marshall, J. A. Leary, T. D. Tilley, *J. Am. Chem. Soc.* **1998**, *120*, 12207–15.

[183] A. A. Dembek, P. J. Fagan, *Organometallics* **1995**, *14*, 3741–5.

[184] U. Koelle, A. Hörnig, U. Englert, *Organometallics* **1994**, *13*, 4064–6.

[185] M. D. Ward, P. J. Fagan, J. C. Calabrese, D. C. Johnson, *J. Am. Chem. Soc.* **1989**, *111*, 1719–32.

[186] A. Schmid, H. Piotrowski, T. Lindel, *Eur. J. Inorg. Chem.* **2003**, *12*, 2255–63.

[187] W. Rigby, J. A. McCleverty, P. M. Maitlis, *J. Chem. Soc., Dalton Trans.* **1979**, *2*, 382–6.

[188] I. Ara, J. R. Berenguer, E. Eguizábal, J. Forniés, E. Lalinde, A. Martín, *Eur. J. Inorg. Chem.* **2001**, *6*, 1631–40.

[189] K. Umakoshi, K. Murata, S. Yamashita, K. Isobe, *Inorg. Chim. Acta* **1991**, *190*, 185–91.

[190] S. H. Liu, S.-Y. Yang, S. T. Lo, Z. Xu, W. S. Ng, T. B. Wen, Z. Y. Zhou, Z. Lin, C. P. Lau, G. Jia, *Organometallics* **2001**, *20*, 4161–9.

[191] K. Mashima, N. Komura, T. Yamagata, K. Tani, *Inorg. Chem.* **1997**, *36*, 2908–12.

[192] K. Mashima, T. Hino, H. Takaya, *J. Chem. Soc., Dalton Trans.* **1992**, *13*, 2099–107.

[193] K. Mashima, T. Hino, H. Takaya, *Tetrahedron Lett.* **1991**, *32*, 3101–4.

[194] W. L. F. Armarego, D. D. Perrin, *Purification of laboratory chemicals*, Edition 4, Oxford: Butterworth-Heinemann, **2000**.

[195] R. Cramer, *Inorg. Synth.* **1974**, *15*, 14–8.

[196] J. L. Herde, J. C. Lambert, C. V. Senoff, *Inorg. Synth.* **1974**, *15*, 18–9.

[197] G. Giordano, R. H. Crabtree, *Inorg. Synth.* **1990**, *28*, 88–90.

[198] M. A. Bennett, T.-N. Huang, T. W. Matheson, A. K. Smith, *Inorg. Synth.* **1982**, *21*, 74–8.

[199] P. M. Treichel, K. P. Wagner, W. J. Knebel, *Inorg. Chim. Acta* **1972**, *6*, 674–6.

[200] C. White, A. Yates, P. M. Maitlis, D. M. Heinekey, *Inorg. Synth.* **1992**, *29*, 228–34.

[201] D. N. Cox, R. Roulet, *Inorg. Chem.* **1990**, *29*, 1360–5.

[202] P. S. Hallman, T. A. Stephenson, G. Wilkinson, *Inorg. Synth.* **1970**, *12*, 237–40.

[203] B. Therrien, T. R. Ward, M. Pilkington, C. Hoffmann, F. Gilardoni, J. Weber, *Organometallics* **1998**, *17*, 330–7.

[204] U. Koelle, J. Kossakowski, *Inorg. Synth.* **1992**, *29*, 225–8.

[205] N. A. Bailey, V. S. Jassal, R. Vefghi, C. White, *J. Chem. Soc., Dalton Trans.* **1987**, *11*, 2815–22.

[206] J. Powell, B. L. Shaw, *J. Chem. Soc. A* **1968**, 583–96.

[207] J. H. van Diemen, J. G. Haasnoot, R. Hage, J. Reedijk, J. G. Vos, R. Wang, *Inorg. Chem.* **1991**, *30*, 4038–43.

[208] F. R. Hartley, *Organomet. Chem. Rev.* **1970**, *6*, 119–37.

[209] A. C. Cope, E. C. Friedrich, *J. Am. Chem. Soc.* **1968**, *90*, 909–13.

[210] Oxford Diffraction Ltd., Abingdon, Oxfordshire, OX141RL, UK, **2002**.

[211] Oxford Diffraction Ltd., Abington, Oxfordshire, UK, **2003**.

[212] G. M. Sheldrick, University of Gottingen, Gottingen (Germany), **1997**.

[213] Brucker AXS, Inc., Madison, Wisconsin, 53719, USA, **1997**.

[214] L. J. Farrugia, *J. Appl. Crystallogr.* **1997**, *30*, 565.

# Curriculum Vitae

**Laurent QUÉBATTE**
26 years old – Single – Swiss

Professional address:

EPFL
Bâtiment BCH
1015 Lausanne
Switzerland
+ 41 21 693 93 13
laurent.quebatte@epfl.ch

Personal address:

Chemin du Stand 18
1024 Ecublens
Switzerland
+ 41 21 691 16 50

## Education and Work Experience

**2001-2005** **Ph.D. in Chemistry**, in progress, at the **Ecole Polytechnique Fédérale de Lausanne (EPFL)**, - Institut des Sciences et Ingénierie Chimiques, advisor: **Prof. Kay Severin**;
*New Polynuclear Catalysts for Atom-Transfer Radical Additions.*

**1999-2001** **Graduate Degree** at the **Université de Lausanne (UNIL)**;
**Diploma work** at the **UNIL** - Institut de Chimie (ICMA), advisor: **Prof. André E. Merbach**;
*Synthesis and Characterization of Gd(III) Complexes for MRI.*
**Specialized practical** at the **UNIL** - ICMA, advisor: **Prof. Geoffrey Bodenhausen**;
*Measurement of coupling constants between $C^{\beta}$ and $C^{\gamma}$ in proteins by 3D NMR.*

**1997-1999** First cycle of Chemistry, at the **EPFL**.

**1994-1997** **Scientific High School Degree**, at the **Centre d'Enseignement Secondaire Supérieur du Nord Vaudois**, Yverdon.

## Research and Teaching Skills

**Scientific Techniques**:

Extensive experience in:
– Organometallic synthesis and catalysis,
– Responsibility for the maintenance and use of GC & GC-MS apparatus,
– Handling of air and moisture sensitive chemical products using Schlenk glassware and glovebox techniques,
– Standard $^{1}$H, $^{13}$C, $^{19}$F, and $^{31}$P NMR spectroscopy.

Basic knowledge in:
– Cloning and gene expression techniques,
– Synthesis of polyaminocarboxylate ligands for MRI contrast agents,
– Measurements of $^{1}$H and $^{17}$O relaxation times,
– IR and UV-vis spectroscopy,
– Understanding of multidimentional NMR pulse sequences.

**Assistantship**:

– Practicals for $1^{st}$ and $3^{rd}$ year students in chemistry,
– Research projects for apprentice chemist and undergraduate exchange students.

## Conferences attended

Oral Presentation, Fall Meeting of the Swiss Chemical Society (SCS), 2004, Zürich

Poster Presentation, Summer School "Frontiers in Catalysis", 2003, Champéry

Poster, SCS Fall Meeting, 2002, Basel

## Publications

— Cover picture, *Angew. Chem. Int. Ed.* **2004**, *43*, issue 12 —
*Combinatorial Catalysis with Bimetallic Complexes: Robust and Efficient Catalysts for Atom-Transfer Radical Additions*
**Laurent Québatte**, Rosario Scopelliti, and Kay Severin
*Angew. Chem. Int. Ed.* **2004**, *43*, 1520–4

*Combinatorial Synthesis of Bimetallic Complexes with Three Halogeno-Bridges*
Sébastien Gauthier, **Laurent Québatte**, Rosario Scopelliti, and Kay Severin
*Chem. Eur. J.* **2004**, *10*, 2811–21

*Atom-Transfer Radical Reactions under Mild Conditions with* $[\{RuCl_2(1,3,5\text{-}C_6H_3{}^iPr_3)\}_2]$ *and* $PCy_3$ *as the Catalyst Precursors*
**Laurent Québatte**, Michel Haas, Euro Solari, Rosario Scopelliti, Quoc T. Nguyen, and Kay Severin
*Angew. Chem. Int. Ed.* **2005**, *44*, 1084–8

*A Bimetallic Ruthenium Ethylene Complex as a Catalyst Precursor for the Kharasch Reactions*
**Laurent Québatte**, Euro Solari, Rosario Scopelliti, and Kay Severin
*Organometallics* **2005**, *7*, 1404–6

*Atom-Transfer Radical Additions with the Cationic Half-Sandwich Complex* $[Cp^{\star}Ru(PPh_3)_2(CH_3CN)]OTf$
**Laurent Québatte**, Rosario Scopelliti, and Kay Severin
*Eur. J. Inorg. Chem.* **2005**, *16*, 3353–8

*Synthesis, Structure, and Recativity of Homo- and Heterobimetallic Complexes of the General Formula* $[Cp^{\star}Ru(\mu\text{-}Cl)_3ML]$ *(LM = (arene)Ru,* $Cp^{\star}Rh$, $Cp^{\star}Ir$*)*
**Laurent Québatte**, Rosario Scopelliti, and Kay Severin
*Inorg. Chem. Commun.* **2005**, *submitted*

# Acknowledgments

First of all, I would like to thank my supervisor Professor Kay Severin for having given me the opportunity to work in one of his fascinating domains, trusted me and kept his door open for discussion at any time.

I am very grateful to Rosario Scopelliti who performed all X-Ray crystallographic analyses, as well as to Euro Solari for the syntheses of several Kharasch catalysts.

My gratitude also belongs to all my colleagues, Marie-Line Lehaire, Sébastien Gauthier, Thomas Brasey, Lionel Tornier, Estelle Burri, Alexander Schiller, Andrey Buryak, Zacharias Grote, Nicolas Christinat, Isabelle Saur and Michel Haas, and to our secretary Christina Zamanos, on whom I could always rely for their ready cooperation and availability, and who have also provided a relaxed working environment which made my time here all the more enjoyable. It was also a real pleasure for me to work with Ioana, Margarita, Lorenz, Leslie, Christoph, Silke, Nina, Stéphane, Fabien and Friederike who spent a short while in the group.

I wish to thank the many people not explicitly mentioned here who helped me one way or another.

Finally, I am fully grateful to my family and again to Marie-Line, who have always supplied me, in good and difficult times, with encouragement and love.